Single-Molecule FRET Reveals Transport Mechanism of ABC Transporters

Husada, Florence

DOI:
10.33612/diss.102141928

Single-Molecule FRET Reveals Transport Mechanism of ABC Transporters

Florence A. Husada

2019

Zernike Institute PhD thesis series 2019-30
ISSN : 1570-1530
ISBN (printed) : 978-94-034-2178-0
ISBN (electronic) : 978-94-034-2177-3

The work published in this thesis was carried out in the research group Molecular Microscopy at the Zernike Institute for Advanced Materials (ZIAM) of the University of Groningen, The Netherlands The research was financially supported by the Netherlands Organization for Scientific Research (NWO) and the Zernike Institute for Advanced Materials.

Cover design by Dina Maniar
Dutch summary by Marijn de Boer and Monique Wiertsema
Printed by ProefschriftMaken | www.proefschriftmaken.nl

rijksuniversiteit groningen

Single-Molecule FRET Reveals Transport Mechanism of ABC Transporters

Proefschrift

ter verkrijging van de graad van doctor aan de
Rijksuniversiteit Groningen
op gezag van de
Rector Magnificus prof. dr. C. Wijmenga
en volgens besluit van het College voor Promoties.

De openbare verdediging zal plaatsvinden op
vrijdag 22 November 2019 om 9.00 uur

door

Florence Agustin Husada
geboren op 1 Augustus 1990
te Bandung, Indonesia

Promotores

Prof. dr. T.M. Cordes

Prof. dr. B. Poolman

Beoordelingscommissie

Prof. dr. R. Ford

Prof. dr. K. Jung

Prof. dr. D.J. Slotboom

CONTENT

Chapter 1

Introduction

Florence A. Husada & Thorben Cordes (unpublished)

Abstract

The cell is the basic membrane-bound unit that contains the fundamental molecules of life, of which all living things are composed. The wall of the cell is something composed by, for example, peptide glycan layer which is not simply a passive barrier, but a major interface between the cell cytoplasm with the exterior. Exchanging essential compounds and wasteful molecules through the membrane requires transporters. Small molecules can potentially pass through the lipid bilayer wall by diffusion and osmosis mechanism, where molecules pass through the pores built by the phospholipid layer. However, the majority of deliverance is accomplished by variety of membrane-affiliated proteins. These proteins distinguish the nutrients to be taken, wasteful products to be excreted or directed between the inside and outside the cell. In this chapter, I introduce the basic features of the biological membrane, protein transporters, and the technique used to examine transport phenomenon. The thesis reveals dynamic information of substrate-binding and transport as well as overpasses the limitation of established structure determinations.

Introduction

Membrane transport

The cell represents the basic structural and functional unit of all living organisms. It is defined by a lipid membrane, which separates the interior from the extracellular space. The self-assembled membrane thus functions as a semi-permeable barrier that sustains life. It has the essential function of compartmenting molecules and it forms a hydrophobic barrier that is relatively impermeable to most (polar) substances. Since it is impermeable for hydrophilic molecules, transporters or chemically selective pores are required for both passive (diffusive) and active (energy-driven) transport processes. To accommodate the diversity of molecules to be acquired from the environment, a cell needs many different transport-systems [1]. These conduct various biochemical functions ranging from nutrient uptake [2], antibiotic and drug resistance [3], antigen presentation [4], cell-volume regulation [5,6] and many others.

In this thesis, I present novel approaches to understand mechanisms of primary-active transporters. The so-called ATP-binding cassette (ABC) transporters [7-11] can be exporters or importers and are involved in various cellular processes [7].

ABC transporters

ABC transporters are ATP-driven transporters mediating import or export of small and large molecules across the cell membrane. They are present in all organisms and represent one of the largest protein super-families with transmembrane spanning segments. ABC transporter stands for ATP-binding cassette transporter that have the ability to bind and hydrolyze ATP for active transport of substrates across the lipid bilayer [12,13]. ABC transporters are found in both prokaryotes and eukaryotes and an essential role for various biological processes [14,15], multidrug resistance [16,17], several human diseases [18]; they have been extensively characterized structurally as well as functionally [19-24]. Several ABC transporters have been crystallized in different conformations, which provide detailed insight in the transport mechanism.

These structural studies reveal that ABC transporters have a common molecular architecture. They consists of two transmembrane domains (TMDs) and two or more intracellular nucleotide ATP-binding domains (NBDs) [25], Figure 1.1. Based on the direction of the translocation, ABC transporters can be classified as exporters or importers. As importers, ABC transporters use an extracellular substrate-binding domain (SBD) to harvest nutrients and other relevant molecules. ABC exporters function without SBDs and excrete toxins, drugs and lipids across membranes [26]. ABC exporters bind their substrates directly within a binding pocket within the TMDs. It is speculated that the binding pocket is either accessible from the membrane or from the cytoplasm, depending on the specific system [27]. ABC transporters are present in organisms from all kingdoms of life. In particular, exporters are found in both eukaryotes and prokaryotes, while importers are specific to prokaryotic organisms [28]. Some

TMDs and NBDs in (bacterial) ABC exporters are fused to one another, resulting in one-, two-, three- or four-chain transporters, in which the order of the domains can vary [29]. For importers, the core TMD and NBD subunits are (often) individual chains, which assemble into homo- or hetero-dimeric TMDs that are bound to homodimeric NBDs [30].

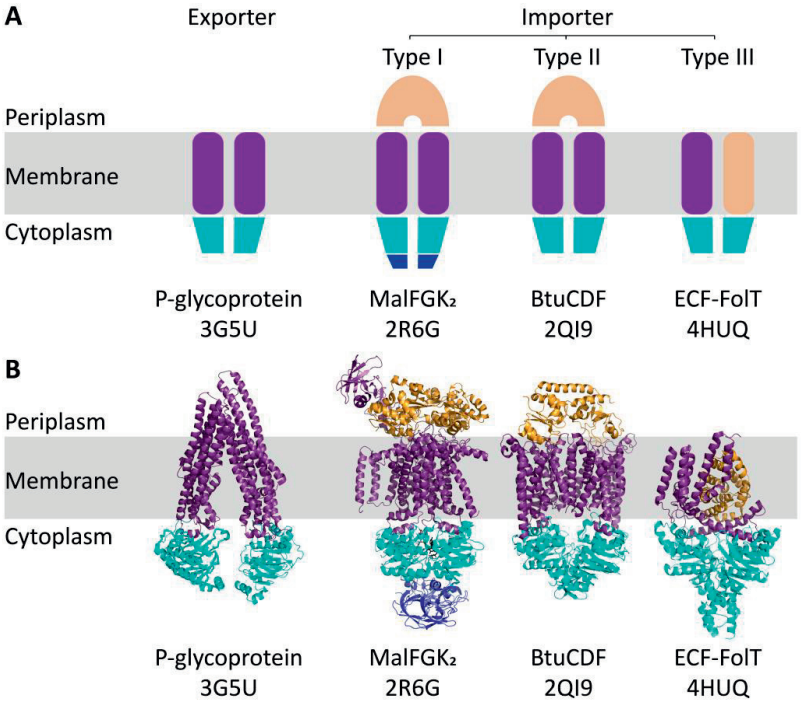

Figure 1.1 | Four distinct folds of ABC transporters in cartoon representation (**A**) and crystal structure (**B**). General architecture of NBDs (cyan), TMDs (purple), SBDs (yellow), and regulatory domains RD (blue, found in the Type I ABC importer $MalFGK_2$). In Type I ($MalFGK_2$) and II (BtuCDF) importers, the transported compounds are delivered to the TMDs by the SBDs, which are located in the periplasm (gram-negative bacteria) or extracellular space (gram-positive bacteria and archaea). In ECF, energy coupling factor (FolT), the SBD is membrane integrated. ABC exporter, e.g., P-glycoprotein, function as a extrusion system for toxins and xenobiotics.

ABC importers

Based on the overall topology and mechanism of transport, a classification of ABC transporters has been proposed [28]: Type I and Type II importers, and energy coupling factor (ECF) transporters (also named Type III importers) (**Figure 1.1**). All three types of ABC importers are found in prokaryotes. Type I and II ABC importers depend on additional soluble SBDs which specialize in distinct substrates [31] for delivery to the TMDs [32,33]. In some cases, the SBD is fused to the TMD into a multi domain protein [5]. ECF transporters do not use periplasmic

and thus soluble SBDs [34] but require an additional small integral membrane domain (S-component), which associates with one transmembrane coupling protein (T-component) [35] and functions as substrate-binding domain.

In general, the type I importers contain fewer and smaller transmembrane helices in comparison to Type II importers. In the absence of SBDs and ligand, type I transporters show negligible levels of ATPase activity; however, activity is stimulated by ligand-loaded SBDs [36,23]. The type I importer class includes the following well-characterized model systems: the maltose transporter $MalFGK_2$ [37,38], Figure 1.1, the methionine transporter MetNI [21] and the molybdate transporters ModBC [39]. In addition to the ABC core domains, some Type I importers feature a regulatory domain (RDattached to the highly conserved NBDs, which controls the function of these importers. These domains are poorly characterized model systems. Substrate or other regulatory proteins such as the glucose-specific enzyme $EIIA^{glc}$ (for the maltose permease[40]) and their binding to the RD controls the conformational states of the NBDs and thus ATP hydrolysis and substrate transport.

Another major difference between type II and type I importers is the differences in the size and overall architecture of the core transporters [22,23]. In general, the Type I importers contain fewer transmembrane helices in comparison with Type II. Type II transporters are generally larger, with the structurally characterized TMD homodimers having 20 TM helices (10 helices per monomer). The Type I importer MetNI has a minimal set of 5 TM helices from each TMD, which forms a homodimer totaling 10 helices [21]. The type II importer category includes: vitamin B12 transporter BtuCD [41-43], heme transporter HmuUV [44], and iron-siderophore transporter FhuD2 [45]. The effects of ligand on Type II complex formation are inverted in Type I transporters, which require nucleotide or substrate for complex formation [46].

The term energy-coupling factor (ECF) transporters was coined in the 1970s [47], and recently classified as a new type of ABC transporter [34,48]. Similar to Type I and II transporters, ECF transporters consist of two nucleotide-binding domains (EcfA and EcfA'), a transmembrane coupling domain (EcfT) and a substrate-binding component (EcfS). The S component is an integral membrane protein that provides substrate specificity to the ECF transporter [49,50]. The structural diversity of ECF transporters was revealed with the full-length structures of the folate [51] and the hydroxymethyl pyrimidine [51] transporters from *Lactobacillus brevis*.

The three different types of ABC importers have overlapping substrate specificities, and hence it is not clear why three different importer folds have evolved [30]. In general, the substrates of type I importers are compounds required in larger amounts, e.g., for metabolism, such as sugars and amino acids [8], whereas Type II importers and ECF transporters are required for transport of compounds such as metal chelates [28] and vitamins [41]. It might be speculated that type I ABC importers are thus more suitable for high capacity, low affinity transport, whereas Type II and ECF importers may better serve for low capacity, yet high affinity transport.

Mechanism of substrate or ligand binding

It is commonly accepted that substrate binding via the extracellular domains of an importer is the initial step of transport. Based on the available crystal structure, the responsible SBDs can exist in several conformations: open-unliganded (O), closed-unliganded (C), open-liganded (OL), closed-liganded (CL) forms and potentially also in intermediate conformations such as partially closed (PC), Figure 1.2. The investigation of different structural states is a way to gain insight into the mechanism of substrate binding by SBDs.

The most simple binding model is the 'lock-and-key' [52], which was introduced by Emil Fischer in 1894. Here both partners, i.e,. protein and ligand, are either rigid or have an binding-compatible conformation. Since crystal structures of SBDs suggest the existence of distinct conformational states of SBDs, the lock-and-key seems to be the most unlikely option. Newer models take conformational plasticity of SBDs into account: the 'induced fit' [53] and 'conformational selection' model [54]. In the induced-fit model, conformational changes occur as a result of substrate binding, which drives the protein from its apo open conformation to a new closed-liganded conformation (**Figure 1.2**). In contrast, the conformational selection model involves fast dynamic transitions from open to semi-closed or closed without the involvement of a substrate. Substrate binding further stabilizes the closed state and therefore shifts the equilibrium of the system towards the closed form [55] (**Figure 1.2**). Also combinations of both mechanisms have been suggested [56].

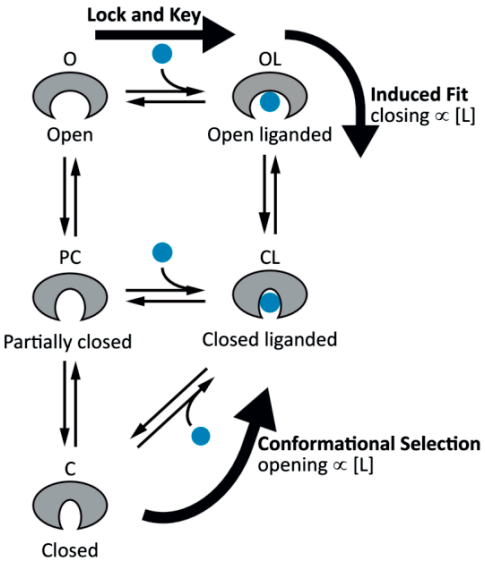

Figure 1.2 | Illustration of conformational states of SBDs and possible binding mechanisms. Lock and key models have an exactly complementary unbound (O) and unbound (OL) conformation. Conformational selection dictates the unbound protein (O) to have a fast dynamics transition to form partially (PC) or fully closed state (C) without the participation of substrate (CL). With the induced-fit model, the bound like conformation state (CL) is formed after interaction with a substrate that induces structural changes of the unbound state (O).

Experimentally, in the case of an induced fit binding mechanism, the closing rate from open to closed state should increase with the substrate concentration. On the contrary, in the conformational selection model, it is the life-time of the closed state that increases with the substrate concentration (assuming that the lifetime of the closed-liganded and close-unliganded cannot be distinguished with the respective technique). Since structural fluctuations can be fast, i.e., on the millisecond and microsecond timescale, it is almost impossible to discriminate between both mechanisms using ensemble structure determination, because these provide only static snapshots of the most stabile conformations. However, discrimination of both mechanisms is possible by employing single-molecule techniques. Single-molecules Förster resonance energy transfer (smFRET) studies on the maltose-binding protein (MalE) [57,58] and glutamine transporter (GlnPQ) [59] have shown that these transporters follow the induced fit mechanism to bind their substrate, unless fluctuations occur on timescales < milliseconds.

Mechanism of transport in ABC importers

The structural diversity among ABC transporters suggests differences in the transport mechanism. Comparison of Type I and II ABC importers show that Type I proteins undergo wide rigid body movements, whereas conformational changes in Type II are restricted to movements of helices and loops in the trans-membrane domains. Regardless of the difference in overall architecture of the core transporters, all type transporters use an alternating access mechanism in which the transporter cycles between inward- and outward- facing conformations, where the translocation pathway and substrate-binding site is exposed to either side of the membrane at any given time

The maltose transporter, $MalFGK_2$ is often referred to as the best characterized system. Here, initiation of the transport occurs by binding of the substrate to substrate-binding protein, MalE (**Figure 1.3 A**, State 1). The substrate-loaded closed MalE binds to inward-facing conformation of transporter (Figure 1.3 A, State 2). In the consensus model, the closed state of MalE triggers a conformational change in $MalFGK_2$ inducing partial closure of MalK dimer (Figure 1.3 A, State 3). Binding of two ATP molecules to the NBD dimer brings the NBDs subunits together as observed in nucleotide-bound MalFGK, resulting in an outward-facing conformation of the transporter (Figure 1.3 A, State 4) [26]. Type I importer structures allowed to indirectly infer the substrate transport mechanism: the open NBDs couple the TMDs to with the inward-facing conformation and the outward-facing conformation of importers can be induced by binding of ATP to the NBDs, resulting in the closed NBD dimer. The alternation between these two conformations allows movement of substrate across the membrane. [26]. Additionally, the regulatory domain of the maltose transporter controls maltodextrin import by MalT and EIIA [60]. This interaction inhibits transport by preventing the closure of the MalK dimer and stabilizing MalFGK in the inward-facing resting state (**Figure 1.3 A, State 5**).

As in Type I ABC transporters, the substrate specificity in Type II transporters is regulated by the substrate-binding protein. The transport mechanism, however, is distinct. This starts with the idea that the TMDs/NBDs of Type II ABC importers are in the outward-facing conformation as the resting conformation (**Figure 1.3 B, State 1**) [46]. The translocation pathway of Type II transporter has been described in great detail for the vitamin B12 transporter, BtuCDF [41]. Again different static conformations of the transporter provide information on the accessibility of the translocation pathway. The mechanism can be described via four states. In the resting state, the translocation pathway is in an outward-facing conformation. It is assumed that the majority of a BtuCD transporter population can be found in the ADP-bound state (**Figure 1.3 B**, State 1; commonly known as the post-hydrolysis state) [43]. Substrate loaded BtuF then binds to BtuCD, delivering substrate to the outward-facing translocation pathway via opening of the trans-membrane domain BtuCD (**Figure 1.3 B**, State 2) [60]. When BtuCD-F binds nucleotide (Figure 1.4 B, State 3), the NBDs close, pulling the transmembrane-helices closer together. This triggers the closing of the periplasmic gate and the opening of the cytoplasmic gate, and thus traps substrate in a large translocation chamber (**Figure 1.3 B**, State 3) [42]. When ATP is hydrolyzed, the NBDs separate, phosphate and ADP depart, and the cytoplasmic gate opens and the translocation chamber collapses with the transmembrane helices squeezing vitamin B12 into the cytoplasm [61,62]. After the departure of substrate, BtuCD-F is in a stable, occluded conformation (**Figure 1.3 B**, State 4) [42], which subsequently returns to the resting state.

Energy-coupling factor (ECF) transporters were recently classified as a new type (III) of ABC transporter [34]. The Crystal structure of the liganded S components in combination with molecular dynamic simulations show that the substrate-binding site is located near the extracellular surface of the proteins, in which the binding site is occluded from the periplasmic side (**Figure 1.3 C**) [49]. The crystal structure of the complete ECF transporter reveals an unusual orientation of the S component, which is lying almost parallel to the plane of the membrane. It has been then proposed that the substrate loaded S component undergoes a major rigid-body movement around an axis in the plane of the membrane [48]. Conformational changes of the ATPase dimer are then transmitted to the TMD and S-component for transport [50]. The cytoplasmic α-helixes loop in the S-component forms a link between substrate-binding site (**Figure 1.3 C**, State 1) and the N-terminal domain that interacts with the ECF in the ECF module (**Figure 1.3 C**, State 3); this structural transition is induced by ATP binding and hydrolysis (**Figure 1.3 C**, State 2) before substrate binding and release from the S-component (**Figure 1.3 C**, State 4) [63].

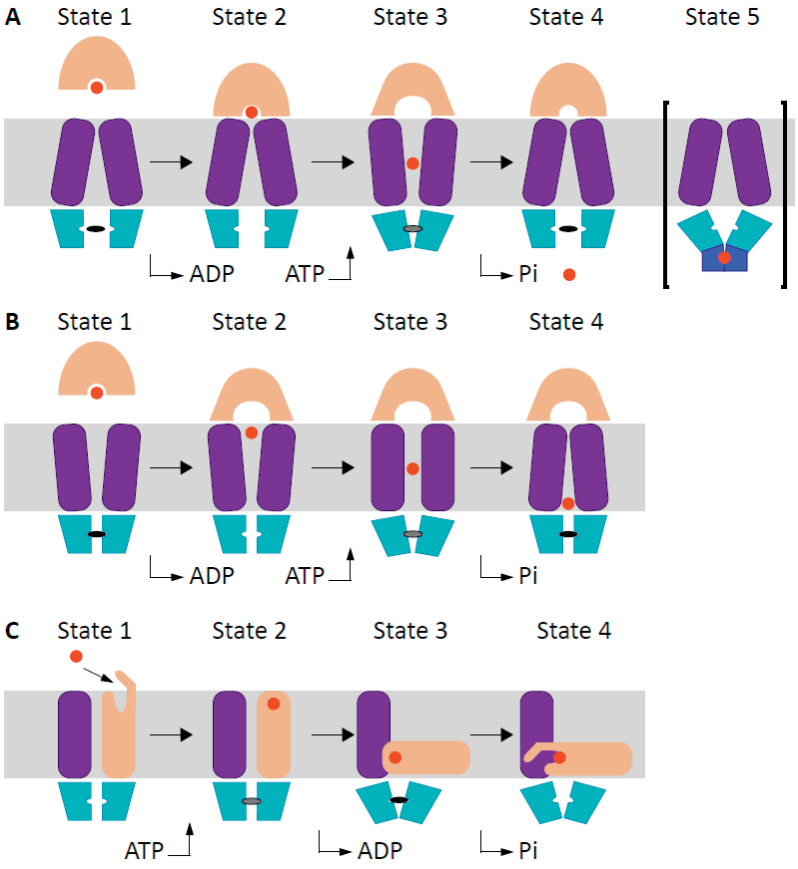

Figure 1.3 | Cartoon sketch of transport mechanisms of ABC importers. TMD are colored purple, NBD cyan, SBD yellow, and the substrate is represented by orange sphere. ATP and ADP are shown as a grey and black sphere, respectively. **A.** Mechanism of Type I transporter, $MalFGK_2$. **B.** Mechanisms of Type II transporter, BtuCDF. **C.** Mechanisms of Type III transporter, FolT.

ABC exporters

The fourth distinct fold of ABC transporters is found in exporters (Figure 1.1). ABC transporters with the exporter fold are present in both prokaryotes and eukaryotes. In all structurally-characterized ABC exporters, the NBDs are directly linked to the TMDs and form one polypeptide chain. ABC exporters thus bind their substrates directly within the TMDs. ABC exporters form a large superfamily of transmembrane proteins responsible for transport of a large diversity of substrates. Some ABC exporters are involved in multidrug resistance [64]. Bacterial ABC exporters are dimers, with each monomer composed of a transmembrane domain (TMD), which forms the translocation pathway across the membrane bilayer and ensures the substrate specificity, and a nucleotide-binding domain (NBD) where binding and hydrolysis of ATP take place [64].

The first high-resolution structure reported for an ABC exporter is the multidrug transporter Sav1866 from *Staphylococcus aureus* [64]. In humans, ABC exporters are crucial participants in lipid, fatty-acid and cholesterol export, their malfunction underlies various diseases [65].

Independent of their function as importers or exporters, all ABC transporters share mechanistic similarities. For both exporters and importers, an alternating access model for transport has been suggested as also described in reference 66. The key feature is the presence of a substrate binding site that can be accessed either via the extracellular- or the intracellular side of the membrane, corresponding to the "outward" and "inward" facing conformations of the transporter, respectively [67] (**Figure 1.4**). The transport event requires ATP binding and hydrolysis to drive the necessary conformational changes, which result in the alternating exposure of the substrate binding site to the two sides of the membrane [68]. There is evidence that the outward facing conformation of an importer is expected to have a higher affinity for substrates than the inward facing conformation, while the opposite relationship will hold for exporters [25].

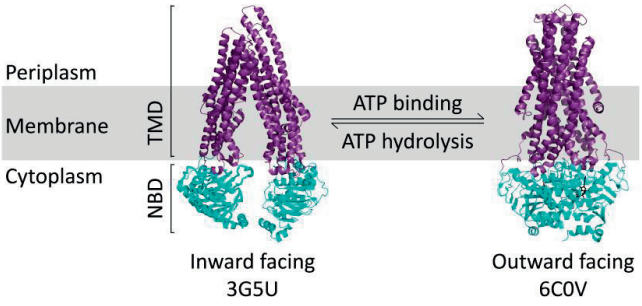

Figure 1.4 | Structural changes in ABC exporters exemplified by crystal structures of P-glycoprotein. The transmembrane domains (purple) and nucleotide-binding domains (cyan) are expressed as a single polypeptide, which associates to form a single large polypeptide with length 170-180 kDa [69]. P-glycoprotein was crystallized in the presence of substrate. In the absence of nucleotide, it adopts an inward facing conformation with the nucleotide-binding domains spread apart (left). In the presence of ATP, the outward facing conformation is adopted (right), where the two nucleotide-binding domain in tightly bound.

Mechanism of transport mechanism in ABC exporters

The transport mechanism of ABC exporters is considered simpler than that of importers because the lack of substrate-binding domains. In an ATP-free (open apo) state, the protein is believed to adopt an inward facing conformation, where the two NBDs are separated and, consequently, the TMDs are open to the cytoplasmic side (**Figure 1.4,** left). Upon the binding of two ATP molecules, the NBDs dimerize, which pushes the coupling helices towards each other; consequently, the TMDs convert into an outward-facing conformation (**Figure 1.4**, right). Upon ATP-hydrolysis, the transporter returns to its inward-facing resting state for the next transport-cycle: the NBD dimer opens, consequently pulling the coupling-helices outward, causing the conversion to an inward-facing conformation. The first half of the

process is thought to be driven by ATP binding and the second half by ATP hydrolysis. However, there is much less understanding of the mechanism by which the energy of ATP is converted into the mechanical motions of the protein or, in other words, the mechanism of chemo-mechanical coupling [67].

Single-molecule techniques for mechanistic studies of ABC transporters

Mechanistic understanding of transport processes requires methods to analyze structures and states but also conformational dynamics of biomacromolecules at room temperature under physiologically relevant conditions. Single-molecule Förster resonance energy transfer (smFRET) has evolved to a versatile tool for exactly this, i.e., the observation of intra- and intermolecular conformational dynamics and interactions of transporter domains [70-73].

In smFRET, energy is transferred from a light-absorbing and emitting donor molecule D to an acceptor A via non-radiative dipole-coupling, with a transfer efficiency E depending on the inverse-sixth-power of the distance R between the donor and acceptor: $E = 1/(1+[R/R_0]^6)$. Here R_0 is the distance at which 50% of the energy is transferred from D to A. The dynamic range of FRET is 3-8 nm which is ideally suitable for use as a molecular ruler. The ability to determine FRET efficiency using a single D/A-pair allows for the study of time-dependent phenomena such as protein- and molecular conformational changes, **Figure 1.5** [74]. To readout conformational states of e.g. SBDs, the protein is labelled at strategic positions that display large distance changes upon conformational transitions.

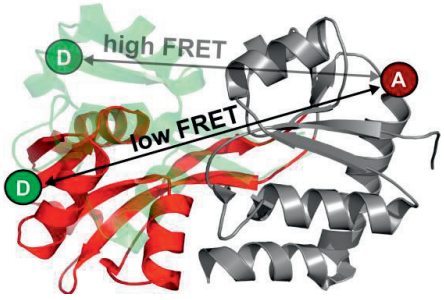

Figure 1.5 | Förster resonance energy transfer assay for monitoring SBD conformational states. Crystal structure of the open ligand-free state of SBD2 of GlnPQ (gray-red, PDB 4KR5 [59]), superimposed onto the structure of one of the rigid domains of the closed ligand-bound state (gray-green, PDB 4KQP). Residues mutated to cysteine for labelling are with D/A. Low FRET efficiency a larger distance between the labelled residues compared to the liganded-closed state.

Thesis outline

This thesis focuses on single-molecule studies of both substrate-binding proteins of ABC importers and ABC exporters via smFRET in order to answer relevant mechanistic questions.

Chapter 1 (this chapter) provides a short yet concise overview on the structures and transport mechanisms of ABC transporters. The focus is to link the information from structural and biochemical studies of ABC transporter to the single-molecule FRET approach.

Chapter 2 introduces protein labelling strategies for fluorescent dyes. This enables smFRET investigations of conformational states and transitions of GlnPQ-SBD1/2, permitting a direct correlation of structural and kinetic information of SBDs. Since information in such assays are restricted by proper labelling of proteins with fluorescent dyes, I present a simple approach to increase the amount of protein with FRET information based on non-specific interactions between a dye and the size-exclusion chromatography (SEC) column material used for protein purification.

Chapter 3 describes the mechanistic studies on the conformational dynamics of the ABC importer GlnPQ from *Lactococcus lactis*. This transporter has different covalently-linked substrate-binding domains (SBDs), thus making it an excellent model system to elucidate the dynamics and role of the SBDs in transport. I demonstrate by single-molecule spectroscopy that the two SBDs intrinsically transit from open to closed ligand-free conformation, and the proteins capture their amino acid ligands via an induced-fit mechanism. High-affinity ligands elicit transitions without changing the closed-state lifetime, whereas low-affinity ligands dramatically shorten it. We show that SBDs in the closed state compete for docking onto the translocator, but remarkably the effect is strongest without ligand. We find that the rate-determining steps depend on the SBD and the amino acid transported. We conclude that the lifetime of the closed conformation controls both SBD docking to the translocator and substrate release.

Chapter 4 provides one of the first smFRET studies on ABC exporters. In this chapter, we analyzed the conformational states and dynamics of the antibacterial peptide exporter McjD from *E. coli* in proteoliposomes. I established smFRET for an ABC transporter in a native-like lipid environment and directly monitored conformational dynamics in both the transmembrane- (TMD) and nucleotide-binding domains (NBD). With this I unravel the ligand-dependencies that drive conformational changes in both domains, i.e., ATP alone controls the NBDs while both ATP and ligand influence the TMD conformational state. Furthermore, we observe intrinsic conformational dynamics in the absence of ATP and ligand in the NBDs on a sub-second timescale, but nearly static TMDs. ATP-binding and hydrolysis on the other hand are slower and can be observed via NBD conformational dynamics on the timescale of several seconds – a value compatible with reported biochemical data.

Publication reported in Scientific Report (2016) 18(6), 33257 describes the possible applications of FRET in studies with diffusing and immobilized molecules, indicating the full

potential of the technique for mechanistic investigations of biomolecular interactions and transport studies. The technique provides a solution to overcome the limitations of FRETs such as their restricted distance ranges and the need for labelling with fluorescent dyes. It allows observing changes in biochemical structure and interactions by following two distances and thus reaction coordinates on two different distance ranges.

Publication reported in eLife Sciences (2019) (8), 44652 facilitates the funding of conformational changes occurring on the OppA and FeuA upon substrate binding detected by using single-molecule approach. The results indicate that OppA and FeuA undergo conformational changes in the presence of substrate as observed by two distinct FRET state (open and closed state) via induced-fit mechanisms.

References

1. Bryan, J., A. Muñoz, X., Zhang, M., Düfer, G., Drews, P., Krippeit-Drews, L., Aguilar, B. (2007) ABCC8 and ABCC9: ABC transporters that regulate K^+ channels. *Pflugers. Arch.* 453,703–718
2. Schuurman-Wolters, G.K., Poolman, B. (2005) Substrate specificity and ionic regulation of GlnPQ from *Lactoccoccus lactis* an ATP-binding cassette tranporter with four extracytoplasmic substrate-binding domains. *J. Biol. Chem.* 280, 23785 – 23790
3. Sharom, F.J. (2008) ABC multidrug transporters: structure, function and role in chemo resistance. Pharmacogenomics. 9, 105 – 127
4. Abele, R., Tampe,R. (2004) The ABCs of immunology: structure and function of TAP, the transporter associated with antigen processing. *Physiology* (Bethesda). 19, 216 – 224
5. Biemans-Oldehinkel, E., Doeven, M.K., Poolman, B. (2006) ABC transporter architecture and regulatory roles of accessory domains. *FEBS Lett.* 580, 1023–1035
6. Biemans-Oldehinkel, E., Mahmood, N.A., Poolman, B.(2006) A sensor for intracellular ionic strength. *Proc. Natl. Acad. Sci. USA.* 103, 10624 – 10629
7. Oldenhinkel, E.B., Doeven, M.K., Poolman, B. (2006) ABC transporter architecture and regulatory roles of accessory domain. *FEBS Letters*. 580, 1023–1035
8. Davidson, A.L., Chen, J. (2004) ATP-binding cassette transporters in bacteria. *Annu. Rev. Biochem.* 73, 241–268
9. Detmers, F.J.M., Lanfermeijer, F.C., Poolman, B. (2000) Peptides and ATP binding cassette peptide transporters. *Res. Microbiol.* 152, 245–258
10. Hollenstein, K., Frei, D.C., Locher, K.P. (2007) Structure of an ABC transporter in complex with its binding protein. *Nat. Letters*. 446, 213–216
11. Akyuz, N., Georgieve, E.R., Zhou, Z., Stolzenberg, S., Cuendet, M.A., Khelashvili, G., Altman, R.B., Terry, D.S., Freed, J.H., Weinstein, H., Boudker, O., Blanchard, S.C. (2015) Transport domain unlocking sets the uptake rate of an aspartate transporter. *Nature*. 518, 68–73
12. Higgins, C.F. (1992). ABC transporters: from microorganisms to man. *Annu. Rev. Cell. Biol*. 8, 67–113
13. Higgins, C.F., Hiles, I.D., Salmond, G.P., Gill, D.R., Downie, J.A., Evans I.J., Holland, I.B., Gray, L., Buckel, S.D., Bell, A.W. (1986). A family of related ATP-binding subunits coupled to many distinct biological processes in bacteria. *Nature.* 323, 448–450
14. Dean, M., Hamon, Y., Chimini, G. (2001). The human ATP-binding cassette (ABC) transporter superfamily. *J. Lipid Res.* 42, 1007–1017

15. Kjelleberg, S., Albertson, N., Flärdh, K., Holmquist, L., Jouper-Jaan, A., Marouga, R., Ostling, J., Svenblad, B., Weichart, D. (1993). How do no differentiating bacteria adapt to starvation? *Antonie. Van. Leeuwenhoek.* 63, 333–341

16. Kerr, I.D., Jones, P.M., George, A.M. (2010). Multidrug efflux pumps: the structures of prokaryotic ATP-binding cassette transporter efflux pumps and implications for our understanding of eukaryotic P-glycoproteins and homologues. *FEBS J.* 277, 550–563

17. Seeger, M.A., Van Veen, H.W. (2009). Molecular basis of multidrug transport by ABC transporters. *Biochim. Biophys. Acta.* 1794, 725–737

18. Fletcher, J.I., Haber, M., Henderson, M.J., Norris, M.D. (2010). ABC transporters in cancer: more than just drug efflux pumps. *Nat. Rev. Cancer.* 10, 147–156

19. Al-Shawi, M.K. (2011). Catalytic and transport cycles of ABC exporters. *Essays. Biochem.* 50, 63–83

20. Goetz, B.A., Perozo, E., Locher, K.P. (2009). Distinct gate conformations of the ABC transporter BtuCD revealed by electron spin resonance spectroscopy and chemical cross-linking. *FEBS Lett.* 583, 266–270

21. Kadaba, N.S., Kaiser, J.T., Johnson, E., Rees, D.C. (2008). The high-affinity E. coli methionine ABC transporter: structure and allosteric regulation. *Science*. 321, 250–253

22. Locher, K.P. (2009). Structure and mechanism of ATP-binding cassette transporters. *Phil. Trans. R. Soc. B. Biol. Sci.* 364, 239–245

23. Oldham, M.L., Davidson, A.L., Chen, J. (2008). Structural insights into ABC transporter mechanism. *Curr. Opin. Struct. Biol.* 18, 726–733

24. Schneider, E., Hunke, S. (1998). ATP-binding-cassette (ABC) transport systems: functional and structural aspects of the ATP-hydrolyzing subunits/domains. *FEMS Microbiol. Rev.* 22, 1–20

25. Rees, D.C., Johnson, E., Lewinson, O. (2009) ABC transporters: the power to change. *Nat. Rev. Mol. Cell Biol*. 10, 218–227

26. Eitinger, T., Rodionov, D.A., Grote, M., Schneider, E. (2011). Canonical and ECF-type ATP-binding cassette importers in prokaryotes: diversity in modular organization and cellular functions. *FEMS Microbiol. Rev.* 35, 3–67

27. van Veen, H.W., Venema, K., Bolhuis, H., Oussenko, I., Kok, J., Poolman, B., Driessen, A.J., Konings, W.N. (1996) Multidrug resistance mediated by a bacterial homolog of the human multidrug transporter MDR1. *Proc. Natl. Acad. Sci. USA.* 93(20), 10668–10672

28. Beek, J.T., Guskov, A., Slotboom, D.J. (2014) Structural diversity of ABC transporters. *J. Gen. Physiol.* 143(4), 419–435

29. Rice, A.J., Aekyung, P., Pinkett, H.W. (2014) Diversity in ABC transporters : Type I, II and III importers. *Crit. Rev. Biochem. Mol. Biol*. 49(5), 426–437

30. Igarashi, Y., Aoki, K.F., Mamitsuka, H., Kuma, K., Kanehisa, M. (2004) The evolutionary repertoires of the eukaryotic-type ABC transporters in terms of the phylogeny of ATP-binding domains in eukaryotes and prokaryotes. *Mol. Biol. Evol*. 21, 2149–2160

31. van der Heide. T., Poolman, B. (2002) ABC transporters: one, two or four extracytoplasmic substrate-binding sites? *EMBO Reports.* 3(10), 938–943

32. Berntsson, R.P.A., Smits, S.H.J., Schmitt, L., Slotboom, D.J., Poolman, B. (2010) A structural classification of substrate-binding proteins. *FEBS Lett.* 584, 2606–2617

33. Quiocho, F.A., Ledvina, P.S. (1996) Atomic structure and specificity of bacterial periplasmic receptors for active transport and chemotaxis: variation of common themes. *Mol. Microbiol.* 20, 17–25

34. Rodionov, D.A., Hebbeln, P., Eudes, A., ter Beek, J., Rodionova, I.A., Erkens, G.B., Slotboom, D.J., Gelfand, M.S., Osterman, A.L., Hanson, A.D., Eitinger, T. (2009) A novel class of modular transporters for vitamins in prokaryotes. *J. Bacteriol.* 191, 42–51

35. Slotboom, D.J. (2014) Structural and mechanistic insights into prokaryotic energy-coupling factor transporters. *Nat. Rev. Microbiol.* 12, 79–87

36. Davidson, A.L., Dassa, E., Orelle, C., Chen, J. (2008) Structure, function, and evolution of bacterial ATP-binding cassette systems. *Microbiol. Mol. Biol. Rev.* 72, 317–64

37. Bao, H., Duong, F. (2012) Discovery of an auto-regulation mechanism for the maltose ABC transporter $MalFGK_2$. *PLoS. One.* 7, 34836

38. Khare, D., Oldham, M.L., Orelle, C., Davidson, A.L., Chen, J. (2009) Alternating access in maltose transporter mediated by rigid-body rotations. *Mol. Cell*. 33, 528–536

39. Gerber, S., Comellas-Bigler, M., Goetz, B.A., Locher, K.P. (2008) Structural basis of trans-inhibition in a molybdate/tungstate ABC transporter. *Science*. 321, 246–250

40. Dean, D.A., Reizer, J., Nikaido, H., Saier, M.H. (1990) Regulation of the maltose transport system of *Escherichia coli* by the glucose-specific enzyme III of the phosphoenolpyruvate-sugar phosphotransferase system. Characterization of inducer exclusion-resistant mutants and reconstitution of inducer exclusion in proteoliposomes. *J. Biol. Chem.* 265, 21005 – 21010

41. Locher, K.P., Lee, A.T., Rees, D.C. (2002) The *E. coli* BtuCD structure: A framework for ABC transporter architecture and mechanism. *Science*. 296, 1091–1098

42. Korkhov, V.M., Mireku, S.A., Hvorup, R.N., Locher, K.P. (2012) Asymmetric states of vitamin B_{12} transporter BtuCD are not discriminated by its cognate substrate-binding protein BtuF. *FEBS Lett.* 586, 972–976

43. Lewinson, O., Lee, A.T., Locher, K.P., Rees, D.C. (2010) A distinct mechanism for the ABC transporter BtuCD-BtuF revealed by the dynamics of complex formation. *Nat. Struct. Mol. Biol.* 17, 332–338

44. Woo, J.S., Zeltina, A., Goetz, B.A., Locher, K.P. (2012) X-ray structure of the *Yersinia pestis* heme transporter HmuUV. *Nat. Struct. Mol. Biol.* 19, 1310–1315

45. Sebulsky, M.T., Shilton, B.H., Speziali, C.D., Heinrichs, D.E. (2003) The role of FhuD2 in iron(III)-hydroxamate transport in *Staphylococcus aureus*. Demonstration that FhuD2 binds iron(III)-hydroxamates but with minimal conformational change and implication of mutations on transport. *J. Biol. Chem*. 278, 49.890–49.900

46. Vigonsky, E., Ovcharenko, E., Lewinson, O. (2013) Two molybdate/ tungstate ABC transporters that interact very differently with their substrate-binding proteins. *Proc. Natl. Acad. Sci. USA* 110, 5440–5445

47. Henderson, G.B., Zevely, E.M., Huennekens, F.M. (1979) Mechanism of folate transport in *Lactobacillus casei*: evidence for a component shared with the thiamine and biotin transport systems. *J. Bacteriol.* 137, 1308–1314

48. Karpowich, N.K., Wang, D.N. (2013) Assembly and mechanism of a group II ECF transporter. *Proc. Natl. Acad. Sci. USA.* 110(7), 2534–2539

49. Erkens, G.B., Berntsson, R.P.A., Fulyani, F., Majsnerowska, M., Vujicic-Žagar, A., Beek, J.T., Poolman, B., Slotboom. D.J. (2011) The structural basis of modularity in ECF-type ABC transporters. *Nat. Struct. Mol. Biol.* 18, 755–760

50. Zhang, P., Wang, J., Shi, Y. (2010) Structure and mechanism of the S component of a bacterial ECF transporter. *Nature*. 468, 717–720

51. Wang, T., Fu, G., Pan, X., Wu, J., Gong, X., Wang, J., Shi, Y. (2013) Structure of a bacterial energy-coupling factor transporter. *Nature*. 497, 272–276

52. Lauria, A., Tutone, M., Almerico, A.M. (2011) Virtual lock-and-key approach: the in silico revival of Fishcer model by means of molecular descriptors. *Eur. J. Med. Chem.* 46(9), 4274–4280

53. Koshland, D.E. (1958) Application of a theory of enzyme specificity to protein synthesis. *Proc. Natl. Acad. Sci. USA.* 44, 98–104

54. Boehr, D.D., Nussinov, R., Wright, P.E. (2009) The role of dynamic conformational ensembles in biomolecular recognition. *Nat. Chem. Biol.* 5(11), 789–796

55. Csermely, P., Palotai, R., Nussinov, R. (2010) Induced fit, conformational selection and independent dynamic segments: an extended view of binding events. *Trends. Biochem. Sci.* 35(10), 539–546

56. Clore, G.M. (2014) Interplay between conformational selection and induced fit in multidomain protein-ligand binding probed by paramagnetic relaxation enhancement. *Biophys. Chem.* 186, 3–12

57. Seo, M.H., Park, J.B., Kim, E.K., Hohng, S.C., Kim, H.S. (2014) Protein conformational dynamics dictate the binding affinity for a ligand. *Nat. Comms.* 5, 3724

58. Kim, E.K., Lee, S.H., Jeon, A., Choi, J.M., Lee, H.S., Hohng, S.C., Kim, H.S. (2013) A single-molecule dissection of ligand binding to a protein with intrinsic dynamics. 9, 313–318

59. Gouridis, G., Schuurman-Wolters, G.K., Ploetz, E., Husada, F., Vietrov, R., de Boer, M., Cordes, T., Poolman, B. (2015) Conformational dynamics in substrate-binding domains influences transport in the ABC importer GlnPQ. *Nat. Struct. Mol. Biol.* 22, 57–64

60. Boos, W., Shuman, H. (1998) Maltose/maltodextrin system of *Escherichia coli*: transport, metabolism, and regulation. *Microbiol. Mol. Biol. Rev.* 62, 204–229

61. Borths, E.L., Poolman, B., Hvorup, R.N., Locher, K.P., Rees, D.C. (2005) In vitro functional characterization of BtuCD-F, the Escherichia coli ABC transporter for vitamin B_{12} uptake. *Biochemistry.* 44, 16301–16309

62. Joseph, B., Korkhov, V.M., Yulikov, M., Jeschke, G., Bordignon, E. (2014) Conformational cycle of the vitamin B_{12} ABC importer in liposomes detected by double electron-electron resonance (DEER). *J. Biol. Chem.* 289, 3176–3185

63. Berntsson, R.P., ter Beek, J., Majsnerowska, M., Duurkens, R.H., Puri, P., Poolman, B., Slotboom, D.J. (2012) Structural divergence of paralogous S components from ECF-type ABC transporters. *Proc. Natl. Acad. Sci. USA*. 28; 109(35), 13990–13995

64. Choudhury, H.G., Tong, Z., Mathavan, I., Li, Y.Y., Iwata, S., Zirah, S., Rebuffat, S., van Veen, H.W., Beis, K. (2014) Structure of an antibacterial peptide ATP-binding cassette transporter in a novel outward occluded state. *PNAS*. 111(25), 9145–9150

65. Ambudkar, S.V., Kimchi-Sarfaty, C., Sauna, Z.E., Gottesman, M.M. (2003) P-glycoprotein: from genomics to mechanism. *Oncogene*. 22, 7468–7485

66. Dawson, R.J.P., Hollenstein, K., Locher, K.P. (2007) Uptake or extrusion: crystal structures of full ABC transporters suggest a common mechanism. *Mol. Micro.* 65, 250–257

67. Arai, N., Furuta, T., Sakurai, M. (2017) Analysis of an ATP-induced conformational transition of ABC transporter MsbA using a coarse-grained model. *Jstage. Jst. Go. Jp.* 14, 161–171

68. Jardetsky, O. (1966) Simple allosteric model for membrane pumps. *Nature*. 211, 969–970

69. Al-Shawi, M.K., Omote, H. (2005). The Remarkable Transport Mechanism of P-glycoprotein; a Multidrug Transporter. *J .Bioenerg. Biomembr.* 37(6), 489 – 496

70. Kalinin, S., Peulen, T., Sindbert, S., Rothwell, P.J., Berger, S., Restle, T., Goody, R.S., Gohlke, H., Seidel, C.A. (2012) Toolkit and benchmark study for FRET-restrained high-precision structural modeling. *Nat. Methods.* 9, 1218–1225

71. Chung, H.S., McHale, K., Louis, J.M., Eaton, W.A. (2012) Single-molecule fluorescence experiments determine protein folding transition path times. *Science.* 335, 981–984

72. Schuler, B., Hofmann, H. (2013) Single-molecule spectroscopy of protein folding dynamics-expanding scope and timescales. *Curr. Opin. Chem. Biol.* 23, 36–47

73. Tsukanov, R., Tomov, T.E., Berger, Y., Liver, M., Nir, E. (2013) Conformational dynamics of DNA hairpins at millisecond resolution obtained from analysis of single-molecule FRET histograms. *J. Phys. Chem. Bio*. 117(50), 16105–16109

74. Ha, T., Enderle, T.H., Ogletree, D.F., Chemla, D.S., Selvin, P.R., Weiss, S. (1996) Probing the interaction between two single molecules: Fluorescence resonance energy transfer between a single donor and a single acceptor. *Proc. Natl. Acad. Sci. USA.* 93,6264–6268

Chapter 2

Watching conformational dynamics of ABC transporters with single-molecule tools

Florence Husada[1], Giorgos Gouridis[1,2], Ruslan Vietrov[2], Gea K. Schuurman-Wolters[2], Evelyn Ploetz[1], Marijn de Boer[1], Bert Poolman[2] and Thorben Cordes[1]

Biochemical Society Transaction. 2015 October 9. 43, 1041–1047
DOI: 10.1042/BST20150140

[1] Molecular Microscopy Research Group & Single-molecule Biophysics, Zernike Institute for Advanced Materials, University of Groningen, Nijenborgh 4, 9747 AG Groningen, The Netherlands

[2] Membrane Enzymology Research Group, Groningen Biomolecular Science and Biotechnology Institute, Netherlands Proteomics Centre & Zernike Institute for Advanced Materials, University of Groningen, Nijenborgh 4, 9747 AG Groningen, The Netherlands

Abstract

ATP-binding cassette (ABC) transporters play crucial roles in cellular processes, such as nutrient uptake, drug resistance, cell-volume regulation and others. Recent findings show that transport is initiated by binding of ligand in the substrate-binding domain. Despite their importance in transporting the substrate across the membrane, all proposed molecular models for either transport or binding are based on indirect evidence, for example interpretation of static crystal structures and ensemble measurements of function. Thus, classical biophysical and biochemical techniques do not readily visualize dynamic structural changes. The conformational states and transitions of ABC-associated substrate-binding domains (SBDs) are visualized with single-molecule FRET, permitting a direct correlation of structural and kinetic information of SBDs. We also delineated the different steps of the transport cycle. Since information in such assays are restricted by proper labelling of proteins with fluorescent dyes, we present a simple approach to increase the amount of protein with FRET information based on non-specific interactions between a dye and the size-exclusion chromatography (SEC) column material used for final purification.

Key words: ABC importer, transport mechanism, SBD, GlnPQ, fluorophore labelling, FRET, single-molecule studies.

Abbreviations: ABC, ATP-binding cassette; NBD, nucleotide binding domain; TMD, transmembrane domain; SBD, substrate binding domain; ALEX, alternating laser excitation; ATP, adenosine triphosphate; DA, donor-acceptor; FRET, Förster resonance energy transfer; SEC, size-exclusion chromatography; smFRET, single-molecule FRET.

Introduction

In prokaryotic ATP-binding cassette (ABC) importers [1–3], substrate-binding proteins or domains (SBDs) [4,5] are used to capture amino acids, sugars [6], vitamins [7], metals [8], peptides [9] and various other ligands before their uphill transport via the core of the ABC transporter: the dimeric transmembrane domain (TMD) and nucleotide binding domain (NBD) [10,11]. Although the molecular model for ligand binding in ABC-related SBDs is still under debate, the consequences of the binding model for transport remains largely elusive [6,12–15]. A key question is which of the conformational states of the SBD interacts with the TMD and leads to a productive transport cycle. It is also uncertain whether the kinetics of substrate binding directly influences the transport rate and if substrate binding and SBD docking to the TMD could trigger events during the translocation cycle [16,17]. To directly observe conformational changes in SBDs and by this to clarify binding models of these ABC-associated proteins, examination of SBD conformational states by means of single molecule FRET (smFRET) is reported [18].

FRET is a 'spectroscopic ruler' that relies on the measurement of energy transfer efficiency between two spectrally distinct fluorophores; the dynamic range is 2–10 nm [2]. In smFRET, a single donor (D) and acceptor (A) pair are excited and detected. Detecting a single molecule over a huge excess of solvent molecules (e.g. 10^{19} water molecules in 1 μL) is challenging due to background contributions by scattering [19,20]. Luckily, fluorescence allows selection of the molecules of interest by distinct absorption and emission spectra [20]. Background is additionally diminished by the reduction of the illuminated volume, for example in a fluorescence microscope [19-21]. The distance between D and A and hence the protein conformation, determines the fluorescence intensities upon D excitation (**Figure 2.1A**). Using FRET as a 1D ruler, one can observe (dynamic) conformational changes within a protein, in-between different proteins or domains. FRET has evolved to be a complementary tool for classical structural biology methods [22,23].

In this chapter, we illustrate the power of using single molecule fluorescence techniques to monitor conformational states and the kinetics of conformational transitions of protein domains such as the SBDs of ABC importers. These approaches unmask heterogeneity, stochastic and dynamic behavior of proteins that are typically hidden in ensemble measurements, such as NMR, EPR and others [24]. We can thus observe directly how binding interactions drive local conformational changes and how these are transmitted to different subunits of an ABC transporter to regulate its function. Although the study of membrane transporters with single-molecule approaches such as electrophysiology was already initiated decades ago, advanced imaging techniques were introduced to the field only recently. The most prominent *in vitro* single-molecule studies, aiming to verify aspects of published reaction models, include investigations of lactose permease [25], secondary active transporters [26], an ABC exporter (P-glycoprotein [27]) and, more recently, ABC-associated SBDs such as maltose-binding protein (MBP) [28,29] and SBDs from other bacterial importers [18].

Methods

Cloning and mutagenesis

To probe conformational changes in SBD1 and SBD2, we introduced two cysteine residues. Quick change mutagenesis approach with *pfu*Ultra was used to introduce two cysteine at strategic positions on the basis of the SBD1 and SBD2 crystal structures. The cysteine residues were introduced at surface-exposed, non-conserved positions and identified using the ConSurf Server. The structures of SBD1 (PDB 4LA9) and SBD2 (PDB 4KR5) in the *apo*protein open state and the closed state with glutamine bound to SBD2 (PDB 4KQP) are available.

The soluble substrate-binding domains were expressed in *Escherichia coli* strain MC1061 carrying pBADnLicSBD1 and pBADnLicSBD2 and derivatives. Site-directed mutagenesis to introduce cysteine pair for the labelling approach was accomplished with the QuickChange Site-Directed Mutagenesis protocol (Stratagene) and mutations were verified by sequence analysis (Seqlab). Briefly, 100 ng of template DNA (pBADnLIC containing either the SBD1 or SBD2 gene) was mixed with 0.3 µM of forward and reverse mutagenic primers in a PCR reaction with *pfu*Ultra High-Fidelity DNA polymerase (Stratagene). A control PCR reaction, in which addition of the polymerase was omitted, was also included. The PCR reaction mixture was treated with *Dpn*I (37 ^{o}C, 5 h) to digest the parental DNA, and this was followed by transformation into *E. coli* DH5α competent cells. The efficiency of the procedure was >90% (verified after sequencing), and the number of colonies varied from 50 to100, whereas in the control PCR reaction, no colonies were observed.

Bacterial strains and growth conditions

His_6SBD1, His_6SBD2, and His_6SBD12 were over-expressed in *E.coli* BL21. The cells were grown in Luria-Bertani media containing 1% w/v pepton, 1% w/v NaCl, 0.5% w/v yeast extract supplemented with 100 µg/ml of ampicillin in shake flasks. Cell was grown at 37 ^{o}C overnight until an OD_{600} of about 1.0. Cell culture was then rejuvenated into production media with dilution of 500X for about 2 hours until an OD_{600} of about 0.5 was reached. Expression was triggered by addition of 0.3% (v/v) L-arabinose 10%, and induction was continued for another 2 h. Cells were harvested by centrifugation (15 min, 6,000 *xg*) and washed once with buffer A (50 mM KPi pH 8.0, 1 M KCl, 20 mM imidazole, 10% glycerol). After resuspension, cells were supplemented with 0.1 mg/ml DNase and 1 mM phenylmethylsulfonyl fluoride PMSF, to be disrupted by cell disrupter with 25,000 psi (Emulsiflex-C5, Avestin). Supernatant was collected after ultracentrifugation (45 min, 150,000 *xg*) and stored at 4 ^{o}C.

Purification of SBD1 and SBD2

For purification step, we used Ni^{2+}-Sepharose resin (5.5 mL bed volume of Ni^{2+}-Sepharose per wet-weight gram of cells). Supernatant (supplemented with 1 mM DTT) was flown into the

resin. Washing step was done with flowing 10 CV (column volume) buffer A and 10CV buffer B (50 mM KPi pH 8.0, 50 mM KCl, 50 mM imidazole, 10% glycerol). The histidine-tagged proteins were eluted in 5 column volumes of buffer C (50 mM KPi pH 8.0, 50 mM KCl, 500 mM imidazole, 10% glycerol). The elution was supplemented with 5 mM EDTA to prevent aggregation and then was concentrated (Vivaspin, Sartorius; ~5 mg/ml), dialyzed in buffer D (50 mM KPi pH 8.0, 50 mM KCl) to remove imidazole for 3 hours. For more protein stability, protein was subsequently dialyzed in buffer E (50 mM KPi pH 7.0; 50 mM KCl; 50% glycerol). The protein was added with 1 mM DTT in final concentration and stored in aliquots at -20 ^{o}C.

Calorimetric measurements

Isothermal titration calorimetry (ITC) experiments were performed with using about 400 µM purified protein. Briefly, the purified SBDs were dialyzed overnight against 50 mM KPi pH 8.0 and 150 mM KCl to have final concentration 20 µM. Isothermal titration experiments were carried out with an ITC-200 (MicroCal, GE Healthcare). 10 times higher glutamine concentration was used as for SBD2 substrate. For these experiments, the substrate was prepared and diluted in the dialysis buffer to minimize mixing effects. Further protein dilution was also done in the dialysis buffer. All experiments were carried out at 25 ^{o}C with a mixing rate of 300 rpm.

Purification of labelled protein

20-40 mg/ml unlabelled SBD1 and SBD2 cysteine-containing derivatives were used in 100 µL total volume buffer labelling A (50 mM KPi pH 7.4, 50 mM KCl and 5% glycerol and 1 mM DTT). Stochastic labelling with maleimide derivatives of donor and acceptor fluorophores was carried out on ~5 nmol of protein; SBD derivatives were labelled with Cy3B- and Atto747N-maleimide in a ratio of protein/Cy3B/Atto647N = 1:4:5. Briefly, purified proteins were treated with 10 mM DTT for at least 30 min to fully reduce oxidized cysteines. After dilution of the protein sample to a DTT concentration of 1 mM, the reduced protein was bound to a Ni^{2+}-Sepharose resin (GE Healthcare) and washed with ten column volumes of buffer labelling A. Simultaneously, the applied fluorophore stocks (50 nmol in powder) dissolved in 5 µl of water-free DMSO, were added at appropriate amounts to buffer A and immediately applied to the protein bound to the Ni^{2+}-Sepharose resin (keeping the final DMSO concentration below 1%). The resin was incubated overnight and kept at 4 ^{o}C (under mild agitation). After labelling, unbound dye was removed by sequential washing with 10 column volumes of buffer B (50 mM KPi pH 7.4, 1 M KCl and 50% glycerol). The protein was eluted in 1.0 mL buffer elution (50 mM KPi pH 7.4, 50 mM KCl, 5% glycerol and 500 mM imidazole) and was applied onto a Superdex-200 column (GE Healthcare) equilibrated with 50 mM KPi pH 7.4, 150 mM KCl. We enriched for protein labelled with donor and acceptor fluorophores by taking advantage of the nonspecific interaction of the Atto647N dye with Superdex-200 column materials.

Single-molecule fluorescence microscopy

Microscope cover slides (no. 1.5H precision cover slides, VWR Marienfeld) were coated with 1 mg/mL BSA for about 30 seconds to prevent quenching of the fluorophore to the glass material. Excess BSA was subsequently washed with imaging buffer containing 50 mM KPi, 150 mM KCl, 1 mM Trolox (photo stabilization agent), and 10 mM Cysteamine, pH 7.4. Purified labelled protein from size exclusion chromatography was further diluted in imaging buffer to obtain 25 pM final concentration. Soluble SBDs proteins were visualized using a built confocal FRET microscopy [30] at room temperature. An excitation light pulses centered at 532 and 640 nm, the correlated wavelength as the used fluorophore (SuperK Extreme, NKT Photonics, Denmark) were used. Alternation between both excitation wavelengths was achieved by modulating the light in 50 µs intervals. The beam was coupled into a single-mode fiber (PM-S405-XP, Thorlabs, United Kingdom) and re-collimated (MB06, Q-Optics/Linos, Germany) before entering an oil immersion objective (60X, NA 1.35, UPLSAPO 60XO, Olympus, Germany). Excitation and emission were separated by a dichroic beam splitter (zt532/642rpc, AHF Analysentechnik, Germany), which is mounted in an inverse microscope body (IX71, Olympus, Germany). Fluorescence emitted by diffusing molecules in solution at the focus was collected by the same oil objective, focused onto a 50 µm pinhole and spectrally separated (640DCXR, AHF Analysetechnik, Germany) onto two APDs (τ-spad, <50 dark-counts/s, Picoquant, Germany) with appropriate spectral filtering (donor channel: HC582/75; acceptor channel: Edge Basic 647LP; both AHF Analysentechnik, Germany).

Scanning confocal microscopy

Confocal scanning experiments were performed using the same homebuilt confocal microscope [30]. Data were recorded with constant 532 nm excitation at an intensity of 0.8 µW (~125 W/cm^2) for OppA and FeuA. A flow-cell arrangement was used as described in [31] for studies of surface-immobilized protein. All experiments were carried out in a degassed buffer (50 mM KPi, pH 7.4, 50 mM KCl) under oxygen-free conditions obtained utilizing an oxygen-scavenging system supplemented with 10 mM of aged Trolox (Merck) as a photostabilizer [32].

Data analysis

Fluorescence photons arriving at the two detection channels (donor detection channel: D_{em}; acceptor detection channel: A_{em}) were assigned to either donor-or acceptor-based excitation based on their photon arrival time [33,34]. Collected photon corresponds to donor-based donor emission F(DD), donor-based acceptor emission F(DA) and acceptor-based acceptor emission F(AA). Fluorophore stoichiometry's S and apparent FRET efficiencies E* were defined by calculating the fluorescent burst yielding in a two-dimensional histogram. Uncorrected

FRET efficiency E* is the proximity between the two fluorophores and is calculated according to:

$$E^* = \frac{F(DA)}{F(DA) + F(DD)}$$

Stoichiometry S is defined as the ratio between the overall green fluorescence intensity over the total green and red fluorescence intensity and describes the ratio of donor-to-acceptor fluorophores in the sample:

$$S = \frac{F(DD) + F(DA)}{F(DD) + F(DA) + F(AA)}$$

One-dimensional E* and S distributions were fitted using a Gaussian function, yielding the mean values of the distribution and an associated standard deviation σ.

Results

Monitoring conformational states of SBDs with smFRET

The core of all ABC-related SBDs, which initiate transport via capturing substrates, consists of two structurally conserved rigid domains connected by a flexible hinge region, which allows a conformational transition from an open to a closed conformational state [35]. We recently studied SBD1 and SBD2 of the ABC transporter for glutamine-importer from *Lactococcus lactis* (GlnPQ), using a combination of single-molecule and biochemical methods to elucidate their exact role and function in transport [18].

To allow FRET investigations of SBDs, two cysteines were introduced at non-conserved and solvent-exposed sites that can be labelled stochastically with maleimide-derivatives of organic fluorophores (**Figure 2.1A**, Cy3B as D and Atto647N as A). The crystal structure of SBD2 in its open state suggests a distance between residues T369C and S451C of 4.9 nm and 4.0 nm for the closed state. In such an assay design, the open conformation of the protein should have low FRET efficiency, whereas the closed conformation should have a higher FRET efficiency; hence, FRET efficiency (E*) is indicative of the conformational state of the protein.

With this assay, we determined the ligand-binding mechanism by stepwise addition of substrate, monitoring the hypothesized transition from open-unliganded to closed-liganded state using alternating laser excitation (ALEX) [36]. This technique allows to study FRET efficiency E* and labelling stoichiometry S of individual molecules during the short millisecond-long transit through the excitation volume of a confocal microscope [2,33]. A single population is observed around an apparent FRET value E* of 0.50 in the apo-state of SBD2 (**Figure 2.1B**). At saturating concentrations of glutamine ($\gg K_d$), the population shifts to a high FRET state E* = 0.69. These observations are in good agreement with expectations from crystal structures, since the apo-state of the protein has a higher distance between both attachment points, whereas the liganded state of the protein shows a smaller separation. Gradual titration of ligand and plotting the relative population of open to closed state yields an apparent K_d -value of $\sim$1 μM that is in full agreement with values derived from isothermal titration calorimetry, as shown in **Figure 2.1C** [18].

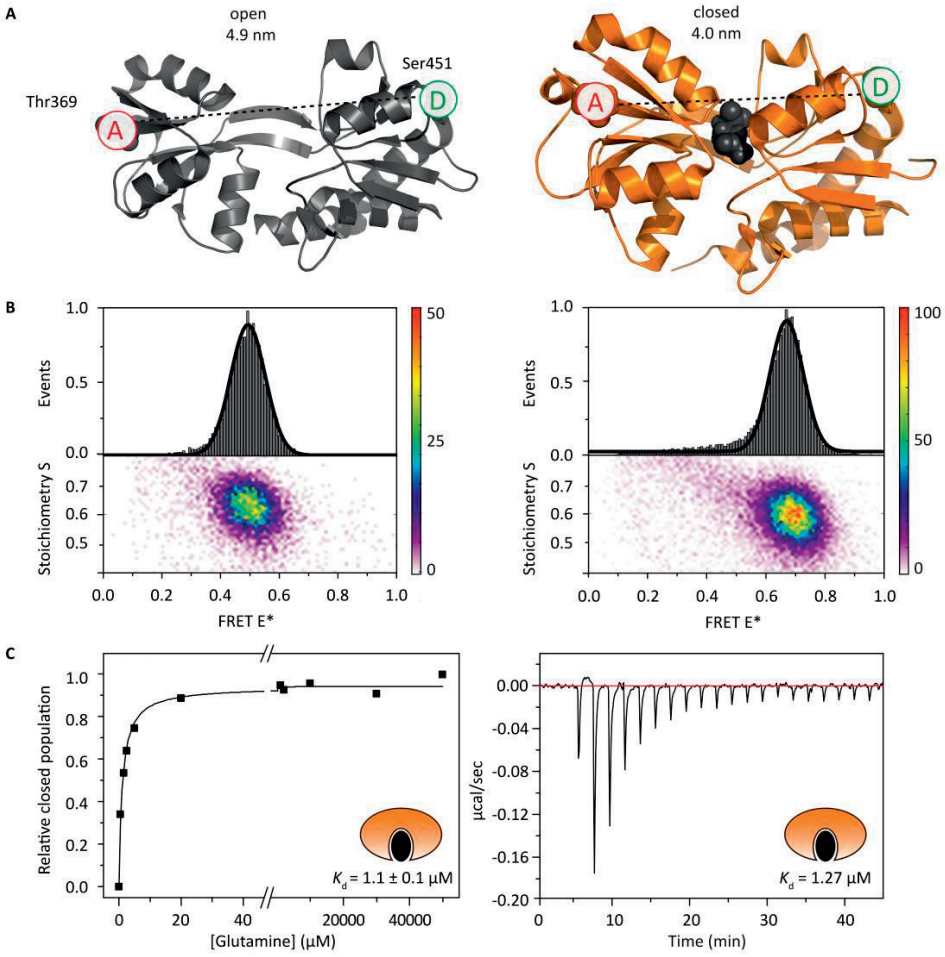

Figure 2.1 | A Left: Crystal structure of the open ligand-free state of SBD2 (grey, PDB 4KR5). Right: Crystal structure of the closed-liganded state (orange, PDB 4KQP). Surface-located and non-conserved residues are mutated to cysteine for labelling. Glutamine (shown in grey spheres) induces the closed state conformation. The residues are 4.9 nm apart in the open state and come to 4.0 nm in the closed state. **B** Confocal single-molecule analysis with ALEX of SBD2 labelled stochastically with Cy3B- and Atto647N-maleimide. SBD2 in the open state has low apparent FRET value of 0.50 (left); with addition of 10 mM glutamine the population shifts to a high FRET of 0.69 (right). **C** Left: ALEX experiments (as in b) were also performed at the indicated concentrations of glutamine. The *K*d value of 1.1 μM was obtained from the ratio of areas [closed-liganded/(open-unliganded + closed-liganded)] between both populations (shown in b). Right: Binding isotherms of the calorimetric titration of SBD2 wild-type with glutamine were performed on a isothermal titration calorimeter (MicroCal VP-ITC, Malvern), ITC measurements were performed in 50 mM KPi pH 7.0, 150 mM KCl at 298 K. Purified SBD2 at a final concentration of 30 μM was placed at the cell in the experiment. Glutamine (2 μl at 500 μM in the syringe) per injections was used to titrate the protein in the cell. The normalized enthalpy changes per glutamine injected is plotted as a function of the protein-to-glutamine ratio, yielding *K*d value of 1.27 μM.

Dynamics of the ligand binding process

To investigate the dynamics of the ligand-binding process, smFRET experiments with identical labelling scheme have to be performed with surface-bound proteins, using a confocal scanning microscope. In accordance with ALEX experiments, SBD2 was predominantly (>95 %) in the open conformation when no ligand was present (**Figure 2.2**, left panel). Importantly, however we observed rare transitions to a high FRET state with identical FRET values as observed for the closed conformation with saturated concentration of glutamine (Figure 2.2, right panel). These data reveal that SBD2 can transit to a closed-unliganded state (lifetime of ~60ms) and does so on average every 2s. It is unclear whether these closing events can trigger ATP-hydrolysis and are one cause for the basal activity of a transporter. In accordance with the K_d-value, SBD2 shows frequent switching between low and high FRET state with even occupation at low ligand concentrations (Figure 2.2, middle panel). These conditions represent direct observation of substrate binding and unbinding events that are coupled with conformational changes in SBD2. Surprisingly, the lifetimes of the closed-liganded and closed-unliganded state were identical within error, thus indicating that the ligand does not 'stabilize' the closed conformation relative to the transition state. The concentration dependence of both on/off-rate clearly follows an induced fit mechanism (or 'Venus fly- trap'), where the on-rate increases with increasing ligand concentration whereas the off-rate is found constant.

To understand the implication of milliseconds-lifetimes of closed-liganded and closed-unliganded states of the SBDs for transport, the single-molecule data were correlated with those obtained from standard biochemical assays. *In vivo* uptake experiments of radio-labelled amino acids were used to determine the transport rates [18]. A direct comparison of the kinetics of the conformational transitions of SBDs with the respective transport rates of wild-type SBDs but also of SBDs with altered conformational dynamics, allowed us to uncover salient features of the transport cycle of type-I ABC importers [18].

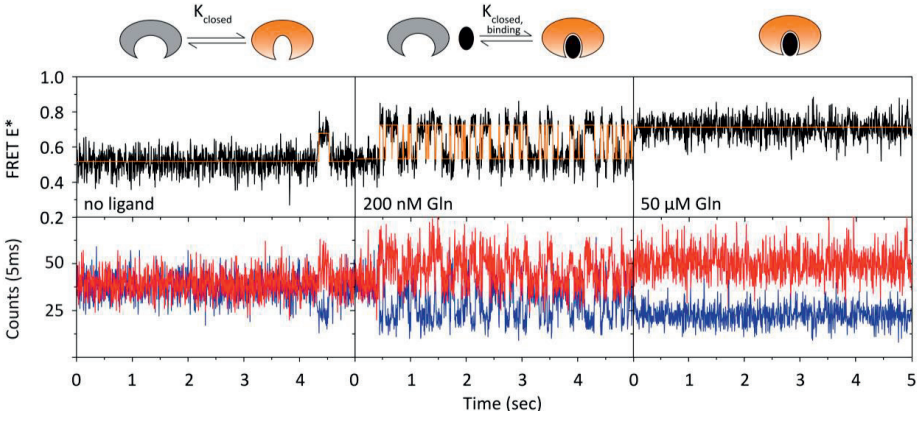

Figure 2.2 | Representative fluorescence time traces of SBD2 labeled with Cy3B- and Atto647N-maleimide with the indicated concentrations of glutamine. SBD2 shows an open state at E* = 0.50 and a closed high FRET state at E* = 0.69 in the presence of saturating concentrations of glutamine. At substrate concentrations around the *K*d, two populations can be resolved.

Advancing single-molecule tools: optimized protein labelling

As shown in Figure 2, single-molecule based assays provide unique opportunities to unravel heterogeneity, to observe rare events and to study unsynchronized biochemical processes even in real time. The observation of individual biomolecules is however complicated by the following major obstacles: (i) a significant number of individual molecules have to be studied to obtain statistically significant information about a biochemical process or a conformational state/transition. (ii) Single-molecule approaches allow for user-based pre-selection of the experimental data, which can ultimately lead to false interpretations and irrelevant models. Both problems can only be overcome by collecting large data sets using automated non-biased data analysis. (iii) smFRET is further complicated by the need for protein species bearing exactly one donor and one acceptor fluorophore. The standard procedure to allow FRET on a protein is stochastic labelling of two (typically engineered) cysteine residues, using reactive fluorophore derivatives, e.g. maleimides. 'Informative' protein molecules are those labelled with both donor and acceptor fluorophore and the yield of these molecules can be 50% at maximum for stochastic labelling since four possible species with equal probability are obtained: donor-only D(cys#1)/D(cys#2), acceptor-only A(cys#1)/A(cys#2) and the donor–acceptor (DA) species D(cys#1)/A(cys#2) and A(cys#1)/D(cys#2).

ALEX- or Pulsed Interleaved Excitation (PIE)- spectroscopy [2,37] provide a bias-free view on the populations of conformational states of freely diffusing proteins. With this knowledge regarding the relevant conformational states from ALEX, single-molecule experiments of surface-immobilized molecules can be obtained without false bias, hence solving problem ii. Often however, additional complications such as labelling efficiency restrict the amount of available information in single-molecule experiments and render the presented strategy not feasible (problems i/iii).

In **Figure 2.3**, we show biochemical and single-molecule data from a typical FRET pair, i.e. donor Cy3B and acceptor Cy5. The chromatogram of the labelled protein shows a single mono-disperse protein species that contains both fluorophores (Figure 2.3A) with ~65% labelling efficiency. Next, we analyzed the different size-exclusion chromatography (SEC)-fractions for the relative population of DA, donor-only and acceptor-only. This percentage was determined from confocal solution ALEX experiments [36] by analyzing single-molecule transits through the confocal volume. Two parameters are obtained: labelling stoichiometry S and apparent FRET efficiency E*. The 2D E*/S histogram reports on apparent FRET E* (*x*-axis), i.e. a measure of the inter-probe distance and the labelling stoichiometry between the two fluorophores on the *y*- axis (Figure 2.3C). Low stoichiometry (<0.3) corresponds to acceptor-only molecules; high stoichiometry (>0.8) corresponds to donor-only molecules; whereas intermediate values ($0.3 < S < 0.8$) correspond to DA molecules. The percentage of the DA population was determined from the areas under the respective S populations. For a standard couple of donor and acceptor, e.g. Cy3B/Cy5, all fractions show an average of 20–30 % DA population (Figure 2.3B) [38]. With this sample, we performed similar experiments as in Figure 2.1C and [18] to see whether the fluorophores have (unwanted) effects on observables such as dissociation

constant. A glutamine titration of SBD2 labelled with Cy3B/Cy5 gives rise to an apparent K_d value ~1.0 µM, which is in full agreement with ITC experiments (Figure 2.3D compared with Figure 2.1C right) and our previous experiments obtained with Cy3B and Atto647N [18].

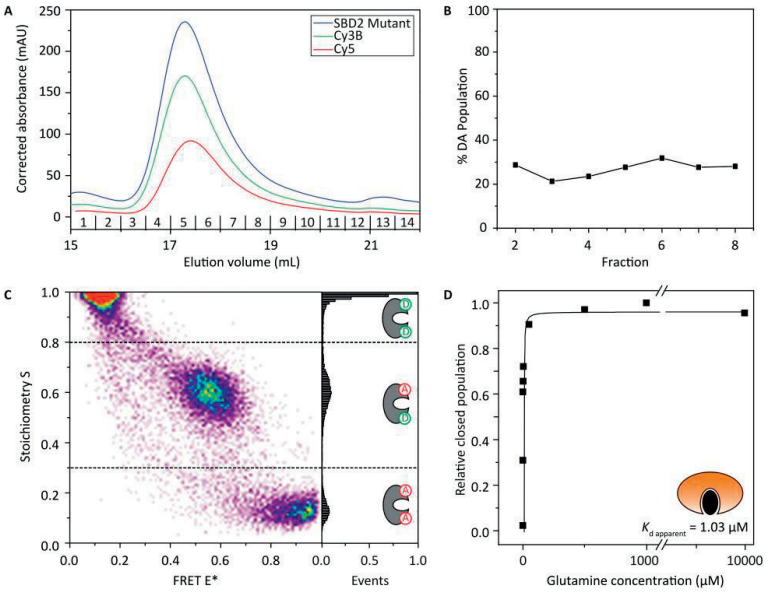

Figure 2.3 | Improved strategy for stochastic labelling of proteins used in smFRET studies. A Chromatogram of SBD2 labelled with Cy3B and Cy5. **B** The percentage of DA population from different fraction was calculated. All fractions have an average of 20-30% of DA population. **C** 2D histogram and 1D histogram of fraction number 5. **D** The *K*d value of SBD2 labelled with Cy3B and Cy5 for glutamine, obtained by plotting the peak value of FRET from a Gaussian fit as a function of its concentration. We obtained similar results after labelling other positions in the SBD or using Cy3B and Atto647N fluorophores [18]. The different 'donor-only', 'DA' and 'acceptor-only' populations are depicted in cartoon style.

We noted, however that the SEC profiles of SBDs labelled with specific fluorophore pairs, e.g. Cy3B/ATTO647N showed a less homogenous labelling ratio (**Figure 2.4**). A relative difference in the retention time of molecules with differing labels offers the interesting possibility to improve the yield of molecules having both donor and acceptor labelling beyond the possible 50% for stochastic labelling. To enrich the population of these molecules, we used the propensity of specific fluorophores (here Atto647N) to interact non-specifically with the SEC column material Superdex-200. SBD labelled with Cy3B and Atto647N was analyzed with SEC, showing an average labelling efficiency of ~67%. As observed, molecules labelled only with Cy3B elute at 17.5 ml (like unlabelled molecules, dashed line; Figure 2.4A). Fraction number 5 has consequently the lowest percentage of DA (~1.5 %), whereas molecules labelled with Atto647N only elute at 21 ml (fraction number 12) with a percentage of DA of ~43 %. Intermediate volumes, e.g. 19 ml (fraction number 8), show the highest percentage of DA population ~59%. Thus, by simply selecting intermediate elution fractions, we were able to

enrich the percentage of double-labelled molecules (Figure 2.4B,C). The ability to enrich for DA molecules is exclusively due to the non- specific interaction of Atto647N with Superdex-200 column material, as molecules labelled with Cy3B and Cy5 elute as a single mono-disperse peak (Figure 2.3A). Importantly, labelling with both pair dyes does not interfere with protein function, as SBD2 labelled with Cy3B–Cy5 has unaffected affinity for glutamine (Figure 2.3D) compared with wild-type SBD2 or other fluorophore pairs such as Cy3B/ATTO647N [18].

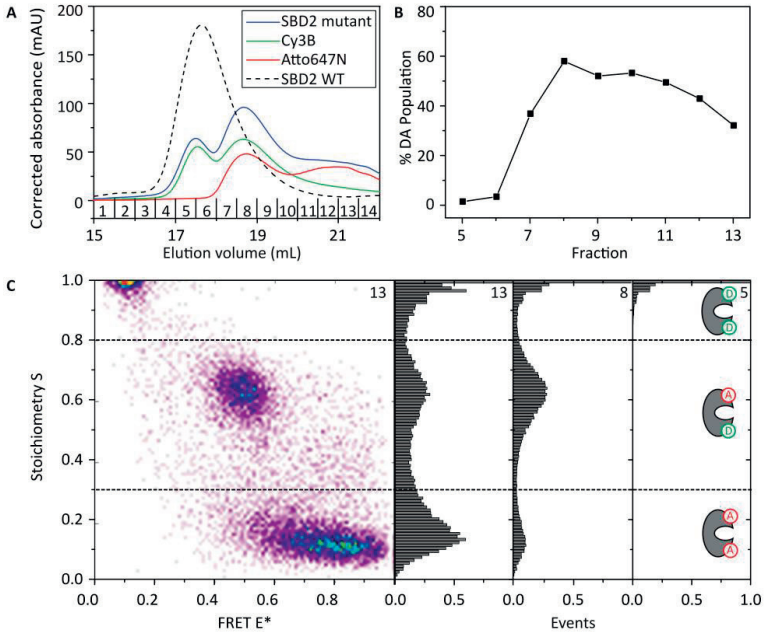

Figure 2.4 | Improved strategy for stochastic labelling of proteins used in smFRET studies. A Chromatogram of SBD2 labelled with Cy3B and Atto647N; unlabelled protein is represented in black dashes. SBD2 labelled with Atto647N is retarded on the column and elutes later than the unlabelled protein. **B** The percentage of DA population from different fractions is depicted. Fraction number 8 has the highest percentage DA population, in agreement with the chromatogram. **C** 2D histogram and 1D histogram of fractions number 13, 8, 5 respectively.

Conclusion

This chapter focused on the use of single-molecule methodology and its practical advancement in terms of labelling to obtain detailed information regarding the conformational states and dynamics of SBDs of type I ABC importers. The knowledge of the binding mechanism and the correlation of kinetic data with *in vivo* transport rates allowed us for the first time to characterize the initial steps of the translocation cycle of an ABC importer. The details of this study are found in [17] and can be summarized as follows: (i) Substrate capturing is accomplished by an induced fit mechanism (or Venus fly-trap), (ii) the lifetime of the closed-liganded state directly influences the rate of transport, (iii) a closed-unliganded state can lock the transport cycle in an non- productive state; (iv) different ligands trigger ATP hydrolysis with different efficiencies; (v) docking efficiency depends on the SBD; (vi) SBD opening seems faster when the SBD is docked/interacting with the transporter.

Our findings contribute to a general understanding of the mechanism of ABC transport, information that became only accessible by combining single-molecule tools with bio-chemical data. Future work will show whether the proposed model for substrate-binding and the resulting implications for transport hold for other types of transporters (type II, energy-coupling-factor ABC transporter or tripartite ATP- independent periplasmic transporters) that also use SBDs for substrate transport [4].

References

1. Cui, J., Davidson, A.L. (2011) ABC solute importers in bacteria. *Essays Biochem*. 50, 85–99
2. Hohlbein, J., Craggs, T.D., Cordes, T. (2014) Alternating-laser excitation: single-molecule FRET and beyond. *Chem. Soc. Rev*. 43, 1156–1171
3. Rees, D.C., Johnson, E., Lewinson, O. (2009) ABC transporters: the power to change. *Nat. Rev. Mol. Cell Biol.* 10, 218–227
4. Berntsson, R.P., Smits, S.H., Schmitt, L., Slotboom, D.J., Poolman, B. (2010) A structural classification of substrate-binding proteins. *FEBS Lett*. 584, 2606–2617
5. Shilton, B.H. (2008) The dynamics of the MBP-MalFGK(2) interaction: a prototype for binding protein dependent ABC-transporter systems. *Biochim. Biophys. Acta.* 1778, 1772–1780
6. Davidson, A.L., Dassa, E., Orelle, C., Chen, J. (2008) Structure, function, and evolution of bacterial ATP-binding cassette systems. *Microbiol. Mol. Biol. Rev.* 72, 317–364
7. Lewinson, O., Lee, A.T., Locher, K.P., Rees, D.C. (2010) A distinct mechanism for the ABC transporter BtuCD-BtuF revealed by the dynamics of complex formation. *Nat. Struct. Mol. Biol.* 17, 332–338
8. Ogunniyi, A.D., Mahdi, L.K., Jennings, M.P., McEwan, A.G., McDevitt, C.A., Van der Hoek, M.B., Bagley, C.J., Hoffmann, P., Gould, K.A., Paton, J.C. (2010) Central role of manganese in regulation of stress responses, physiology, and metabolism in *Streptococcus pneumoniae*. *J. Bacteriol.* 192, 4489–4497
9. Lanfermeijer, F.C., Detmers, F.J., Konings, W.N., Poolman, B. (2000) On the binding mechanism of the peptide receptor of the oligopeptide transport system of *Lactococcus lactis. EMBO J.* 19, 3649–3656
10. Hollenstein, K., Dawson, R.J., Locher, K.P. (2007) Structure and mechanism of ABC transporter proteins. *Curr. Opin. Struct. Biol*. 17, 412–418
11. Zolnerciks, J.K., Andress, E.J., Nicolaou, M., Linton, K.J. (2011) Structure of ABC transporters. *Essays Biochem.* 50, 43–61
12. Bucher, D., Grant, B.J., McCammon, J.A. (2011) Induced fit or conformational selection? The role of the semi-closed state in the maltose binding protein. *Biochemistry.* 50, 10530–10539
13. Frauenfelder, H., Sligar, S.G., Wolynes, P.G. (1991) The energy landscapes and motions of proteins. *Science.* 254, 1598–1603
14. Hammes, G.G., Chang, Y.C., Oas, T.G. (2009) Conformational selection or induced fit: a flux description of reaction mechanism. *Proc. Natl. Acad. Sci. U.S.A*. 106, 13737–13741

15. Silva, D.A., Bowman, G.R., Sosa-Peinado, A., Huang, X. (2011) A role for both conformational selection and induced fit in ligand binding by the LAO protein. *PLoS Comput. Biol.* 7, e1002054

16. Jones, P.M., O'Mara, M.L., George, A.M. (2009) ABC transporters: a riddle wrapped in a mystery inside an enigma. *Trends Biochem. Sci.* 34, 520–531

17. Wilkens, S. (2015) Structure and mechanism of ABC transporters. *F1000prime reports*. 7, 14

18. Gouridis, G., Schuurman-Wolters, G.K., Ploetz, E., Husada, F., Vietrov, R., de Boer, M., Cordes, T., Poolman, B. (2015) Conformational dynamics in substrate-binding domains influences transport in the ABC importer GlnPQ. *Nat. Struct. Mol. Biol.* 22, 57–64

19. Ha, T., Enderle, T., Ogletree, D.F., Chemla, D.S., Selvin, P.R., Weiss, S. (1996) Probing the interaction between two single molecules: fluorescence resonance energy transfer between a single donor and a single acceptor. *Proc. Natl. Acad. Sci. U.S.A.* 93, 6264–6268

20. Jameson, D.M., Croney, J.C., Moens, P.D. (2003) Fluorescence: basic concepts, practical aspects, and some anecdotes. *Methods Enzymol.* 360, 1–43

21. Kastantin, M., Schwartz, D.K. (2011) Connecting rare DNA conformations and surface dynamics using single-molecule resonance energy transfer. *ACS Nano.* 5, 9861–9869

22. Kalinin, S., Peulen, T., Sindbert, S., Rothwell, P.J., Berger, S., Restle, T., Goody, R.S., Gohlke, H., Seidel, C.A. (2012) A toolkit and benchmark study for FRET-restrained high-precision structural modeling. *Nat. Methods.* 9, 1218–1225

23. Muschielok, A., Andrecka, J., Jawhari, A., Bruckner, F., Cramer, P., Michaelis, J. (2008) A nano-positioning system for macromolecular structural analysis. *Nat. Methods.* 5, 965–971

24. Christoph Göbl, N.T. (2012) Application of solution NMR spectroscopy to study protein dynamics. *Entropy.* 14, 581–598

25. Majumdar, D.S., Smirnova, I., Kasho, V., Nir, E., Kong, X., Weiss, S., Kaback, H.R. (2007) Single-molecule FRET reveals sugar-induced conformational dynamics in LacY. *Proc. Natl. Acad. Sci. U.S.A.* 104, 12640–12645

26. Erkens, G.B., Hanelt, I., Goudsmits, J.M., Slotboom, D.J., van Oijen, A.M. (2013) Unsynchronised subunit motion in single trimeric sodium-coupled aspartate transporters. *Nature*. 502, 119–123

27. Verhalen, B., Ernst, S., Borsch, M., Wilkens, S. (2012) Dynamic ligand-induced conformational rearrangements in P-glycoprotein as probed by fluorescence resonance energy transfer spectroscopy. *J. Biol. Chem*. 287, 1112–1127

28. Kim, E., Lee, S., Jeon, A., Choi, J.M., Lee, H.S., Hohng, S., Kim, H.S. (2013) A single-molecule dissection of ligand binding to a protein with intrinsic dynamics. *Nat. Chem. Biol.* 9, 313–318

29. Seo, M.H., Park, J., Kim, E., Hohng, S., Kim, H.S. (2014) Protein conformational dynamics dictate the binding affinity for a ligand. *Nat. Commun.* 5, 3724

30. van der Velde, J.H.M., Ploetz, E., Hiermaier, M., Oelerich, J., de Vries, J.W., Roelfes, G., Cordes, T. (2013) Mechanism of Intramolecular Photostabilization in Self-Healing Cyanine Fluorophores. *Chem. Phys. Chem.* 14, 4084–4093

31. Roy, R., Hohng, S., Ha, T. (2008) A practical guide to single-molecule FRET. *Nature methods.* 5(6), 507–516

32. Cordes, T., Vogelsang, J., Tinnefeld, P. (2009) On the mechanism of Trolox as antiblinking and antibleaching reagent. *Journal of the American Chemical Society.* 131(14), 5018–5019

33. Kapanidis, A.N., Lee, N.K., Laurence, T.A., Doose, S., Margeat, E., Weiss, S. (2004) Fluorescence-aided molecule sorting: analysis of structure and interactions by alternating-laser excitation of single molecules. *Proc. Natl. Acad. Sci. U.S.A.* 101, 8936–8941

34. Kapanidis, A.N., Laurence, T.A., Lee, N.K., Margeat, E., Kong, X.X., Weiss, S. (2005) Alternating-laser excitation of single molecules. *Acc. Chem. Res.* 38, 523–33

35. Tang, C., Schwieters, C.D., Clore, G.M. (2007) Open-to-closed transition in apo maltose-binding protein observed by paramagnetic NMR. *Nature.* 449, 1078–1082

36. Lee, N.K., Kapanidis, A.N., Wang, Y., Michalet, X., Mukhopadhyay, J., Ebright, R.H.,Weiss, S. (2005) Accurate FRET measurements within single diffusing biomolecules using alternating-laser excitation. *Biophys. J.* 88, 2939–2953

37. Muller, B.K., Zaychikov, E., Brauchle, C., Lamb, D.C. (2005) Pulsed interleaved excitation. *Biophys. J*. 89, 3508–3522

38. Kapanidis, A.N., Weiss, S. (2002) Fluorescent probes and bio-conjugation chemistries for single-molecule fluorescent analysis of biomolecules. *J. Chem. Phys.* 117, 11

Chapter 3

Conformational dynamics in the substrate-binding domains influences transport in the ABC importer GlnPQ

Giorgos Gouridis[1,2], Gea K. Schuurman-Wolter[1], Evelyn Ploetz[2], Florence Husada[2], Ruslan Vietrov[1], Marijn de Boer[1,2], Thorben Cordes[2], Bert Poolman[1]

An extended version of this chapter was published in Nature Structural & Molecular Biology. 2015 January. 22(1), 57–64 DOI: 10.1038/nsmb.2929

[1] Department of Biochemistry, Groningen Biomolecular Sciences and Biotechnology Institute, University of Groningen, Nijenborgh 4, 9747 AG Groningen, The Netherlands

[2] Molecular Microscopy Research Group, Zernike Institute for Advanced Materials, University of Groningen, Nijenborgh 4, 9747 AG Groningen, The Netherlands

F.A.H. conducted research (plasmid construction, mutagenesis, protein production, protein purification, surface preparation, fluorescence labelling, smFRET experiments), analyzed data, produced figures and contributed towards writing of the manuscript.

Abstract

The conformational dynamics in ABC transporters is largely elusive. The ABC importer GlnPQ from *Lactococcus lactis* has different covalently linked substrate-binding domains (SBDs), thus making it an excellent model system to elucidate the dynamics and role of the SBDs in transport. We demonstrate by single-molecule spectroscopy that the two SBDs intrinsically transit from open to closed ligand-free conformation, and the proteins capture their amino acid ligands via an induced-fit mechanism. High-affinity ligands elicit transitions without changing the closed-state lifetime, whereas low-affinity ligands dramatically shorten it. We show that SBDs in the closed state compete for docking onto the translocator, but remarkably the effect is strongest without ligand. We find that the rate-determining steps depend on the SBD and the amino acid transported. We conclude that the lifetime of the closed conformation controls both SBD docking to the translocator and substrate release.

Key words: ABC importer, transport mechanism, SBD, GlnPQ, fluorophore labelling, FRET, single-molecule studies.

Abbreviations: ABC, ATP-binding cassette; NBD, nucleotide binding domain; TMD, transmembrane domain; SBD, substrate binding domain; ALEX, alternating laser excitation; ATP, adenosine triphosphate; DA, donor-acceptor; FRET, Förster resonance energy transfer; SEC, size-exclusion chromatography; smFRET, single-molecule FRET.

Introduction

ATP-binding cassette (ABC) transporters are integral membrane proteins found in all kingdoms of life [1]. The importers are involved in uptake of cellular building blocks and nutrients and also in large-scale accumulation of compatible solutes for cell-volume regulation [2,3] and of signaling molecules for intercellular communication [4,5]. ABC exporters are involved in extrusion of drugs and antibiotics [6], lipid translocation [7], antigen presentation [4] and numerous other functions [8]. Both importers and exporters consist of two transmembrane domains (TMDs) and two cytoplasmic nucleotide-binding domains (NBDs), which power transport through hydrolysis of ATP. Besides TMDs and NBDs, the ABC importers use SBDs or substrate-binding proteins (SBPs) to capture substrates from the environment and deliver them to the translocator. The SBDs are fused to the TMD, whereas SBPs are separate polypeptides, either present in the periplasm or associated with the membrane via a lipid or protein anchor [9]. A subset of ABC transporters has two or even three SBDs fused in tandem [9, 10], thus giving rise to four or six receptor domains per functional complex. Despite the difference in the number of SBDs and their linkage to the cell surface, the basic transport mechanism of ABC importers could be similar. However, very little is known of how ABC importers interact with multiple (and structurally distinct) SBDs. Do the SBDs operate independently of each other, and do they function via a similar mechanism? Do multiple SBDs increase the substrate spectrum and/or transport capacity? Do the SBDs compete for docking onto the TMD, and in which conformation do they interact? Importantly, the transporters with multiple SBDs fused to the TMDs offer unique possibilities for probing the rate-determining steps in translocation and the influence of the dynamics of SBDs in translocation.

In this study, we focus on GlnPQ (**Figure 3.1A**) from the Gram-positive bacterium *L. lactis*, which uses two different SBDs for import of asparagine, glutamine and glutamate [10, 11]. The overall fold of the two SBDs of GlnPQ is very similar even though their primary sequences diverge by more than 50%. Numerous crystal structures of SBDs [12] and some structural information from NMR are available [13], but the mechanism of ligand binding ('induced fit' versus 'conformational selection') is still under debate [14, 15]. What remains ambiguous, however, is how the binding mechanism influences the transport process. Moreover, there is no consensus on the conformations of SBDs that lead to a productive translocation cycle. To discriminate between the different models of substrate delivery and translocation by ABC importers and to understand the role of the individual SBDs in the transport process, a variety of different studies have been carried out. A number of crystal structure of GlnPQ are available of full-length ABC importer [10]. Crystal structures provide crucial snapshots of discrete states of the translocation cycle but do not resolve the dynamics of the processes.

Additionally, 'bulk' biochemical experiments cannot provide insights into rare and/or transient events that are crucial for the transport process because these are lost in the ensemble averaging. Here, we used single-molecule Förster resonance energy transfer (smFRET) to probe conformational dynamics of the SBDs and correlated these findings with

isothermal titration calorimetry (ITC) to determine the specificity and thermodynamics of ligand binding. In addition, we monitored the overall transport process to relate differences in binding activity and protein conformation to translocation efficiency. With this unique combination of techniques, we present new mechanistic insight into the transport mechanism of ABC importers: (i) SBDs of GlnPQ bind their ligands via an induced-fit mechanism; (ii) the lifetime of the closed ligand-bound state determines the rate of transport; and (iii) the closed ligand-free state of SBD2 inhibits transport via SBD1.

Methods

Labelling of SBDs derivatives

Experimental procedures are described in the "Methods" of chapter 2 in this study..

Uptake experiments in whole cells

Uptake experiments were done as described in Wolters *et al.* [11] (experiments were done in the collaboration with Membrane Enzymology group). *L. lactis* cells were grown in GM17 to an OD_{600} of 0.4, induced for 1 hour with 0.01% of culture supernatant of the nisin A–producing strain NZ9700 (containing 10 mg/L of nisin A) and harvested by centrifugation for 10 min at 4,000 *xg*. After being washed twice with 10 mM PIPES-KOH, 80 mM KCl, pH 6.0, cells were resuspended to OD_{600} 50 in the same buffer. Uptake experiments were performed at final protein concentrations of 2.5–250 mg/mL in 30 mM PIPES-KOH, 30 mM MES-KOH, and 30 mM HEPES-KOH, pH 6.0. Before the transport assays, the cells were equilibrated and energized at 30 ^{o}C for 3 min in the presence of 10 mM glucose plus 5 mM $MgCl_2$. After 3 min, the uptake reaction was started by addition of either [^{14}C]glutamine or [^{3}H]asparagine; the specific radioactivity was adjusted in the different experiments to have disintegrations per minute (d.p.m.) at least ten-fold above the background. The final amino acid concentrations are indicated in the figures, tables and/or figure legends. At given time intervals, samples were taken and diluted in 2 mL ice-cold 100 mM LiCl. Samples were rapidly filtered through 0.45-mm cellulose nitrate filters (Whatman/GE Healthcare), and the filter was washed once with ice-cold 100 mM LiCl. The radioactivity on the filters was determined by liquid scintillation counting.

Results

GlnPQ is essential for amino acid uptake

As previously reported [10,11], we determined the structures and amino acid specificity of SBD1 and SBD2 of GlnPQ from *L. lactis* GKW9000 (**Figure 3.1A**). We obtained the ligand dissociation (K_d) values with ITC measurement. SBD1 binds asparagine with high affinity (K_d = 0.2 μM) as well as glutamine with low affinity (K_d= 92 μM), whereas SBD2 binds only glutamine with high affinity (K_d = 0.9 μM). To determine the contribution of the SBDs on amino acid transport, we deleted the chromosomal GlnPQ-encoding genes (denoted *glnPQ*) in *L. lactis* NZ9000 and complemented the null strain (GKW9000). *In vivo* uptake experiments showed that transport of glutamine no longer occurred in *L. lactis* GKW9000 (**Figure 3.1B**) either complemented or not complemented with GlnPQ-ΔSBD, whereas some residual asparagine uptake activity (due to an endogenous transport system) was present (**Fig. 3.1C**).

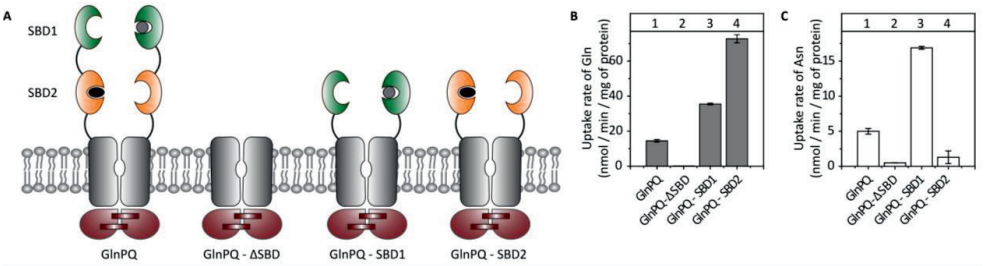

Figure 3.1 | **ABC importer GlnPQ and amino acid transport**. **A** Schematic of GlnPQ, featuring two fused SBDs (SBD1 (green) and SBD2 (orange)) per TMD, as well as of GlnPQ derivatives lacking both SBDs (GlnPQ-ΔSBD) or carrying only a single SBD (GlnPQ-SBD1 and GlnPQ-SBD2). **B** Whole-cell uptake assays with 250 μM [^{14}C]glutamine **C** or 250 μM [^{3}H]asparagine in *L. lactis* GKW9000.

We assessed the relationship between substrate binding and the kinetics of the whole transport process. We examined GlnPQ and 'simplified' transporters with either of the two SBDs deleted (GlnPQ-SBD1 and GlnPQ-SBD2). In GlnPQ, SBD2 is situated nearer to the translocator, whereas SBD1 is situated further. GlnPQ-SBD1 mediates transport of both asparagine (**Figure 3.1C**) and glutamine (**Figure 3.1B**). The maximal transport rate (V_{max}) of glutamine was approximately two-fold higher than that of asparagine (**Figure 3.1B,C**). In contrast, GlnPQ-SBD2 mediates transport of only glutamine, with an approximately two-fold-higher V_{max} than that of GlnPQ-SBD1. The higher rates of transport of GlnPQ-SBD1 and GlnPQ-SBD2 relative to GlnPQ reflect to the more complete and effective transport process with a single SBD. The K_m value for glutamine transport via SBD2 approaches the K_d value for its binding to SBD2. However, the K_m value for asparagine transport via SBD1 is two orders of magnitude higher than the corresponding K_d value, whereas the *K*m value for glutamine transport is approximately seven-fold lower than the K_d value. These remarkable observations suggest that the rate-determining step in the overall translocation can vary with the SBD used and the substrate transported. To incorporate the relation between substrate binding and transport kinetics, we investigated first the conformational dynamics at the single-molecule level.

Cloning, expression and purification of SBD1 and SBD2 derivatives

Crystal structure of the SBDs had been reported in Fulyani *et.al* [10]. Based on that, we generated cysteine mutants for labelling with maleimide-based fluorophores. The distance-dependent transfer of energy between donor and acceptor fluorophores is used to probe the conformational states receptor molecules (**Figure 3.2**). The distances between fluorophores were designed to be between 3 and 6 nm in both states; typical distance changes are between 0.5 and 1.3 nm (**Table 3.1**). Conformational state changes toward ligand binding are not dependent on the position of the dyes. We determined ligand binding by stepwise addition of substrate, monitoring the transition from O to CL based on the crystal structure.

	Open (Å)	Closed (Å)	Distance changes (Å)
SBD1 (A136C-S221C)	48.1	52.7	5.4
SBD1 (T159C-G87C)	44.8	33.8	11.0
SBD2 (T369C-S451C)	49.0	40.1	8.9
SBD2 (H392C-H319C)	47.8	34.8	13.0

Table 3.1 | Expected distances and distance changes of SBDs upon ligand binding based on the crystal structure. The structures of SBD1 and SBD2 in the *apo*protein open state and the closed state with glutamine bound to SBDs are available. Both conformations were overlapped to examine the state changes. The cysteine residues were introduced at surface- exposed, non-conserved positions and identified using the ConSurf Server.

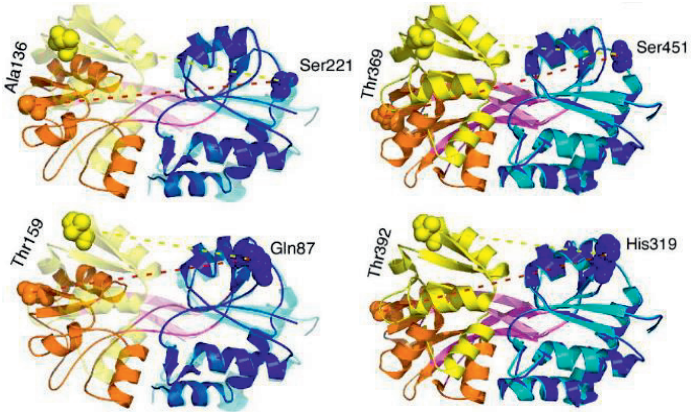

Figure 3.2 | Residues of mutation of SBD1 (left) and SBD2 (right). Crystal structure of the open ligand-free state of SBD1 (PDB 4LA9) and SBD2 (PDB 4KR5), superimposed onto the structure of one of the rigid domains of the closed ligand-bound state SBD1 (PDB is not available when this study was done) and SBD2 (PDB 4KQP). Residues mutated to cysteine for labelling are shown in spheres. Magenta color represents hinge of the two dimers; orange-blue structure represents open conformation of the protein; and yellow-light blue represents close conformation of the protein. Dots are residues to be mutated into cysteine.

The genes encoding SBDs mutants were cloned in *Escherichia coli* DH5α and expressed in *E. coli* BL21. SDS-PAGE shows the protein expression before and after induction with 0.3% L-arabinose. SBD1 has molecular weight of 24 kDa, SBD2 has molecular weight of 25 kDa, while SBD1+2 in tandem has molecular weight of about 50 kDa (**Figure 3.3A**). To analyze the binding mechanism of SBDs, proteins were purified using Ni-NTA (nickel-nitrilotriacetic acid) affinity chromatography, resulting in more than 98%?? pure protein (**Figure 3.3B**).

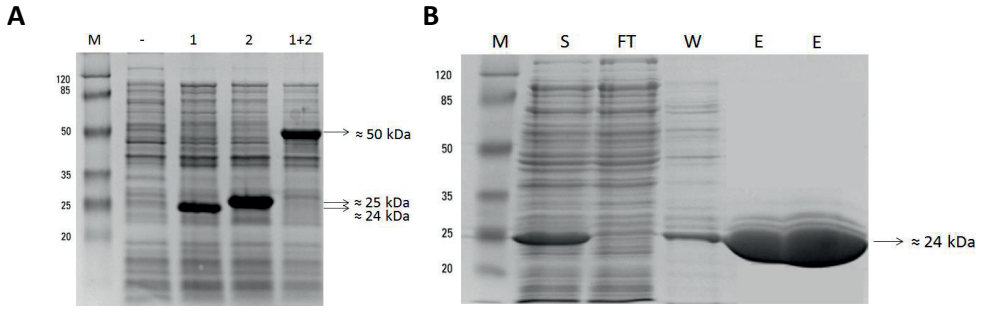

Figure 3.3 | SBDs expression and purification. A SDS-PA gel stained with coomassie brilliant blue of SBD-expressing constructs. M is protein marker; (-) proteins which are expressed naturally by *E. coli* BL21; (1) is SBD1; (2) is SBD2; (1+2) is SBD1+2 tandem. Proteins were expressed upon induction with 0.3% L-arabinose. **B** SDS-PA gel with coomassie brilliant blue staining for the expressed and purified proteins. M is protein marker; S is supernatant of the protein; FT is flow through protein after eluted from Ni-NTA column; W is protein solution after washing with wash buffer; E is protein solution after eluting with elution buffer.

Conformational states at the single-molecule level

We examined the conformational states of the SBDs by smFRET [16] and observed conformational changes as a change in FRET efficiency. FRET is referred to as a `spectroscopic/molecular ruler´, for example to measure the distance between two active sites on a protein that have been labelled with suitable donor-acceptor chromophore. Therefore monitoring the conformational changes through the amount of FRET between the fluorophores. By design, the open conformation of the protein should feature a low FRET efficiency, whereas the closed conformation should have a higher FRET efficiency (**Figure 3.4A**). We determined ligand binding by stepwise substrate addition, monitoring the hypothesized transition from O to CL.

SBD2 labelled at T369C and S451C showed a single population normally distributed around an apparent lower FRET value (E*) of 0.52 (**Figure 3.4B**). Saturating concentrations of 50 mM glutamine (more than ten-fold K_d) shifted the population to a high FRET state (E* = 0.68), whereas we observed both states at K_d concentrations around the of SBD2 for glutamine. In agreement with expectations from crystal structures, the low FRET state corresponds to the O state, whereas the high FRET state is indicative of the CL state.

SBD1 labelled at T159C and G87C shifted from a low-FRET (O) conformation to the CL state upon binding of asparagine. In contrast to the effect of asparagine, saturating concentrations of glutamine shifted SBD1 from the open state at E* = 0.63 to an intermediate value of E* = 0.74 (**Figure 3.4D**), which is lower than that observed with asparagine (E* = 0.83) (**Figure 3.4C**). Given the time resolution of alternating-laser excitation (ALEX) experiments [17,18] and the width of the FRET distributions, this is likely to be caused by fast conformational dynamics between an O and a partial closed (PC) or C state on the sub-millisecond time scale. In the presence of glutamine, the SBD1 population gradually shifted to higher FRET values, and the

peak had its maximal width at concentrations close to the K_d value. The apparent K_d values of SBDs can be determined from the ratio of the areas (CL/(O+CL)) between open and closed ligand-bound population as the function of ligand concentration (**Figure 3.4B-D**, right panel). The dissociation constant value reported here is in excellent agreement with values determined by ITC approach as reported in reference number 11.

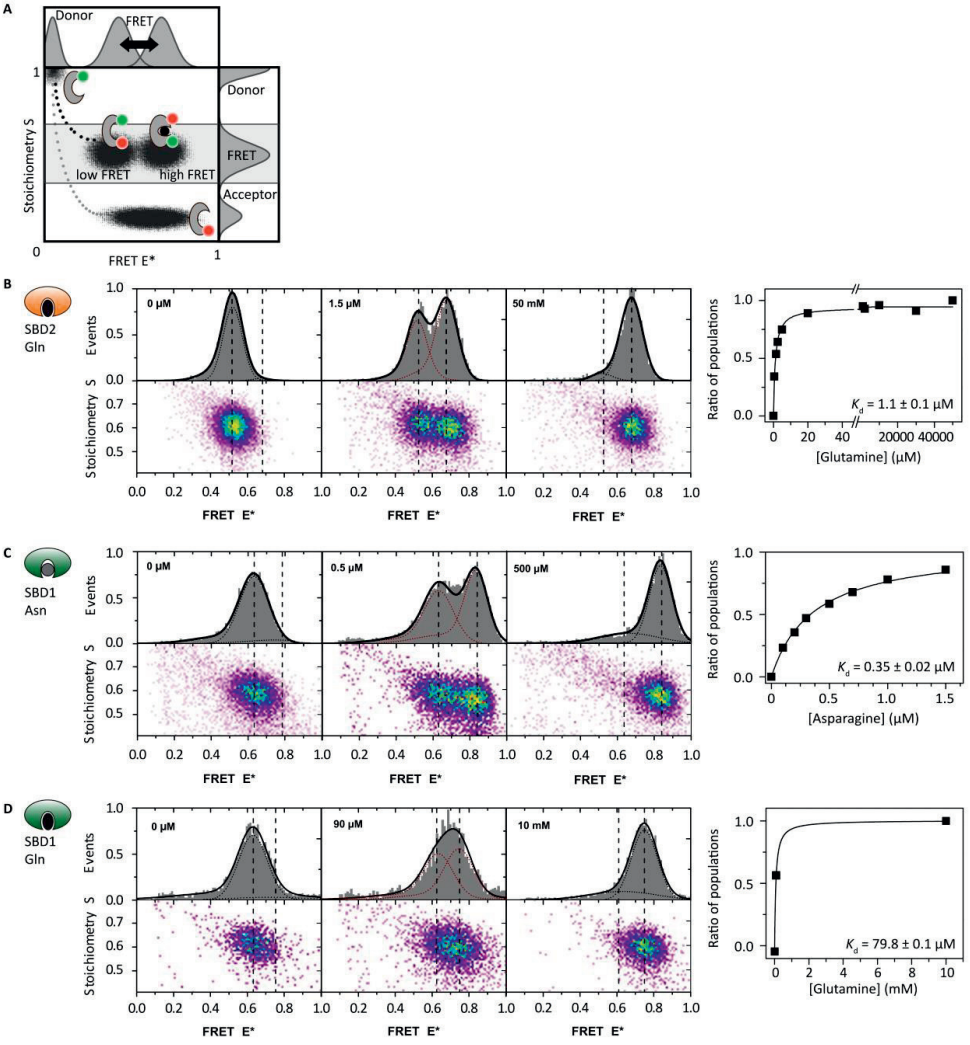

Figure 3.4 | ALEX histogram of SBDs. A ALEX in 2D histogram separating FRET efficiency E* and stoichiometry S. Separation of stoichiometry distinguish populations donor-only, acceptor-only, donor-acceptor; while E* is a measure for inter-probe distance. **B** (left) ALEX histograms for SBD2 labelled with Cy3B- and Atto647Nmaleimide. The one-dimensional E*-histogram displays values in the range of S = 0.4-0.8 (donor-acceptor labelling). E* is characteristic for the conformational state of the proteins, for instance the open-unliganded state has low FRET while the closed-liganded has high FRET SBD2 shows an open state at E* = 0.52 and a closed high FRET state at E* = 0.68 in the presence of saturating concentrations of glutamine. At substrate concentrations around the K_d,

two populations can be resolved. (right) Ligand dissociation constants (K_d) derived from obtaining the ratio of areas (CL/(O+CL)) between open and closed ligand-bound populations as the function of ligand concentration. **C** (left) ALEX histograms for SBD1 labelled with Cy3B- and Atto647Nmaleimide. SBD1 shows an open state at E* = 0.63 and a closed high FRET state at E* = 0.83 at saturating concentrations of asparagine. At substrate concentrations around the K_d, both populations can be resolved. **D** Upon addition of glutamine, E* in SBD1 gradually shifts from a low FRET state at E* = 0.63 to a state with E* = 0.74, which is lower than what is observed for asparagine. K_d values determination is not provided.

To verify that the cysteine mutations do not influence SBD function, we analyzed one extra double cysteine derivative of SBD1 and SBD2 by FRET which are SBD1 A136C S221C and SBD2 T369C S451C respectively (**Figure 3.5**). The results of both double-cysteine derivatives of SBD1 and SBD2 show consistent results. SBD2 (T392C H319C) labelled with Cy3B- and Atto647N-maleimide occurs from the open state as the unbound state and converts to full closed bound state with glutamine. SBD1 (A136C S221C) labelled with Cy3B- and Atto647N-maleimide converts from open state to closed state with asparagine via fast transitions. Two distinguished population in the K_d concentration cannot be resolved anymore, because the distance change between A136 and S221 is smaller than that of SBD1 (T159C G87C)

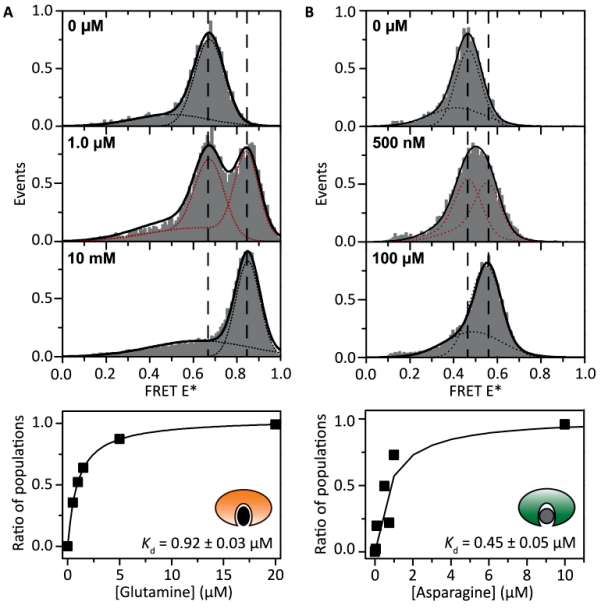

Figure 3.5 | Influence of the cysteine mutations on the ligand dissociation constants of SBD1 and SBD2. A SBD2 transits from O (E* = 0.69) to CL (E* = 0.85) at the indicated concentrations of glutamine; the *K*d = 0.92±0.03 µM. **B** SBD1 transits from E* = 0.46 to 0.56 in the presence of asparagine; the *K*d = 045±0.04 µM with faster transition then the other cysteine mutant. SBD1 data with glutamine bounded is not provided, assuming it has the same rapid transitions.

We conclude from the smFRET measurements in solution that (i) apo-SBD1 and apo-SBD2 are predominantly (>95%) in the open conformation; (ii) SBD1 and SDB2 transit to a closed state upon binding of high-affinity ligands, presumably via an induced-fit mechanism; and (iii) binding of glutamine to SBD1 is of low affinity and induces fast transitions between two distinct conformational states.

Binding mechanism of SBD1 and SBD2 at the single-molecule level

In the induced-fit mechanism [19], the ligand-bound conformation (CL) is formed only after interaction with a ligand binding which leads to specific induced structural changes (**Figure 3.6**). In the conformational-selection model, the unbound protein (O) explores to bound conformations (C) with predominantly fast dynamics [13,15]. Ligand binding, in the conformational-selection model, stabilizes the C form and thereby drives the equilibrium to the CL form.

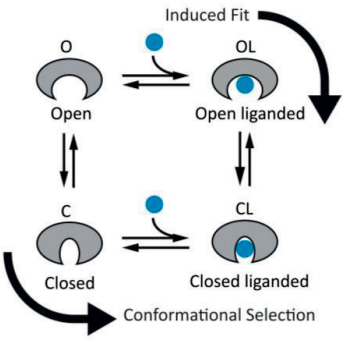

Figure 3.6 | SBDs in a known ligand binding mechanisms. Conformational transitions in SBDs according to the induced-fit or the conformational selection binding mechanisms proportional to ligand concentration.

To investigate the dynamics of conformational changes in SBDs, we carried out smFRET experiments with surface-bound proteins, using a confocal scanning microscope (**Figure 3.7A**) [20]. In accordance with the ALEX experiments, both SBDs were predominantly in the open conformation when no ligand was present (SBD2 in **Figure 3.7B**; SBD1 in **Figure 3.7C**); representative fluorescent time traces of the *apo*-proteins showed E* values of ~0.50 for SBD2 and ~0.63 for SBD1, which we assign to the open ligand-free state of the proteins. Importantly, in the absence of substrate, we observed rare transitions to a state with FRET efficiencies of ~0.70 for SBD2 and ~0.83 for SBD1, which are identical to values for the closed conformation observed with the high-affinity ligands. The average dwell times of the closed ligand-free state (τ_{closed}) are ~60 ms for SBD2 and ~240 ms for SBD1 which are identified by plotting time traces with ligand concentration. In contrast, we could not observe the closing state of the single molecule of SBD1 when binding low-affinity ligand glutamine (**Figure 3.7D**). This indicates the rapid transitions between open and closed states lower than our technique

lifetime resolution ~1ms. These fast transitions are distinct from the intrinsic slow transitions. This implies that glutamine shortens the lifetime of the closed state. With our current time resolution, we cannot rule out that SBD1 shows either fast sub-millisecond dynamics between O and CL or a structurally distinct partially closed state when the low-affinity ligand is bound.

To determine which binding mechanisms contemplated in SBDs, we investigated the lifetime of the open and closed conformations as a function of substrate concentration. We detected substrate concentration is dependent to the closing-rate whereas substrate concentration is independent lifetime of the open conformation. The lifetimes of the closed state were similar in the absence and presence of high-affinity ligand for both SBD2 (glutamine) and SBD1 (asparagine), thus indicating that the ligand does not 'stabilize' the closed conformation relative to the transition state (**Figure 3.7B** for SBD2). In contrast, we found that the transitions between open and closed states were extremely fast (<1 ms) when the low-affinity ligand glutamine binds to SBD1 (**Figure 3.7C**). This implies that glutamine shortens the lifetime of the closed state. With our current time resolution, we cannot rule out that SBD1 shows either fast sub-millisecond dynamics between O and CL or a structurally distinct partially closed state when the low-affinity ligand is bound.

We conclude from the smFRET measurements on surfaces that (i) SBD1 and SBD2 display intrinsic dynamics to the closed conformation; (ii) the binding of high-affinity ligands enhances transition of SBD1 and SBD2 to the closed state more frequently but without relative stabilization of this conformation; (iii) binding of glutamine to SBD1 shortens the closed-state lifetime; and (iv) in all cases, the binding reaction is dependent on the substrate addition, whereas the release reaction is independent of ligand concentration. Collectively, these data are compatible with the induced-fit mechanism, despite the unique feature of intrinsic closing of the binding sites.

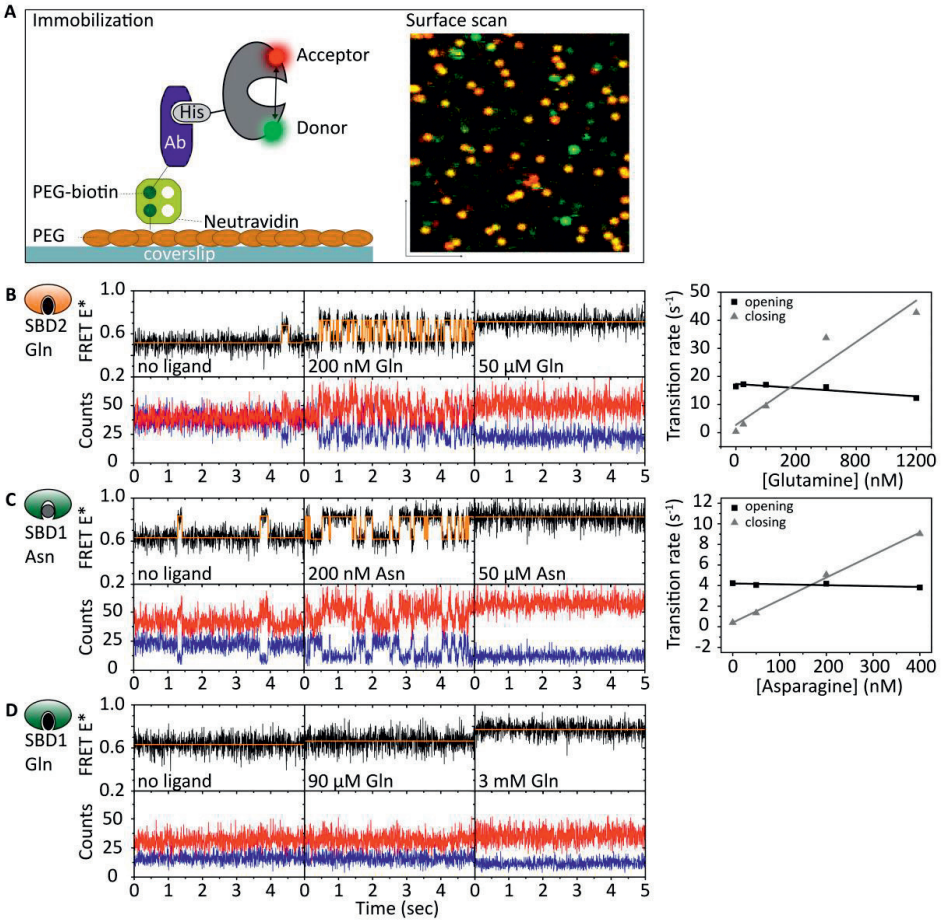

Figure 3.7 Single-molecule dynamics of surface-tethered SBDs probed by confocal scanning smFRET. A (left) Schematic showing the immobilization of SBDs to the surface: histidine-tagged, dye-labelled SBDs were immobilized to a PEG-biotin–coated surface in a flow cell by biotinylated anti-His_5 antibody (Ab). (right) A typical surface scan is shown in false-color representation at right (orange, double-labelled SBDs; green, SBDs with donor fluorophore only; red, SBDs with acceptor fluorophore only). **B-D** Representative fluorescence time traces (blue, donor signal; red, acceptor signal; black, FRET signal; orange, fit) of SBDs labelled with Cy3B- and Atto647N-maleimide for SBD2 (T369C S451C) with the indicated concentrations of glutamine **B**, SBD1 (T159C G87C) with asparagine **C** and SBD1(T159C G87C) with glutamine **D**. Distribution between opening ($\tau_{opening}$) and closing ($\tau_{closing}$) rate constants of SBD2 (**B** right) and SBD1 (**C** right), determined from the transition rates of surface-immobilized molecules as a function of substrate concentration. The $\tau_{closing}$ was obtained from the slope of the linear fit and $\tau_{opening}$ follows zero-order kinetics.

Cooperativity of fused SBDs toward ligand binding

To observe the cooperativity between SBD1 and SBD2 (**Figure 3.8**), each SBD was analyzed when fused to another SBD. Both pairs of mutation were engineered in the fused protein. SBD1 labelled in (Q87CT159C) as the tandem protein showed clear populations of both the

open and closed state. Without ligand, the distance between the two fluorophores gave E* = 0.57. After addition of saturated concentration of asparagine, E was shifted to 0.78. Those E* values were lower than E* values observed in SBD1 protein because of there is difference in the folding protein which might due to slightly different folding of the fused SBDs. Glutamine is bound in the SBD1 tandem protein with high affinity and fast transitions. Two distinct population between open and closed is not observed. Whereas in SBD2 (S451C T369C) as the tandem showed distinguished open and closed state. These behavior fits perfectly with the single SBDs mechanism. Therefore, we concluded that there are no significant distinctness of the cooperation between two SBDs, either in the binding affinity as well as in binding mechanism. In the publication of this study, we reported the effect of having two SBDs with competition of substrate transport. We found that high affinity binding proceeds and the lifetime of the closed state of the substrate-binding domain is a determining factor for the rate of transport. The closed state of the SBD will interact with the TMD resulting transport of the substrate. The opening of the substrate-binding domains seems to be linked to the transition of the TMD from inward to outward facing conformation.

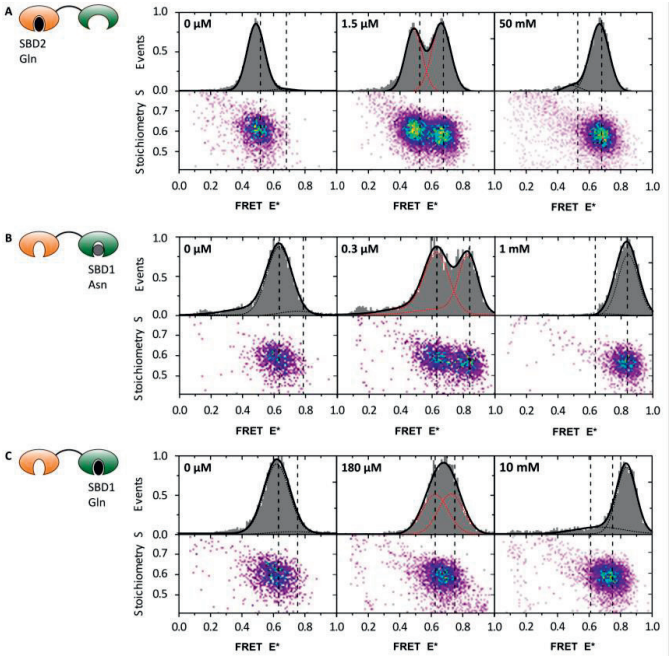

Figure 3.8 | ALEX histogram of fused SBD1 SBD2. A ALEX histograms for SBD12 (S451C T369C) labelled with Cy3B- and Atto647N in the SBD2. E* is characteristic for the conformational state of the proteins, for instance the open-unliganded state has low FRET while the closed-liganded has high FRET SBD2 shows an open state at E* = 0.52 and a closed high FRET state at E* = 0.68 in the presence of saturating concentration of glutamine. At substrate concentrations around the K_d, two populations can be resolved. **B** SBD1 shows an open state at E* = 0.63 and a closed high FRET state at E* = 0.83 at saturating concentrations of asparagine. At substrate concentrations around the K_d, both populations can be resolved. **C** Upon addition of glutamine, E* in SBD1 gradually shifts from a low FRET state at E* = 0.63 to a state with E* = 0.74, which is lower than what is observed for asparagine. Fused SBD1 and SBD2 does not significantly interfere the conformational state changes upon substrate binding.

Interaction between closed state of SBD2 with the translocator

It is still debated how and which states of SBDs dock on the translocator complex [21,22]. GlnPQ is an excellent model system to address these questions because (i) it has multiple SBDs that can be competing with each other for interaction with the TMDs; (ii) the covalent linkage of the SBDs to the TMD ensures a high and fixed concentration of receptor protein available for transport; and (iii) the selectivity of the SBDs is different, thus allowing the paths of transport from SBD1 and SBD2 and their mutual influence to be dissected. Because both SBD1 and SBD2 show intrinsic closing without involvement of the ligand, we can directly probe whether the closed ligand-free state of, or example, SBD2 competes with SBD1-facilitated transport of asparagine, the amino acid that is not bound by SBD2.

We designed a mutation on SBD2 that abolishes glutamine binding (binding site of SBD2 and the position of the D417F substitution shown in **Figure 3.9A**). D417F is no longer transporting glutamine SBD2 (D417F) did not undergo detectable conformational changes upon addition of 20 mM glutamine (**Figure 3.9B**). With surface-immobilized protein, we found that SBD2 (D417F) is solely in the open conformation and lacks the capacity to transit intrinsically to the closed state (**Figure 3.9C**). Over periods of 30–60 s we did not find a single closing event, thus indicating that the protein is trapped in the open ligand free state.

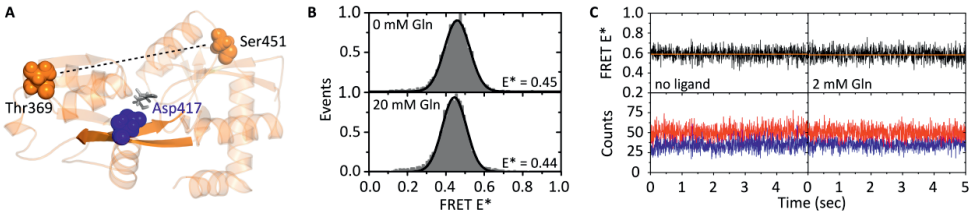

Figure 3.9 | The closed ligand-free state of SBD2 inhibits transport via SBD1. **A** Crystal structure of the closed state of SBD2 showing the positions (T369C and S451C, orange spheres) used for fluorophore labelling (as in **Figure 3.2**). Asp417 (blue spheres); glutamine (gray sticks) and the hinge region (two nontransparent B-sheets) are depicted. **B** SBD2 (D417F) has lost the capacity to transit from the open state to a closed state. E*-S histograms of SBD2 (D417F) labelled with Cy3B and Atto647N show a single distribution for the unliganded state at E* = 0.45 (top). Addition of 20 mM glutamine (bottom) does not alter the E* value or the width of the distribution. Thus, SBD2 (D417F) does not undergo detectable conformational changes, irrespective of the presence of ligand. **C** smFRET analysis of SBD2 (D417F) labelled at Cys369 and Cys451 with Cy3B- and Atto647N-maleimide.

We investigated the impact of the D417F mutation in the context of the full-length transporter (**Figure 3.10A**). We found that GlnPQ (D417F) has about 50% of the glutamine-uptake activity of GlnPQ (**Figure 3.10B**). Strikingly, the rate of asparagine uptake by GlnPQ (D417F) was almost three-fold higher than that of GlnPQ, although both proteins were expressed at similar levels (**Figure 3.10B** top bar). This suggests that the open ligand-free conformation of SBD2 (D417F) no longer (or poorly) interacts with the TMDs. It implies that in GlnPQ, SBD2 competes with SBD1 for delivery of the substrate to the TMD, even in the absence of the SBD2 substrate.

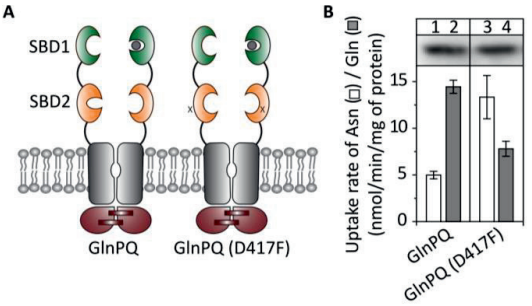

Figure 3.10 | The closed ligand-free state of SBD2 inhibits transport via SBD1. **A** Schematic of GlnPQ and GlnPQ (D417F). **B** Transport assay with 250 MM [^{3}H]asparagine (open bars) and [^{14}C]glutamine (filled bars) in *L. lactis* GKW9000 complemented with either GlnPQ or GlnPQ (D417F). Error bars, s.e.m. calculated from independent cell cultures (*n* = 3).

Conclusion

The constructs of the mutation in SBD1, SBD2, and SBD1+2 tandem were successfully generated and expressed. The SBD proteins were also successfully purified and labelled with Cy3B (donor) and Atto647N (acceptor) at strategic positions. As indicated for the mutant SBD2 S451C T369C, the static crystal structures suggest that the distance of the fluorophore was 4.9 nm (low FRET) for the open and 4.0 nm for the closed conformation (high FRET). Our results showed only a single peak in the absence of the ligand as well as for saturating concentrations of glutamine. Close to the K_d-value of ~1.0 μM, clear populations of both species can be observed. Similar results were found for different labelling positions in GlnPQ-SBD2 (mutant H319CT392C), indicating a similar binding mechanism independent of the labelling position.

Substrates are captured via SBDs, which then undergo a conformational change to a closed state, according to the induced-fit mechanism. Occasionally, the SBDs of GlnPQ intrinsically close. Furthermore, the lifetime of the closed state varies with the SBD and substrate, and C or CL inhibit transport differently.

In summary, we find that high-affinity binding proceeds via the induced-fit mechanism, and the lifetime of the closed state of the substrate-binding domain is a determining factor for the rate of transport. The opening of the substrate-binding domains seems to be linked to the transition of TMD from inward to outward facing. Moreover, we find that SBDs compete with each other in the closed state, but the extent of inhibition is stronger without ligand. Our findings contribute to a general understanding of the mechanism of ABC transport, information obtained for the first time, to our knowledge, by single-molecule structural studies and a kinetic analysis of substrate translocation.

References

1. Higgins, C.F. (1992) ABC transporters: from microorganisms to man. *Annu. Rev. Cell Biol.* 8, 67–113
2. Biemans-Oldehinkel, E., Doeven, M.K., Poolman, B. (2006) ABC transporter architecture and regulatory roles of accessory domains. *FEBS Lett.* 580, 1023–1035
3. Biemans-Oldehinkel, E., Mahmood, N.A., Poolman, B. (2006) A sensor for intracellular ionic strength. *Proc. Natl. Acad. Sci. U.S.A.* 103, 10624–10629
4. Doeven, M.K., Abele, R., Tampe, R., Poolman, B. (2004) The binding specificity of OppA determines the selectivity of the oligopeptide ATP-binding cassette transporter. *J. Biol. Chem.* 279, 32301–32307.
5. van der Heide, T., Poolman, B. (2000) Osmoregulated ABC-transport system of *Lactococcus lactis* senses water stress via changes in the physical state of the membrane. *Proc. Natl. Acad. Sci. U.S.A.* 97, 7102–7106
6. Sharom, F.J. (2008) ABC multidrug transporters: structure, function and role in chemoresistance. *Pharmacogenomics.* 9, 105–127
7. Nagao, K., Kimura, Y., Mastuo, M., Ueda, K. (2010) Lipid outward translocation by ABC proteins. *FEBS Lett.* 584, 2717–2723
8. Holland, I.B., Cole, S.P., Kuchler, K., Higgins, C.F. (2003) ABC Proteins: from Bacteria to Man *Academic Press*.
9. van der Heide, T., Poolman, B. (2002) ABC transporters: one, two or four extracytoplasmic substrate-binding sites? *EMBO Rep.* 3, 938–943
10. Fulyani, F., Wolters, G.K.S., Zagar, A.V., Guskov, A., Slotboom, D.J., Poolman, B. (2013) Functional diversity of tandem substrate-binding domains in ABC transporters from pathogenic bacteria. *Structure* 21, 1879–1888
11. Schuurman-Wolters, G.K., Poolman, B. (2005) Substrate specificity and ionic regulation of GlnPQ from *Lactococcus lactis*: an ATP-binding cassette transporter with four extracytoplasmic substrate-binding domains. *J. Biol. Chem.* 280, 23785–23790
12. Berntsson, R.P.A., Smits, S.H.J., Schmitt, L., Slotboom, D.J., Poolman, B. (2010) A structural classification of substrate-binding proteins. *FEBS Lett.* 584, 2606–2617
13. Tang, C., Schwieters, C.D., Clore, G.M. (2007) Open-to-closed transition in apo maltose-binding protein observed by paramagnetic NMR. *Nature* 449, 1078–1082
14. Csermely, P., Palotai, R., Nussinov, R. (2010) Induced fit, conformational selection and independent dynamic segments: an extended view of binding events. *Trends Biochem. Sci.* 35, 539–546

15. Kim, E., Lee, S., Jeon, A., Choi, J.M., Lee, H.S., Hohng, S., Kim, H.S. (2013) A single-molecule dissection of ligand binding to a protein with intrinsic dynamics. *Nat. Chem. Biol.* 9, 313–318

16. Ha, T., Enderle, T., Ogletree, D.F., Chemla, D.S., Selvin, P.R., Weiss, S. (1996) Probing the interaction between two single molecules: fluorescence resonance energy transfer between a single donor and a single acceptor. *Proc. Natl. Acad. Sci. U.S.A.* 93, 6264–6268

17. Kapanidis, A.N., Lee, N.K., Laurence, T.A., Doose, S., Margeat, E., Weiss, S. (2004) Fluorescence-aided molecule sorting: analysis of structure and interactions by alternating-laser excitation of single molecules. *Proc. Natl. Acad. Sci. U.S.A.* 101, 8936–8941

18. Lee, N.K., Kapanidis, A.N., Wang, Y., Michalet, X., Mukhopadhyay, J., Ebright, R.H.,Weiss, S. (2005) Accurate FRET measurements within single diffusing biomolecules using alternating-laser excitation. *Biophys. J.* 88, 2939–2953

19. Mao, B., Pear, M.R., Mccammon, J.A., Quiocho, F.A. (1982) Hinge-bending in L-arabinose- binding protein: the venus-flytrap model. *J. Biol. Chem.* 257, 1131–1133

20. van der Velde, J.H.M., Ploetz, E., Hiermaier, M., Oelerich, J., de Vries, J.W., Roelfes, G., Cordes, T. (2013) Mechanism of Intramolecular Photostabilization in Self-Healing Cyanine Fluorophores. *Chem. Phys. Chem.* 14, 4084–4093

21. Bao, H., Duong, F. (2013) ATP alone triggers the outward facing conformation of the maltose ATP-binding cassette transporter. *J. Biol. Chem.* 288, 3439–3448

22. Khare, D., Oldham, M.L., Orelle, C., Davidson, A.L., Chen, J. (2009) Alternating access in maltose transporter mediated by rigid-body rotations. *Mol. Cell.* 33, 528–536

Chapter 4

Conformational dynamics of the ABC transporter McjD seen by single-molecule FRET

Florence Husada[1], Kiran Bountra[2,3], Konstantinos Tassis[1], Marijn de Boer[1], Maria Romano[2,3], Sylvie Rebuffat[4], Konstantinos Beis[2,3], and Thorben Cordes[1,5]

[1] Molecular Microscopy Research Group, Zernike Institute for Advanced Materials, University of Groningen, Nijenborgh 4, 9747 AG Groningen, The Netherlands

[2] Department of Life Sciences, Imperial College London, Exhibition Road, London, South Kensington, SW7 2AX, United Kingdom

[3] Rutherford Appleton Laboratory, Research Complex at Harwell, Didcot, Oxfordshire, OX11 0FA, United Kingdom

[4] Communication Molecules and Adaptation of Microorganisms Laboratory, Sorbonne University, Mueum National d'Histoire Naturelle, Centre National de la Recherche Scientifique, CP 54, 57 rue Cuvier 75005 Paris, France

[5] Physical and Synthetic Biology, Faculty of Biology, Ludwig Maximilians-Universität München, Großhadernerstrasse 2-4, 82152 Planegg-Martinsried, Germany F.A.H. conducted research (surface preparation, fluorescence labelling, smFRET experiments), analyzed data, produced figures and contributed writing of the towards manuscript.

Abstract

ABC transporters utilize ATP for export processes to provide cellular resistance against toxins, antibiotics, and harmful metabolites in eukaryotes and prokaryotes. Based on static structure snapshots, it is believed that they use an alternating access mechanism, which couples conformational changes to ATP binding (outward-open conformation) and hydrolysis (inward-open) for unidirectional transport driven by ATP. Here, we analyzed the conformational states and dynamics of the antibacterial peptide exporter McjD from *Escherichia coli* using single-molecule Förster resonance energy transfer (smFRET). For the first time, we established smFRET for an ABC exporter in a native-like lipid environment and directly monitor conformational dynamics in both the transmembrane- (TMD) and nucleotide-binding domains (NBD). With this, we unravel the ligand dependences that drive conformational changes in both domains. Furthermore, we observe intrinsic conformational dynamics in the absence of ATP and ligand in the NBDs. ATP binding and hydrolysis on the other hand can be observed via NBD conformational dynamics. We believe that the progress made here in combination with future studies will facilitate full understanding of ABC transport cycles.

Key words: antibacterial peptide ABC transporter, membrane protein, ABC exporter, type I ABC transporter, transporter structure

Abbreviations: ABC, ATP-binding cassette; NBD, nucleotide binding domain; TMD, transmembrane domain; SBD, substrate binding domain; ALEX, alternating laser excitation; ATP, adenosine triphosphate; DA, donor-acceptor; FRET, Förster resonance energy transfer; SEC, size-exclusion chromatography; smFRET, single-molecule FRET.

Introduction

ABC transporters are essential membrane proteins found in both eukaryotic and bacterial cells that facilitate the uphill transport of ions and chemically diverse compounds in an ATP-dependent manner [1]. They are involved in numerous cellular processes including nutrient import, metal homeostasis, detoxification and antigen processing. The ABC exporter family plays a major role for the extrusion of toxic compounds and has relevance for human diseases, tumor resistance and bacterial virulence. All ABC transporters share a common architecture consisting of a transmembrane domain (TMD) for substrate-recognition and transport, and a nucleotide binding domain (NBD) that converts the chemical energy of ATP into conformational changes for transport [2]. The structures of several homodimeric [3-5] and heterodimeric ABC transporters [6,7] revealed distinct conformations and suggest, in combination with biophysical studies (e.g., EPR and NMR) [8-12] that they undergo large conformational changes during transport. Their complex architecture is, however, a fundamental hurdle to fully understand the coupling between conformational changes, substrate-binding, ATP-binding and –hydrolysis and transport. Such detailed mechanistic models of transport would not only require the knowledge of conformational states from static structural snapshots but also their interconversion dynamics.

Based on the available structural, biophysical and biochemical data for exporters, two transport mechanisms have been proposed, the alternating access mechanism [3,4,8,13] and the outward-only mechanism [5]. ABC exporters that use the alternating access mechanism switch between inward- and outward-facing states with transmembrane helices intertwining, which exposes the ligand binding site alternatively to the inside or outside of the membrane, a process that is believed to couple to ATP-binding and hydrolysis. The outward-only mechanism was proposed in light of the structural and functional data of the lipid-linked oligosaccharide flippase PglK from *Campylobacter jejuni* [5]; the inward-facing conformation is not required for substrate translocation since it can be directly recruited from the membrane and ATP hydrolysis at the NBDs is transmitted to the TMD to drive substrate release.

ABC transporters that utilize the alternating access mechanism undergo large conformational changes during the transport cycle suggested by crystal structures [3] and EPR-based Double Electron Electron Resonance (DEER) measurements [12,15,16] of the lipid A flippase MsbA from *E. coli.* Although, the DEER measurements proposed that ATP triggers the opening of the TMD to the periplasmic side for release of the substrate, it is unclear how precisely these changes are coupled to ATP binding and hydrolysis. It has been proposed that homodimeric transporters employ this mechanism. Opening of the TMD of heterodimeric ABC transporters is coupled to ATP hydrolysis rather than binding due to the nature of their NBDs that contain a consensus and degenerate site for ATP hydrolysis [9,10,16].

In contrary, we have shown that the antibacterial peptide ABC transporter McjD, which confers bacterial cells with self-immunity against the antibacterial peptide MccJ25, adopts

distinct conformations to other bacterial exporters including MsbA [8,13]. We have determined the crystal structure of McjD in two distinct conformations, apo inward-occluded and nucleotide-bound outward occluded [8,13]. In both conformations, the TMD is occluded to either side of the membrane that was also supported by PELDOR measurements in bicelles and predictive cysteine cross-linking in *E. coli* membranes [8]. Occluded conformations have also been reported for other ABC transporters including the peptidase-containing ATP-binding cassette transporter (PCAT1) from *Clostridium thermocellum* [17], PglK from *C. jejuni* [5] and the Type-1 secretion system ABC transporter AaPrtD from *Aquifex aeolicus* [18]. Unlike MsbA and PglK, McjD appears to be unique since it does not display any domain intertwining in the presence or absence of nucleotides. We have biochemically shown that McjD adopts a transient outward-open conformation that it is probably not long lived or well populated to be trapped by PELDOR [8]. The NBDs of McjD do not completely disengage compared to MsbA or PglK. Although, both MsbA and McjD utilize the alternating access mechanism for export of their substrate, the overall mechanism is not fully conserved. MsbA has been shown to adopt stable inward- and outward-open TMD conformations during the transport cycle [12,15,16] while McjD only samples these states transiently [8].

So far, however, all the conformations that have been reported for ABC transporters are static and do not provide insights on the conformational changes and dynamics that govern the movement of NBDs upon ATP binding and hydrolysis or that of the TMDs during substrate transport across the membrane bilayer. In recent years, it has, however, become apparent that transporters show conformational dynamics and that those have to be understood and characterized. For this single-molecule Förster-resonance energy transfer (smFRET) has been used to monitor these conformational dynamics of transporters, e.g., the P-type Ca^{2+}-ATPase (LMCA1) from *Listeria monocytogenes* [19], secondary transporters such as the aspartate/Na^+ symporter from *Pyrococcus horikoshii* [20] and the leucine/Na^+ symporter LeuT from *Aquifex aeolicus* [21]. While there are also smFRET studies of ABC importers regarding the conformational dynamics of the substrate binding domains (SBDs) [22] or interactions of SBD-TMD [23], there are no studies of conformational dynamics and crosstalk between TMDs and NBDs in ABC exporters in native-like lipid environment [16].

Here, we have analyzed the antibacterial peptide exporter McjD from *E. coli* in proteoliposomes using smFRET via labelling of specific residues in the TMD and NBDs to monitor the conformational dynamics during the transport cycle. The developed assay has the potential to provide full understanding of the transport mechanism and can be used for both ABC importers and exporters. In this study, it was used to answer the following mechanistic questions regarding McjD: i) How exactly is ATP binding or hydrolysis coupled to the opening of the TMD? In McjD crystal structures and PELDOR data in the presence of the ATP-analogue adenosine 5'-(β,γ-imido)triphosphate (AMPPNP) (mimicking ATP binding) and ADP-vanadate (mimicking ATP hydrolysis) could not reveal an open cavity [8,13]. ii) What are the intrinsic and ligand-induced conformational dynamics of McjD as a model system for ABC exporters and on what timescales do they occur?

To answer these questions, we have studied McjD reconstituted in liposomes under equilibrium conditions to obtain a picture of the stable conformational states, and non-equilibrium conditions to understand how conformational changes are triggered by substrates using smFRET. We demonstrate that the NBDs have intrinsic conformational dynamics in their apo state on the 100 ms timescale, while the TMDs remain static. ATP-binding and hydrolysis on the other hand takes much longer and it is observed via NBD conformational dynamics on the timescale of several seconds, which is a value compatible with reported biochemical data on McjD. Our assays also show that the TMD remains occluded in the presence of nucleotides and only opens when both the substrate MccJ25 and ATP are present. Our study represents major advances in using smFRET for mechanistic studies of ABC transporters in a native environment. Furthermore, this is the first report showing that an ABC exporter requires both ATP and substrate binding to drive the formation of the outward-open conformation. Thus, we propose that opening of the McjD cavity is tightly coupled to both ATP and MccJ25 binding and present a refined model for the transport cycle.

Methods

Gene isolation, protein expression and purification

The full length cys-less *mcjD* was subcloned into the pET-28b vector with a non-cleavable His_8-tag from the pWaldo-McjD-GFPd vector [13]. Single cysteine mutations at positions Y64, L67 and C547 were introduced using the Quick Change Site-Directed mutagenesis kit (Agilent Technologies). Expression and purification of the McjD mutants were performed as previously described [13,8]. McjD mutants for FRET were purified in a final buffer of 20 mM TrisCl pH 7.5, 150 mM NaCl and 0.03 % (w/w) DDM.

MccJ25 purification

Peptide MccJ25 was expressed and purified as previously described in Zirah *et al*. 2011 [24]. MccJ25 was produced from E.coli K12 MC4100 harboring cultures with plasmid pTUC202 and then purified from the supernatants by solid phase extraction using Sepak Plus C8 cartridges (Waters). The fractions containing the peptide were further purified by HPLC on a Capcell reverse-phase C18 semipreparative column (300 × 7 mm, 5 µm, 120 Å; Shiseido).

Protein labelling

For labelling, 200 µg McjD was incubated with 1 mM DTT for 30 min on ice to fully reduce oxidized cysteines. The protein was passed through a Superdex-200 column (GE Healthcare) equilibrated in deoxygenized buffer of 20 mM TrisCl pH 7.5, 150 mM NaCl, and 0.03% (w/w) DDM. Fractions containing McjD were pooled and diluted at a final concentration of 5 nmol. For labelling, Alexa Fluor 555 C2 Maleimide (Thermo Fisher Scientific) and Alexa Fluor 647 C2 Maleimide (Thermo Fisher Scientific) were added to McjD at a ratio of 1:4:5 for McjD: Alexa 555: Alexa 647. The protein mixture was degassed under argon for 5 min followed by labelling for 5 hours at 277 K with gentle shaking. The protein was passed through a 2 mL Zeba spin desalting column (Thermo Fisher Scientific) equilibrated in the same freshly deoxygenized buffer. Labelled McjD was subsequently applied into a Superdex-200 column (GE Healthcare). Fractions with optimal labelling efficiency were collected for reconstitution.

ATPase assays

The ATPase activity of the labelled McjD-63C, McjD-67C and McjD-547C were measured as described previously [13]. Ligand-induced ATPase activity was measured in the presence of 0.5 mM MccJ25.

Preparation of biotynilated liposomes

Biotinylated lipids were prepared from a synthetic lipid mixture of 67% (w/w) 1,2-dioleoyl-sn-glycero-3-phosphoethanolamine (DOPE), 23% (w/w) 1,2-dioleoyl-sn-glycero-3-phospho-(19-rac-glycerol) (DOPG), 7% (w/w) cardiolipin, and 3% (w/w) 1,2-dioleoyl-sn-glycero-3-phosphoethanolamine-N-(cap biotynil) (biotin-DOPE) (Avanti). Approximately 100 µL of lipid mixture at 20 mg/mL dissolved in chloroform was dried under vacuum rotary evaporation 30 ^{o}C for about 30 min until a dry film was observed. 1 mL diethyl ether was used to dissolve the lipid film and the lipid mixture was further dried by evaporation. Lipids were then hydrated in a buffer containing 20 mM TrisCl pH 7.5, 150 mM NaCl to a final concentration of 20 mg/mL (w/v). The lipid suspension was sonicated on ice for 16 cycles (15s on, 45s off) with an amplitude setting of 70% to generate unilamellar vesicles. Vesicles were flash frozen in liquid nitrogen and subsequently thawed slowly at room temperature. The freeze-thaw process was repeated two times for homogenous product. Prepared liposomes were aliquoted and stored in -80 ^{o}C.

Reconstitution of McjD in proteoliposomes

Labelled McjD mutants were reconstituted in either polar lipids for ALEX measurements or biotinylated proteoliposomes for surface measurements using the rapid dilution method as previously described [2]. Synthesized liposome was sonicated in water bath for 15 minutes to dissolve the lipid. Labelled McjD was added at a ratio of 1:1000 (w/w) protein to lipid. Reaction was followed with incubation on ice for about 5 minutes. Reaction was diluted further into 4 mL of liposome buffer (20 mM TrisCl pH 7.5, 150 mM NaCl) and incubated again on ice for 5 minutes. Proteoliposomes were collected by centrifugation at 33,000 *×g* for 30 min, resuspended to 100 µL of the buffer and then used in experiments. Proteoliposomes were stabile for few hours. Freshly prepared reconstitution is recommended.

Single-molecule fluorescence microscopy and data analysis

Experimental protocol was done as mentioned in the “Methods” of chapter 1 in this study.

Confocal scanning microscopy and data analysis

Protocol was adapted as previously described in [22]. Microscope cover-slides (No. 1.5, Marienfeld, Germany) were cleaned by sonication in a series of solvents, followed by plasma etching (Plasma Etch, PE-25- JW) for 10 min. Functionalization with PEG-Silane (6-9 PE units, CAS 65994-07-2) and Biotin-PEG-Silane (MW3400, Laysan Inc., United States) was done in toluene (55 ^{o}C overnight) and flow cells were assembled [25].

To immobilize labelled McjD within these flow cells, the surface was incubated for 10 min with a solution containing 0.2 mg/ml neutravidin (Invitrogen, United States) in 20 mM TrisCl pH 7.5, 150 mM NaCl. Unbound neutravidin was flushed away in the same buffer. Non-specific binding of labelled McjD to the PEG-surface was tested by incubation with 50 pM of labelled protein immediately without having neutravidin coverage. All experiments were carried out in a degassed buffer under oxygen-free conditions, utilizing an oxygen scavenging system supplemented with 10 mM aged Trolox as a photostabilization agent [26].

To measure conformational kinetics of McjD, the same custom-built confocal microscope was used [27]. Surface-scanning was performed using a XYZ-piezo stage with 100×100×20 µm range (P-517-3CD with E- 725.3CDA, Physik Instrumente, Germany). The detector signal was registered using a Hydra Harp 400 picosecond event timer and a module for time-correlated single photon counting (both Picoquant, Germany). The data, i.e., time traces and scanning images, were extracted using custom made LabVIEW software [28,29]. Data were recorded with constant 532 nm-excitation at an intensity of 0.5 µW (~125 W/cm2). A typical 10-µm-sized false-color image is shown in **Figure 4.7**. After each surface scan, the positions of labelled proteins were identified manually; the position information was used to subsequently generate time traces. Subsequently, FRET trajectories, i.e. donor and acceptor traces of double-labelled SBDs, were recorded (seen as orange spot in the false color representation, **Figure 4.6**).

Results

Single-molecule FRET monitors the conformational states of the ABC exporter McjD

smFRET has emerged as a tool for investigating conformational dynamics of biomacromolecules over the past 20 years. This approach relies on mapping a relevant reaction coordinate, i.e., for ABC transporters spatial separation of characteristic residues between TMD and NBD domains, and provides “low resolution” structural information in the form of a distance. On the other hand, however, it is a very powerful technique to measure real-time conformational changes and dynamics unlike other biophysical techniques such as EPR, where the sample has to be frozen. In this paper, we have established smFRET to directly monitor the conformational states of ABC transporters. Our assay is tailored to monitor conformational states and dynamics during substrate export and relies on the use of single cysteines at the periplasmic side of the TMD, Y64C, and L67C (**Figure 4.1A**) and the cytosolic NBDs, native C547, of McjD ((Figure 4.1A); all single mutants were introduced to cys-less McjD (via mutation of native cysteines to serine).

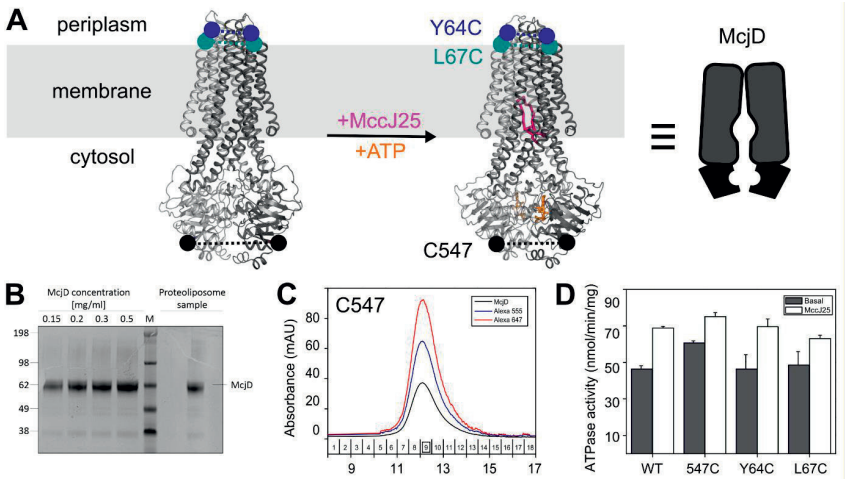

Figure 4.1 | Biochemical characterization of McjD and smFRET assay design. A) Schematic representation of the smFRET assay using crystal-structure snapshots of McjD. On the right side McjD is also shown as a cartoon. In the crystal structure nucleotides and ATP-Mg in orange sticks, the peptide MccJ25 in pink. Each half transporter is colored in dark and light grey. McjD is shown in a view along the plane of the membrane which is depicted in light grey. Colored balls show the position of the cysteines used for probing conformational changes. PBD codes for McjD in inward-occluded conformation are 5OFP (left) [8] and in the outward-occluded conformation 4PL0 (right) [13]. **B)** Coomassie stained SDS-PAGE of McjD-C547 reconstituted in liposomes. The amount reconstituted was evaluated against detergent purified protein. **C)** Chromatogram of McjD C547 (black) labelled with Alexa 555 (blue) and Alexa 647 (red) maleimide fluorophore. The fraction containing the highest degree of labelling is marked by a square. **D)** The ATPase activity of all labelled variants C547, Y64C, L67C was determined in liposomes and compared to wild-type, wt. All labelled McjD variants show basal- and ligand-induced ATPase activities in liposomes comparable to that of wild type protein, indicating that labelling does not interfere with their activity.

It can be clearly seen that due to the homodimeric nature of McjD, introduction of one cysteine results in the possibility to label the protein with two fluorophores that is required for FRET, i.e., a donor and an acceptor fluorophore. Furthermore, structural analysis suggests that the apo conformation of McjD has distinct distances between the two labelled positions for C547 but not for the nucleotide-bound conformation (Y64C and L67C) that allows assessment of the biochemical and conformational states of McjD via smFRET. The FRET efficiency changes are related to the distance of the respective mutants and thus indicates the changes that occur upon addition of ATP or the substrate MccJ25. For example, the crystal structure estimates that the nucleotide-free form of McjD should show a larger NBD separation (low FRET) while this should be shorter in the nucleotide-bound form (high FRET) [8,13].

McjD was purified in detergent and reconstituted into proteoliposomes as previously described (Figure 4.1B) [8,13]. McjD was labelled stochastically with Alexa555 and Alexa647 for smFRET experiments. The gel-filtration purification of donor-acceptor-labelled McjD is shown in Figure 4.1C. The detergent-solubilized protein runs as a mono-disperse peak with significant absorption at both the donor and acceptor wavelengths at 532 nm and 640 nm, respectively (Figure 4.1C). The labelling efficiency of the two fluorophores was determined to be ~60%. All mutants were biochemically characterized using a previously published ATPase assay [8,13]. Neither the introduction of cysteines nor addition of fluorescent labels affected the activity of the transporter in proteoliposomes; this is indicated by the similar basal and ligand induced ATPase activity compared to wild type McjD (Figure 4.1D).

We first assessed the conformational states of McjD under equilibrium conditions in the detergent-solubilized state. We used three different labelling positions in McjD to monitor the conformational states of the periplasmic TMD region and the cytosolic ATPase domain (Figure 4.1A and **4.2A**). Since detergent-solubilized McjD diffuses freely in solution, we used confocal microscopy with alternating laser excitation (ALEX) to relate FRET efficiency values of single McjD molecules with their conformational states (**Figure 4.2B**).

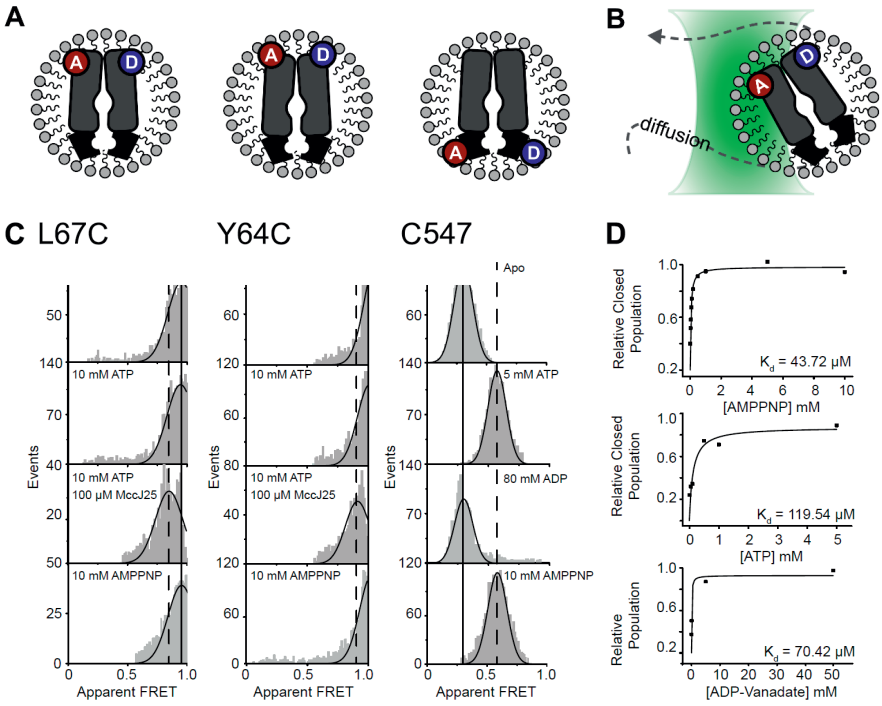

Figure 4.2 | Freely diffusing McjD in detergent studied by smFRET. Schematic overview of McjD labelling schemes and **B** diffusion-based experiments using confocal microscopy. Stochastic labelling is performed in NBD mutants (native cysteine 547) and TMD mutants (Y64C; L67C). **C** Confocal single molecule analysis with ALEX of labelled McjD in detergent. TMD mutants, Y64C and L67C, have primary high FRET and are shifted to lower FRET with addition of ATP and MccJ25. The NBD mutant C547 is shifted to higher FRET with nucleotide addition. **D** Ligand binding affinity values of McjD for AMPPNP (top), ATP (middle), and ADP-vanadate (bottom), obtained from the ratio of areas (C/(O+CL)) between open and closed ligand-bound populations at the indicated substrate concentration.

From the available crystal structures, we can extract C_a-C_a distances between the two labelling positions. It is worthwhile to note that in our smFRET assays, we do not determine absolute distances, but only use relative distance changes via the setup-dependent apparent FRET efficiency E*. The qualitative relation between E* and the C_a-C_a distances do, however, allow us to assess whether FRET experiments relate well to distances expected from the crystal structures. For the periplasmic TMD mutants, Y64C and L67C, the crystal structures predict C_a-C_a distances of 2.7 nm and 2.9 nm, respectively (without taking any fluorophore properties into account). The Förster radius of Alexa555/647 is R_0 = 5.1 nm. At this distance FRET efficiency is theoretically expected to be 0.5; interprobe distances above this value have thus smaller values of E* while shorter distances are expected to show larger E*-values. Since C_a-C_a distances are much shorter than R_0, we expect high FRET efficiency values significantly above 0.5. The data are fully coherent with the crystal structure predictions as seen from **Figure 4.2C**, whereas a FRET distribution of apo McjD centers around 0.95 (L67C) and ~1.05

(Y64C). The distance extracted for C547, located at the NBDs, from the crystal structure of the apo McjD is 4.8 nm, in agreement with the mean observed FRET efficiency of apo-McjD of ~0.31. All interpretations are supported by comparison of the observed E*-values of McjD with respect to static dsDNA ruler structures (**Figure 4.4**) that is described in a Chapter 3.

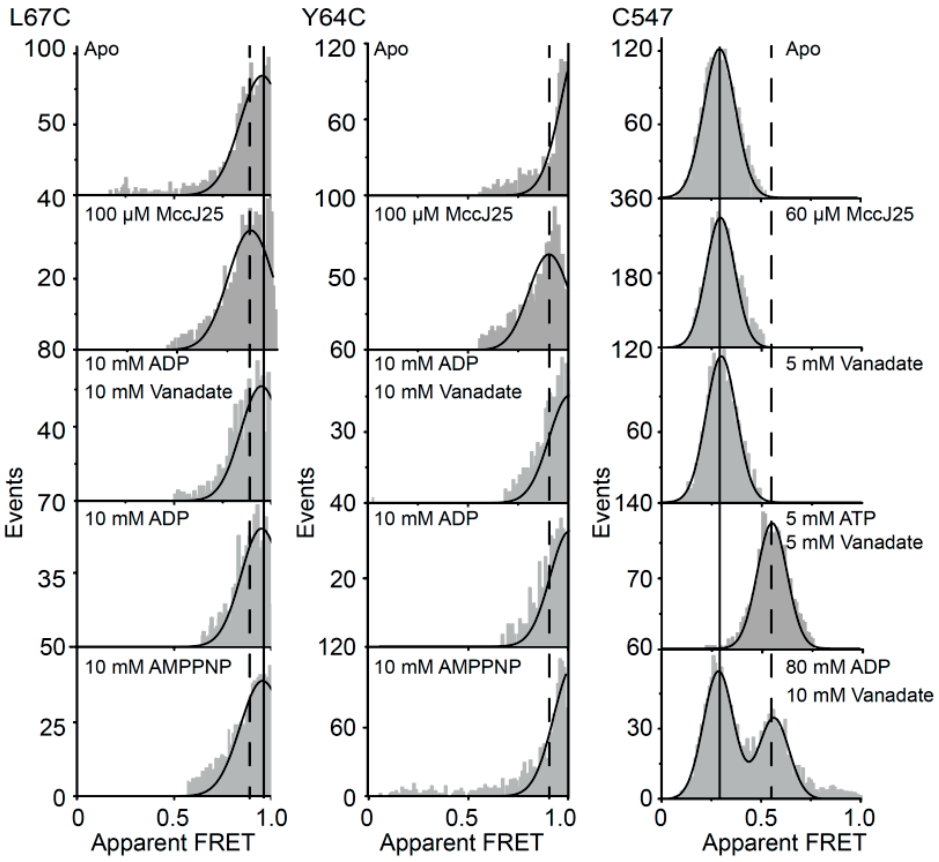

Figure 4.3 | Additional data for detergent-solubilized McjD. Confocal single molecule analysis of labelled McjD and variants in detergent using ALEX. Mean values of ligand-free conditions are shown as a reference with a solid marker while ligand-bound mean values are shown dashed.

Having established that our smFRET assays are coherent with structural predictions, we tested conditions that mimic relevant stages of the ABC transport cycle. From diffusion-based experiments, these show the statistically relevant states and related conformations of McjD for: (i) ATP-binding and hydrolysis and turnover with/without substrate, (ii) the pre-hydrolysis state using the ATP-analogue AMPPNP, (iii) the transition-state during ATP-hydrolysis with ATP-Vanadate and finally (iv) the post-hydrolysis state using either ADP-vanadate or ADP (**Figure 4.2** & **Figure 4.3**).

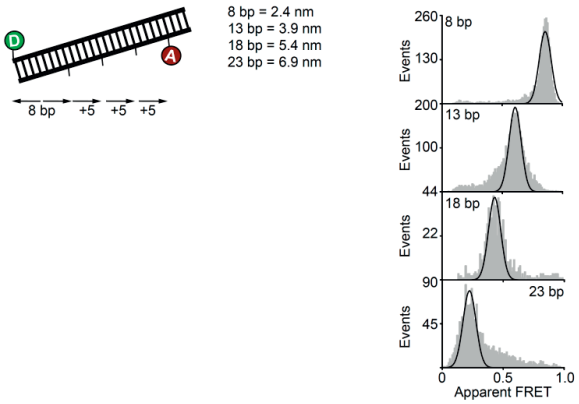

Figure 4.4 | Static dsDNA control experiments. Schematic representation of the smFRET assay using labelled double-stranded DNA with Alexa 555 and Cy5 fluorophores as indicated. Distances were calculated by multiplication of 0.34 nm times number of base pairs for estimation of molecular distances. Experimental data similar to those shown in Figure 2 are shown, which establish the validity of experimental results and interpretations given in the main text.

For both TMD mutants, the addition of ATP, its non-hydrolysable or transition-state analogues did not alter their conformational states (Figure 4.2C). Interestingly, the addition of MccJ25 and ATP triggered opening of the periplasmic gate as observed by a small but significant shift towards lower FRET efficiency values that is consistent with opening of the TMD. Strikingly, the observation of opening occurs under equilibrium conditions and indicates that the outward-open conformation is visited by McjD during the transport cycle and is triggered by both ATP and the MccJ25 peptide. We observe a slightly smaller opening of the TMDs in the absence of nucleotides but the presence of MccJ25 can induce an open TMD. We have shown, however, that McjD transports MccJ25 in an ATP-dependent manner. We explain the observations by the fact that ABC exporters can transport their substrates bidirectionally, and this previously described effect manifests in a structural reorientation of the TMD and opening that is similar to that observed during transport with MccJ25 and ATP but only occurs at high concentrations of peptide via rebinding [32].

On the contrary, the NBDs were very sensitive to ATP (and analogues) and show pronounced conformational changes upon ATP, AMPPNP, ADP, ATP-vanadate and ADP-vanadate addition (Figure 4.2C). Peptide addition after ATP does not alter the observed conformational state any further. The only conditions that are incompatible with conformational change are sole addition of either peptide or vanadate alone. The conformational changes occur with apparent affinities in the 50-100 µM range for ATP, AMPPNP and ADP-vanadate (**Figure 4.2D**), matching reported values for binding affinities of similar ATPases [13]. The data show that binding of the nucleotides ATP, AMPPNP and ADP-vanadate at the NBDs trigger conformational changes into their closed dimer form (Figure 4.2C). It is only after ATP-hydrolysis (ADP-vanadate, **Figure 4.3** and ADP, **Figure 4.2**) that a subtle reopening of the NBDs is seen that is linked to a reset of the transporter.

Altogether, the data based on detergent-solubilized McjD suggest that it uses an alternating access mechanism, where conformational changes are triggered by ATP (engagement of the NBDs from inward-open to outward-occluded) and substrate binding (opening of the TMD to outward-open). Since we also find subtle differences between the pre- and post-hydrolytic states, ATP hydrolysis seems to only reset the transporter whereas ATP binding is coupled to conformational changes in the NBD and TMD. The data also suggest tight coupling between ATP and MccJ25 binding and subsequent substrate transport and suggest that hydrolysis is only required for resetting the system. Since the detergent environment is not very physiologically relevant, we further verified these results (and their interpretations) with surface-immobilized liposome-reconstituted McjD.

McjD displays similar conformational states and changes in detergent and proteoliposomes

For studies of surface-immobilized liposomes containing one transporter for smFRET, we used a low protein to lipid ratio of ~1:1000 (w/w). We observed the time-duration of fluorescence bursts in a confocal microscope with McjD in detergent and in proteoliposomes, and we measured nearly identical values in the range of 10-20 ms (**Figure 4.5**) as reported for other diffusing liposome systems [30]. Finally, we verified random insertion (inside-out and inside-in) of McjD into the proteoliposomes with a ratio of approximately 60:40 (**Figure 4.5**).

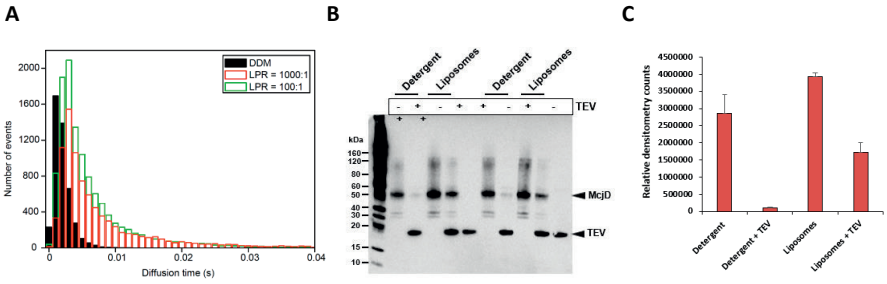

Figure 4.5 | Support for liposome-incorporation of McjD into proteoliposomes. A Comparison of lifetime of the diffusing labelled McjD in detergent-solubilized and reconstitution of proteoliposomes. Different ratio of lipid to protein does not have any significant effect. Proteoliposomes have longer diffusion time due to steric hindrance of the lipid environment, whereas it does not exist in the detergent-solubilized condition. **B** Western blot showing orientation of McjD in proteoliposomes. Detergent purified McjD-His (~50KDa) and liposome reconstituted McjD-His were incubated with TEV protease (~20KDa), which carries a His-tag, at a 1:1 molar ratio of protein to TEV. The reactions were visualized before and after TEV cleavage by anti-His Western blot. The McjD His-tag is located at the C-terminus of the NBDs. McjD-His molecules facing the interior of the liposomes are inaccessible for TEV cleavage whereas the ones facing outside are accessible for cleavage. Comparison of the TEV-treated and untreated McjD-His-containing liposomes shows that cleavage is not complete, suggesting that McjD-His has inserted in the liposomes in different orientations. As a control experiment, detergent-purified McjD-His (~50 KDa) can no longer be detected after TEV treatment suggesting full removal of the His-tag. The reaction conditions for each lane are shown above the gel. Bands corresponding to McjD-His and TEV protease-His are labelled. **C** Densitometry quantification of McjD orientation. The ratio of inside to outside McjD-His in liposomes was quantified by measuring the Western blot band intensities before and after TEV protease incubation. Values represent mean densitometry counts calculated from two independent liposome preparations and indicate a proportion of 44:56 ± 4.0 % McjD-His inside to outside. Error bars are shown (mean ± standard deviation, *n* = 2).

McjD reconstituted in liposomes was immobilized in custom-made flowcells on PEGylated coverslips via liposomes containing biotin-DOPE (**Figure 4.6A**). Confocal scanning microscopy was performed as described before and single liposomes could be identified with 10x10 µm search areas (Figure 4.6A). Individual McjD transporters with donor and acceptor dye were identified manually. In the data evaluation process, we discarded events with donor- or acceptor only character or where >1 bleaching step was seen in either detection channel. Using this procedure, we observed fluorescence transients with a time-resolution of 10 ms and observation times of multiple seconds (**Figure 4.6B**, donor = blue, acceptor = red, FRET = black, orange = most probable state-trajectory of Hidden Markov Model (HMM); see also Material and Methods). FRET histograms were obtained by projection of all E* values from multiple traces (N > 50) for each condition; see Figure 4.6B, right.

The observed FRET efficiency values for apo-McjD in proteoliposomes are fully consistent but not identical with our detergent data. Both TMD mutants show high E* values, mean of 0.69 (L67C) and 0.81 (Y64C), (**Figure 4.3**). The differences between both mutants, not the absolute FRET values, are consistent with the detergent indicating that the FRET assay correctly monitors TMD conformation in the liposomes. Also, the conformational changes triggered by addition of peptide and ATP shift the values toward of 0.52 for both mutants (Figure 4.3, L67C,

Y64C). The fact that the FRET changes are more pronounced in the liposomes represents the increased sensitivity of the FRET assay since the larger absolute distances for both TMD mutants in the liposomes make FRET more sensitive (FRET has the greatest sensitivity for structural changes around the Förster radius). In summary, the TMD shows opening in the presence of both ATP and MccJ25. Considering the absolute values of apparent FRET seems to indicate overall larger opening of the TMD in liposomes compared to detergent environment.

The cumulative FRET histograms for both TMD mutants also comply with the fact that only 60% of McjD transporters have the correct orientation (cytosolic NBD facing the outside of the liposome) to react to addition of MccJ25 and ATP, while 40% all of molecules stay in the apo state (**Figure 4.6**). We observed a bimodal distribution of the Y64C in its apo state which we associate to be more dynamic since it is located further up TM1, compared to L67C, and it is likely be less restricted in motion by the proteoliposome's lipid bilayer, thus showing a broader distribution. This will not manifest itself in detergent experiments since here the overall distances are shorter and thus less ideal for the dynamic range of FRET to capture it. The NBD FRET data for C547-McjD in liposomes are almost identical with the detergent ones and show low-FRET apo molecules shifting toward a high-FRET ATP-bound state (Figure 4.3) The only minor difference concerns the FRET efficiency of the ATP-bound state which seems slightly more expanded in the liposomes.

Altogether, the combined data of detergent-solubilized and liposome-reconstituted McjD are consistent – a finding that is interesting in itself. Furthermore, the data remain fully compatible with the alternating access mechanism, where conformational changes are triggered by ATP (closing of NBDs from inward-open) and substrate binding (opening of the TMD for outward-open). The data also suggest tight coupling between ATP and MccJ25 binding and subsequent substrate transport and suggest that hydrolysis is required for resetting the transporter.

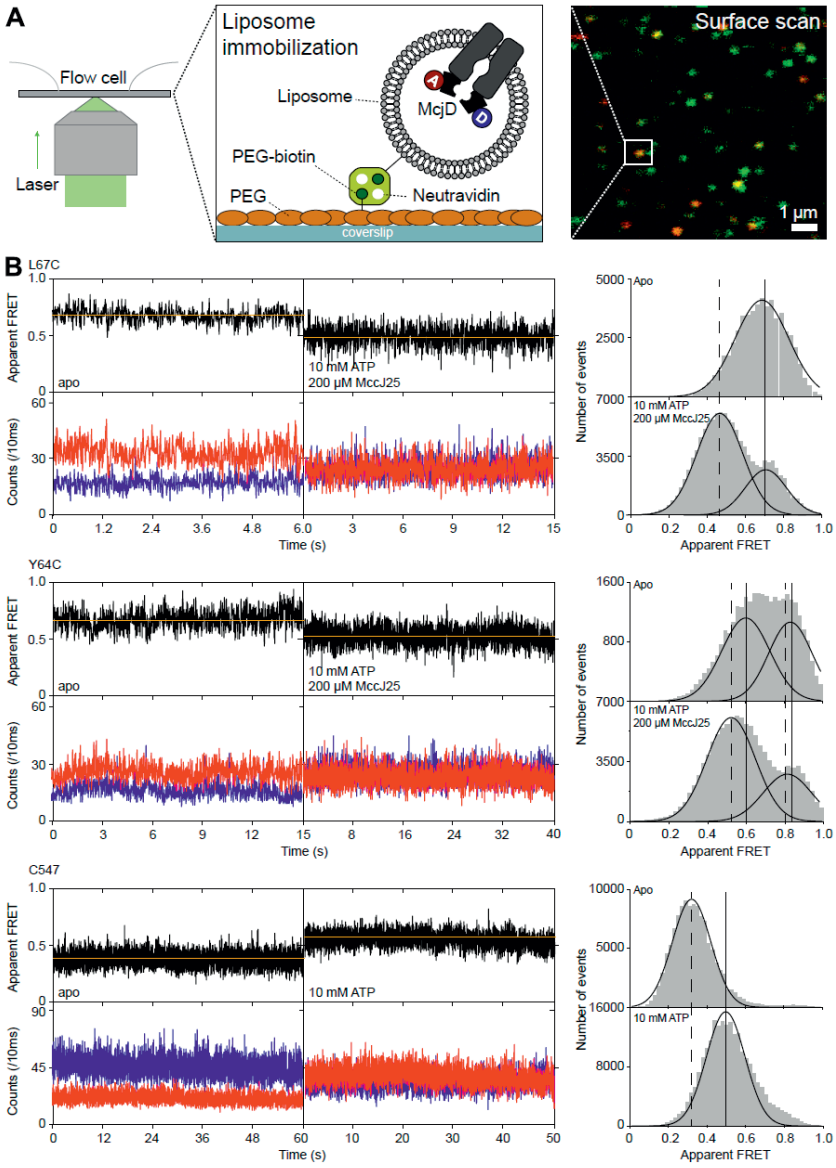

Figure 4.6 | Conformational states of surface-immobilized McjD in proteoliposomes. A schematic showing the immobilization of McjD to the surface: labelled McjD reconstituted in biotinylated DOPE lipid was immobilized to a Peg-biotin-coated surface in a flow cell via a neutravidin-tag on the proteoliposome. A typical surface scan is shown in false-color representation at right (orange, double-labelled McjD; green, McjD with donor fluorophore only; red, McjD with acceptor fluorophore only). **B-D** Representative fluorescence time traces (blue, donor signal; red, acceptor signal; black, FRET signal; yellow, fit) of McjDs labelled with Alexa555 and Alexa647-maleimide with indicated concentrations of corresponding substrate **B** McjD L67C with 10 mM ATP and 200 µM MccJ25 **C** McjD Y64C with 10 mM ATP and 200 µM MccJ25 **D** McjD C547 with 10 mM ATP. Right panel is the projections of accumulated time traces in the absence and presence of substrate for each mutant. We note that differences between the setup dependent apparent FRET values are not influencing our interpretations since only relative changes of FRET efficiency are interpreted.

We also verified ATP-induced NBD switching with detergent solubilized McjD on the surface to exclude unwanted effects due to immobilization (**Figure 4.7**).

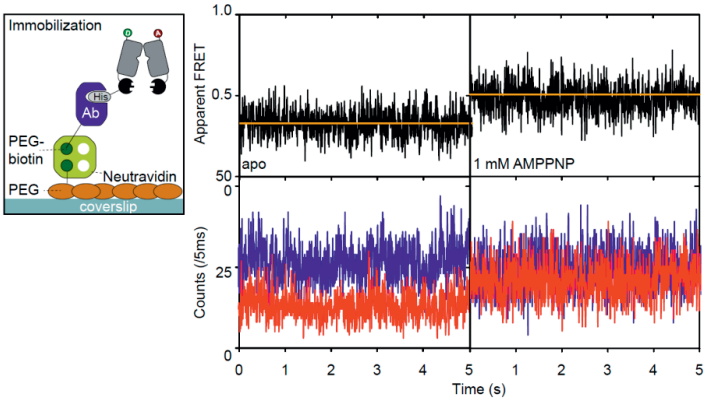

Figure 4.7 | Conformational states of surface-immobilized McjD in detergent environment. A schematic showing the immobilization of McjD to the surface: labelled McjD tagged into PEG-biotin and Histidine antibody. A typical surface scan is shown in false-color representation at right (orange, double-labelled McjD; green, McjD with donor fluorophore only; red, McjD with acceptor fluorophore only). Representative fluorescence time traces (blue, donor signal; red, acceptor signal; black, FRET signal; yellow, fit) of McjDs labelled with Alexa555 and Alexa647-maleimide with indicated concentrations of corresponding substrate 1 mM AMPPNP**.**

The NBDs show conformational dynamics in the absence of ligands while TMDs are static

We used smFRET to investigate intrinsic conformational dynamics of McjD, in the absence of any ligand or nucleotide. For this we used a time-resolution and data binning of 10 ms. For both TMD mutants we did not find any intrinsic FRET changes that go beyond experimental noise, when analysing data sets with N > 100 molecules. All traces look similar to those shown in Figure 4.6B (L64C, Y67C, apo). These data suggest that the TMD shows no detectable conformational changes on timescales > 10 ms in the absence of substrate and ATP.

In contrast, a significant fraction of 15% of all McjD-C547 FRET traces showed short stepwise changes of FRET efficiency from the lower apo level of 0.3 to values > 0.5, similar to those found in the presence of ATP (**Figure 4.8A**, apo vs. ATP-bound). The dwells in the high-FRET state are short and the transitions in FRET efficiency were accompanied by anticorrelated change of donor- and acceptor fluorescence intensity. These transitions occur with low frequency and on average only once per trace (Figure 4.8B). A histogram of all observed transition dwells revealed an average lifetime of 82 ± 25 ms of the dimerized ATP-free NBD state from an exponential fit of the dwell-time distribution (Figure 4.8C).

These data support the interpretation of intrinsic conformational flexibility of the NBD domains but high structural rigidity in the TMD in the absence of ATP and MccJ25. The flexibility of the NBD domains might also be a basis for the observed basal ATPase activity of McjD and other ABC transporters. The findings show that ATPase activity needs to be less controlled than TMD movements since TMDs represent gate towards the extracellular milieu.

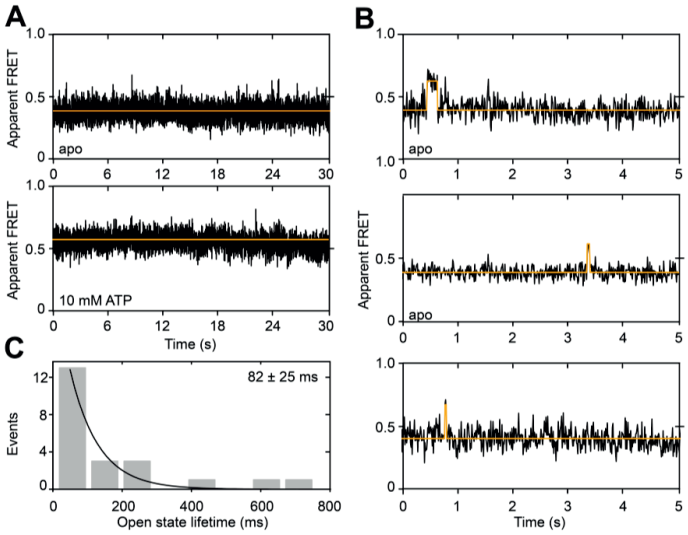

Figure 4.8 | Intrinsic conformational dynamics of the NBDs in surface-immobilized McjD in proteoliposomes. A Representative FRET fluorescence time traces (black, FRET signal; yellow, fit) of McjD NBD C547 labelled with Alexa 555 and Alexa 647-maleimide in apo conditions at 10 ms time resolution. Our study shows that ~85% of all apo-McjD traces show no significant fluctuations beyond shot-noise. Apo-McjD is thus predominantly in the low FRET and thus open state with E* values <0.3. **B** Within the complete data set of N = 80 traces of apo-McjD comprising donor and acceptor, ~15%, show infrequent fluctuations to a higher FRET efficiency state with a lifetime of **C** 82 ± 25 ms where E* values > 0.5 are observed. The data set represents a total recording time of 4.6 mins with a temporal resolution of 10 ms.

ATP-induced conformational dynamics of the NBDs of McjD

Finally, we aimed to study ligand-induced movements of McjD (**Figure 4.9**). The complexity of the McjD system and its "ligands" MccJ25 and ATP would require testing of multiple conditions, i.e., equilibrium and non-equilibrium cases. Both peptide transport or AMPPNP would require triggered addition of the compounds; such experiments are best studied with TIRF-microscopy with a flow-cell arrangement to quickly exchange buffer and to trigger conformational changes of the transporter at distinct time points [23]. Confocal scanning microscopy, as used in this study, does not have the parallelized detection and high throughput of widefield single-molecule methods but better time-resolution to detect e.g., fast events such as intrinsic conformational dynamics (Figure 4.8).

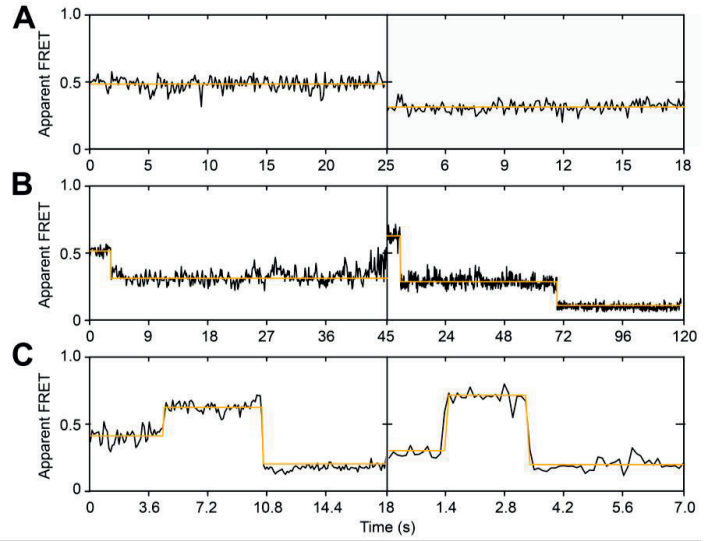

Figure 4.9 | ATP-induced conformational dynamics of the NBDs in surface-immobilized McjD in proteoliposomes. A Representative FRET time traces (black, FRET signal; yellow, fit) of McjD NBD C547 labelled with Alexa 555 and Alexa 647-maleimide in apo conditions at 10 ms time resolution. This panel shows stable ATP-loaded (left) and ATP-free (right) McjD. **B** Representative FRET time traces that show switching between ATP-loaded (high FRET >0.5) and ATP free McjD (E* ~ 0.3) at 2 s (left) and 5 s (right). The traces show photobleaching events after ca. 40 s (left, donor-bleaching) and 70 s (right, acceptor-bleaching). **C** Representative FRET time traces that show switching between ATP free McjD (E* ~ 0.3) and ATP-loaded (high FRET >0.5) at ~4s s (left) and ~1.4 s (right). The traces show photobleaching events of the acceptor after ~10 s (left) and ~3.3 s (right).

Consequently, we decided to study the basal ATPase activity of liposome-reconstituted McjD with our confocal scanning setup and imaged McjD-C547 at concentrations of 120 µM ATP, i.e., concentrations close to the K_d-value. From our previously measured basal catalytic ATPase activity of McjD in liposomes [13] with a k_{cat} of ~3.5 min^{-1}, we expect that associated conformational dynamics occur on a timescale of tens of seconds. Consistent with that the experiments show mostly stable FRET traces with either high or low FRET values corresponding to the two conformational states of the NBDs that were already described in Figure 4.6, since transitions will occur on timescales longer than the average photobleaching lifetime of ~10-20 s. The mix of both types of traces also represents the fact that the protein is half occupied with ATP and half free, either after ATP hydrolysis or prior to ATP binding (**Figure 4.9A**). Short-lived traces that have the transporter in the inside-in orientation could not be considered for the data analysis due to their short photobleaching lifetime and the low likehood to detect a transition.

Strikingly, we find examples were switching between both FRET states occurs either from high to low (Figure 4.9B) or low to high (Figure 4.9C) with final photobleaching. These data represent the first direct observation of intrinsic (Figure 4.8) and ligand-induced conformational dynamics (Figure 4.9) of an ABC transporter and reveal the relevant timescales

of 100 ms and seconds for conformational switching in the NBD domains, respectively. These data are under active ATP hydrolysis conditions and we cannot distinguish between occupation of the NBDs by ATP or ADP (as a result of ATP hydrolysis). Our attempts to prepare the ATPase deficient E506Q mutant in our C547 construct resulted in aggregated protein, thus limiting our in-depth interpretation of these data.

The impact of conformational changes in transport

From structural and biochemical studies, it is unclear what is the driving force behind NBD dimerization in the presence of nucleotides. It has been proposed that nucleotide binding brings the NBDs closer to each other but there is no clear consensus on how transporters that display large degree of disengagement can form a closed dimer; binding of substrate at the TMD has been proposed to bring them closer as a result of inducing conformational changes at the TMD upon binding [3].

Our detergent data revealed that the TMD of McjD does not adopt an outward-open conformation in the presence of nucleotides alone consistent with our previous PELDOR experiments (**Figure 4.2C**) [8]. Addition of both ATP and the peptide MccJ25, however, resulted in lower E* values suggesting that TMs1-2 from one protomer have moved toward the opposite protomer for opening of the periplasmic side of the TMD and release of the peptide (Figure 4.2C). Here, we provide the first direct observation that McjD undergoes conformational changes in its TMD and adopts an outward-open conformation. Strikingly, we also observed similar conformational changes in surface-immobilized McjD in proteoliposomes (**Figure 4.6B**). We observe two main populations, one that has a low E* and one with a high E* value suggesting that some McjD molecules have opened up to release the bound peptide, and some are reverting back to the occluded conformation upon substrate release; we cannot exclude that the population with the high E* values is McjD bound to ATP but not MccJ25. In the ALEX data, we cannot distinguish these individual populations but the histogram analysis shows a rather broad distribution that could be a mixture of similar states. These data suggest that there is a tight coupling between ATP and substrate binding and subsequent release that is significantly different from other ABC transporters. Furthermore, it is the first report to show that both ATP and substrate are required to induce conformational changes in the TMD.

Our smFRET data in detergent and liposomes revealed that the NBDs of McjD adopt very similar disengagement with E* values of 0.3 and larger E* values of 0.5 upon nucleotide binding. These trends are in perfect agreement with our crystal structures [8] and suggest that, although the crystal structures have been obtained using detergent-purified protein, they represent relevant conformations of the transport cycle as supported by the direct comparison of detergent and liposome smFRET data.

From structural and biochemical studies, the driving force behind NBD dimerization in the presence of nucleotides remains unclear although molecular simulations have tried to address the dimerization process [33]. It has been proposed that nucleotide binding brings the NBDs closer to each other, but there is no clear consensus on how transporters that display large degree of disengagement can form a closed dimer; binding of substrate at the TMD has been proposed to bring them closer as a result of inducing conformational changes at the TMD upon binding [3]. Our smFRET data from surface-immobilized McjD in proteoliposomes revealed that the NBDs display conformational dynamics in the absence of substrates rather than being static NBDs.

ATP binding alone driving the closure of the NBDs, our data suggest that the apo NBDs can sample the dimerized state without any nucleotide (Figure 4.8). This is the first direct observation that apo NBDs can sample a dimerized state and it is in agreement with our previous cysteine cross-linking studies at the NBDs that showed cross-linking in the absence of CuCl2, suggesting a very close proximity to each other [8]. Unlike the NBDs that show detectable intrinsic conformational fluctuations, the TMD of McjD did not reveal any dynamics in the absence of ligands and even in the presence of nucleotides alone, suggesting that opening of the periplasmic gate is even more tightly coupled to ATP and MccJ25 binding.

In light of the smFRET data and previous structural work we can provide a very detailed mechanism for the transport of MccJ25 outside of the producing cells. We propose that in the absence of substrate (futile ATP hydrolysis), the NBDs sample different conformations, including a nearly closed dimer, that is driven to full closure upon the presence of ATP (**Figure 4.10**). As we have previously shown, the TMD does not open up in the presence of nucleotides alone and in addition our smFRET data did not show any dynamics either. On the other hand, in the presence of both ATP and MccJ25 (transport cycle), the TMD of McjD opens to release the bound peptide and collapses to an occluded conformation that is in agreement with our structural and PELDOR measurements.

In conclusion, all our data suggest that ATP and MccJ25 binding is tightly coupled to the opening of the TMD that is distinct from other multidrug ABC transporters. We have shown that McjD can only transport MccJ25 and no other antibacterial peptides or drugs [31], and these data confirm that this tight regulation of opening the TMD to the periplasm might be a unique mechanism of natural product self-immunity ABC transporters that distinguishes them from multidrug transporters that only require ATP binding to open their TMD; i.e. we propose that for multidrug transporters if a ligand can fit in their cavity, they will transport it since its binding is not coupled to the opening of the TMD, whereas more specific ABC transporters will only open the cavity in the presence of a single specific substrate.

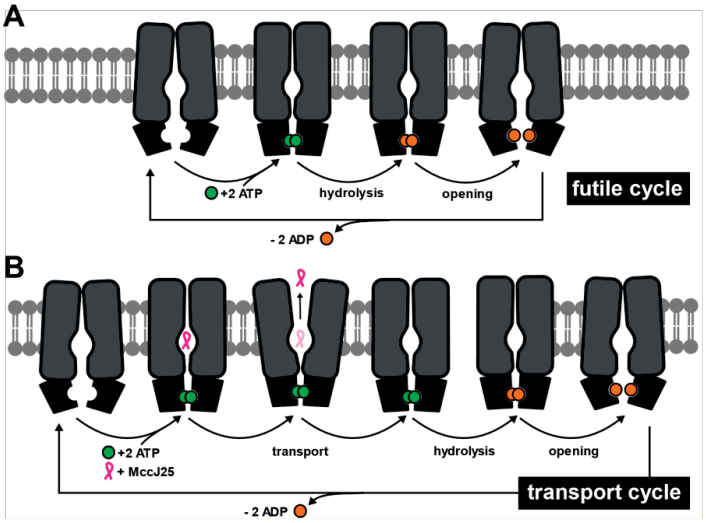

Figure 4.10 | Refined transport mechanism of ABC exporter McjD based on structural, biochemical and biophysical data. Schematic representation of the smFRET assay using crystal-structure snapshots of McjD. Binding of ATP alone (futile cycle) is not coupled to an opening of the TMD that remains occluded. The smFRET data did not reveal any dynamics either. On the other hand, the NBDs are more dynamic and they can sample a nearly closed dimer that is driven to full closure in the presence of ATP. Binding of both ATP and MccJ25 is coupled to an open TMD, that reverts back to an occluded conformation upon substrate release. ATP hydrolysis and ADP release resets the transporter to a new transport cycle.

Conclusion

ABC transporters utilize the alternating access mechanism to transport the substrate. This usually undergoes large conformational changes upon ATP binding and hydrolysis [3,4], whereas McjD appears to be more "rigid"[8]. Our only evidence that McjD adopts an outward-open conformation was from transport data using a cross-link between TMs1-2 and TMs1'-2' [8]. We have speculated that this conformation might not be sufficiently well populated or long-lived to be studied by EPR techniques, therefore, we have probed the opening of the McjD TMD by smFRET by placing fluorescent dyes at TM1 and 1'. MsbA adopts an outward open conformation in the presence of nucleotides by movement of TMs1-2 towards the opposite protomer that causes subunit intertwining [8]. Our detergent ALEX data revealed that the TMD of McjD does not adopt an outward open conformation in the presence of nucleotides alone, which is consistent with our previous DEER measurements (Figure 4.2C) [8]. Addition of both ATP and peptide MccJ25 resulted in lower E* values suggesting that TMs1-2 from one protomer has moved towards the opposite protomer, which resulted in the opening of the periplasmic side of the TMD for release of the peptide (Figure 4.2C).

This is the first direct observation that McjD undergoes conformational changes in its TMD and adopts an outward-open conformation. We also observed similar conformational changes in surface-immobilized McjD in proteoliposomes (Figure 4.6B). We observe two main populations, one that has a low E* and one with a high E* value suggesting that some McjD molecules have opened up to release the bound peptide, and some are reverting back to the occluded conformation upon substrate release; we cannot exclude that the population with the high E* values is McjD bound to ATP but not MccJ25. In the ALEX data, we cannot distinguish these individual populations but the histogram analysis shows a rather broad distribution that could be a mixture of similar states. These data suggest that there is a tight coupling between ATP and substrate binding and subsequent release that is significantly different from other ABC transporters. This report shows that both ATP and substrate are required to induce conformational changes in the TMD.

Since ATP binding is coupled to opening of the TMD, we also used a native cysteine, C547, at the NBDs in order to monitor how ATP binding and hydrolysis affects their conformation. The crystal structures of exporters display varying degrees of NBD disengagement in the absence of nucleotides [3,5,8,17]. It has been suggested that it could be a detergent artefact or a real dynamic nature of the NBDs. DEER data of ABC transporters in liposomes and bicelles show broad lines for apo NBDs [8,11,12,15] further suggesting that in the absence of nucleotides the NBDs can have different degrees of disengagement. Upon nucleotide binding, the NBDs dimerise and display nearly identical distances across different transporters [3,5,8,17]. Our smFRET data in detergent and liposomes revealed that the NBDs of McjD adopt very similar disengagement with E* values of 0.3 and larger E* values of 0.5 upon nucleotide binding. These values are also in close agreement to our crystal structures [8] and suggest that although the crystal structures have been obtained using detergent purified protein, they represent relevant conformations of the transport cycle as supported by the direct comparison of detergent and liposome smFRET data.

References

1. Holland, B., Cole, S.P.C., Kuchler, K., Higgins, C.F. (2003) ABC Proteins From Bacteria to Man. *Academic Press*
2. Beis, K. (2015) Structural basis for the mechanism of ABC transporters. *Biochem. Soc. Trans.* 43, 889–893
3. Ward, A., Reyes, C.L., Yu, J., Roth, C.B., Chang, G. (2007) Flexibility in the ABC transporter MsbA: Alternating access with a twist. *Proc. Natl. Acad. Sci. USA.* 104, 19005–19010
4. Dawson, R.J., Locher, K.P. (2006) Structure of a bacterial multidrug ABC transporter. *Nature.* 443, 180–185
5. Perez, C., Gerber, S., Boilevin, J., Bucher, M., Darbre, T., Aebi, M., Reymond, J.L., Locher, K.P. (2015) Structure and mechanism of an active lipid-linked oligosaccharide flippase. *Nature.* 524, 433–438
6. Hohl, M., Briand, C., Grutter, M.G., Seeger, M.A. (2012) Crystal structure of a heterodimeric ABC transporter in its inward-facing conformation. *Nat. Struct. Mol. Biol.* 19, 395–402
7. Noll, A., Thomas, C., Herbring, V., Zollmann, T., Barth, K., Mehdipour, A.R., Tomasiak, T.M., Bruchert, S., Joseph, B., Abele, R., Olieri, V., Wang, M., Diederichs, K., Hummer, G., Stroud, R.M., Pos, K.M., Tampe, R. (2017) Crystal structure and mechanistic basis of a functional homolog of the antigen transporter TAP. *Proc. Natl. Acad. Sci. USA.* 114, E438–E447
8. Bountra, K., Hagelueken, G., Choudhury, H.G., Corradi, V., El Omari, K., Wagner, A., Mathavan, I., Zirah, S., Yuan Wahlgren, W., Tieleman, D.P., Schiemann, O., Rebuggat, S., Beis, K. (2017) Structural basis for antibacterial peptide self-immunity by the bacterial ABC transporter McjD. *EMBO J.* 36(20), 3062–3079
9. Barth, K., Hank, S., Spindler, P.E., Prisner, T.F., Tampe, R., Joseph, B. (2018) Conformational Coupling and trans-Inhibition in the Human Antigen Transporter Ortholog TmrAB Resolved with Dipolar EPR Spectroscopy. *J. Am. Chem. Soc.* 140, 4527–4533
10. Timachi, M.H., Hutter, C.A., Hohl, M., Assafa, T., Bohm, S., Mittal, A., Seeger, M.A., Bordignon, E. (2017) Exploring conformational equilibria of a heterodimeric ABC transporter. *Elife.* 6, e20236
11. Zou, P., Bortolus, M., Mchaourab, H.S. (2009) Conformational cycle of the ABC transporter MsbA in liposomes: detailed analysis using double electron-electron resonance spectroscopy. *J. Mol. Biol.* 393, 586–597

12. Dong, J., Yang, G., Mchaourab, H.S. (2005) Structural basis of energy transduction in the transport cycle of MsbA. *Science.* 308, 1023–1028

13. Choudhury, H.G., Tong, Z., Mathavan, I., Li, Y.Y., Iwata, S., Zirah, S., Rebuffat, S., van Veen, H.W., Beis, K., (2014) Structure of an antibacterial peptide ATP-binding cassette transporter in a novel outward occluded state. *PNAS*. 111(25), 9145–9150

14. Mi, W., Li, Y., Yoon, S.H., Ernst, R.K., Walz, T., Liao, M. (2017) tructural basis of MsbA-mediated lipopolysaccharide transport. *Nature.* 549, 233–237

15. Borbat, P.P., Surendhran, K., Bortolus, M., Zou, P., Freed, J.H., Mchaourab, H.S. (2007) Conformational motion of the ABC transporter MsbA induced by ATP hydrolysis. *PLoS. Biol.* 5, e271

16. Mishra, S., Verhalen, B., Stein, R.A., Wen, P.C., Tajkhorshid, E., Mchaourab, H.S. (2014) Conformational dynamics of the nucleotide binding domains and the power stroke of a heterodimeric ABC transporter. *Elife.* 3, e02740

17. Lin, D.Y., Huang, S., Chen, J. (2015) Crystal structures of a polypeptide processing and secretion transporter. *Nature.* 523, 425–430

18. Morgan, J.L.W., Acheson, J.F., Zimmer, J. (2017) Structure of a Type-1 Secretion System ABC Transporter. *Structure.* 25, 522–529

19. Dyla, M., Terry, D.S., Kjaergaard, M., Sorensen, T.L., Lauwring A.J., Andersen, J.P., Rohde, K.C., Altman, R.B., Nissen, P., Blanchard, S.C. (2017) Dynamics of P-type ATPase transport revealed by single-molecule FRET. *Nature.* 551, 346–351

20. Akyuz, N., Altman, R.B., Blanchard, S.C., Boudker, O. (2013) Transport dynamics in a glutamate transporter homologue. *Nature.* 502, 114–118

21. Zhao, Y., Terry, D., Shi, L., Weinstein, H., Blanchard, S.C., Javitch, J.A. (2010) Single-molecule dynamics of gating in a neurotransmitter transporter homologue. *Nature.* 465, 188–193

22. Gouridis, G., Schuurman-Wolters, G.K., Ploetz, E., Husada, F., Vietrov, R., de Boer, M., Cordes, T., Poolman, B. (2015) Conformational dynamics in substrate-binding domains influences transport in the ABC importer GlnPQ. *Nat. Struct. Mol. Biol.* 22, 57–64

23. Goudsmits, J.M.H., Slotboom, D.J., van Oijen, A.M. (2017) Single-molecule visualization of conformational changes and substrate transport in the vitamin B_{12} ABC importer BtuCD-F. *Nat. Commun.* 8, 1652

24. Zirah, S., Afonso, C., Linne, U., Knappe, T.A., Marahiel, M.A., Rebuffat, S., Tabet, J.C. (2011) Topoisomer differentiation of molecular knots by FTICR MS: lessons from class II lasso peptides. *J. Am. Soc. Mass. Spectrom.* 22, 467–479

25. Roy, R., Hohng, S., Ha, T. (2008) A practical guide to single-molecule FRET. *Nature methods.* 5(6), 507–516

26. Cordes, T., Vogelsang, J., Tinnefeld, P. (2009) On the mechanism of Trolox as antiblinking and antibleaching reagent. *Journal of the American Chemical Society.* 131(14), 5018–5019

27. van der Velde, J.H.M., Ploetz, E., Hiermaier, M., Oelerich, J., de Vries, J.W., Roelfes, G., Cordes, T. (2013) Mechanism of Intramolecular Photostabilization in Self-Healing Cyanine Fluorophores. *Chem. Phys. Chem.* 14, 4084–4093

28. Vogelsang, J., Cordes, T., Forthmann, C., Steinhauer, C., Tinnefeld, P. (2009) Controlling the fluorescence of ordinary oxazine dyes for single-molecule switching and super resolution microscopy. *Proc. Natl. Acad. Sci. U.S.A.* 106, 8107–8112

29. Vogelsang, J., Cordes, T., Tinnefeld, P. (2009) Single-molecule photophysics of oxazines on DNA and its application in a FRET switch. *Photochem. Photobiol. Sci.* 8, 486–496

30. Seo, M.H., Park, J., Kim, E., Hohng, S., Kim, H.S. (2014) Protein conformatinal dynamics dictate the binding affinity for a ligand. *Nat. Commun.* 5, 3724

31. Romano, M., Fusco, G., Choudhury, H.G., Mehmood, S., Robinson, C.V., Zirah, S., Hegemann, J.D., Lescop, E., Marahiel, M.A., Rebuffat, S., De Simone, A., Beis, K. (2018) Structural Basis for Natural Product Selection and Export by Bacterial ABC Transporters. *ACS. Chem. Biol*. 13(6), 1598–1609

32. Grossmann, N., Vakkasoglu, A.S., Hulpke, S., Abele, R., Gaudet, R., Tampe, R. (2014) Mechanistic Determinants of the Directionality and Energetics of Active Export by a Heterodimeric ABC Transporter. *Nat. Commun.* 5, 5419

33. Szollosi, D., Szakacs, G., Chiba, P., Stockner, T. (2018) Dissecting the Forces that Dominate Dimerization of the Nucleotide Binding Domains of ABCB1. *Biophys. J*. 114, 331 – 342

Chapter 5

Summary and outlook

Summary

Single-molecule methods are nowadays widely used to study complex biological processes such as active membrane transport. In contrast to classic bulk biochemistry experiments, the approaches presented in this thesis show the behavior of individual molecules and avoid ensemble averaging. Strikingly, in our work we could demonstrate real-time observation of conformational changes of membrane transporters under near-native condition to understand their structure-function relationships. In the different thesis chapters, I focused on single-molecule studies of proteins and domains belonging to ABC transporters.

Chapter 1 provided a comprehensive overview of the biological significance and mechanisms of primary active membrane transporters, the ATP-binding cassette transporters. These are known to be present in all organisms, represent one of the largest super families of membrane transporters and are central to many important biomedical phenomena and diseases [1]. As I outline in the chapter, a vast of structural information of ABC transporter has been collected and was used to establish mechanistic transport models, which, however, need further verification via additional techniques that provide dynamic information (as provided in this thesis).

In **Chapter 2**, I describe the development of novel techniques for fluorescence labelling of ABC transporter domains for Förster Resonance Energy Transfer (FRET) investigations. I outline a general FRET-labelling strategy that is applied to the substrate-binding domains (SBDs) of the amino-acid importer GlnPQ of *L. lactis*. With the improved labelling scheme, I demonstrate donor-acceptor containing SBDs of up to 70%. Our studies also show that the fluorophores have little to no influence on the biochemical properties of the SBDs based on the finding of comparable binding affinity between calorimetry and single-molecule experiments. Furthermore, I outline our experimental strategy (used in chapter 4) to visualize conformational states of GlnPQ-SBDs in solution and their interconversion dynamics.

Although a lot of structural information is available for ABC transporters, the conformational dynamics in ABC transporters are largely elusive, but such data is required for full mechanistic understanding of transport. This limitation is partially resolved in **Chapter 3** where I link structural and dynamic information of the ABC importer model system GlnPQ from *L. Lactis*. Our findings suggest that amino-acid substrates of the transporter are captured via SBDs, which undergo conformational changes from an open-unliganded to a closed-liganded state using to an induced-fit mechanism. Our FRET-results showed only a single low-FRET peak in the absence of the ligand as well as for saturating concentrations of substrate (high FRET). Identical results were found for different FRET-labelling positions, indicating the absence of artefacts. A direct correlation of kinetic data, i.e., the release time of the substrate from the SBD with *in vivo* transport rates allowed us for the first time to characterize the initial steps of the translocation cycle of an ABC importer. In detail, the lifetime of the closed state of the SBD can be one of the determining

factors for the overall rate of transport. From a kinetic rate model, we further suggest that the opening of the substrate-binding domains is linked to the transition of the transmembrane pump switching from an inward to outward facing conformation. These findings contribute to a general understanding of the mechanism of ABC transport, information that became only accessible by combining single-molecule tools with bio-chemical data.

In all preceding chapters the smFRET approach was employed to the soluble domains of ABC importers. In **Chapter 4** it was successfully adopted for an ABC exporter, McjD, in a near-native lipid environment. The single-molecule data confirm existing believes of conformational control of ATP-binding and hydrolysis for the nucleotide binding domains, NBDs of McjD: ATP triggers closing and hydrolysis induces dissociation of the NBDs. Surface-immobilized McjD in proteoliposomes revealed that the NBDs also display fast conformational dynamics even in the absence of ATP. So, rather than ATP binding alone driving the closure of the NBDs, the data suggest that the apo NBDs can sample a nearly closed state without any nucleotide. Nucleotides, however, drive the NBDs to a fully closed dimer state and stabilize the closed dimer state and thus prohibit reverting back to an open dimer. Unlike the dynamic NBDs, the TMDs of McjD did not reveal any conformational fluctuations in the absence or even presence of nucleotides alone, suggesting that opening of the periplasmic gate is tightly coupled to ATP and binding of the substrate of McjD, the lasso-peptide MccJ25. With smFRET we could also for the first time show the opening of the TMDs of McjD, something that was not yet accomplished with standard structural biology techniques. In summary, our smFRET data suggest that ATP and MccJ25 binding are tightly coupled to the opening of the TMDs which is distinct from multidrug ABC transporters which are less selective for their transported ligands.

Outlook

The pioneering single-molecule studies presented in this thesis on the SBD, TMD and NBD domains of different ABC transporters pave the way for future mechanistic studies that will allow to fully unravel the transport mechanisms of these important molecular machines. A long-term goal behind our research was to identify crucial aspects of conformational changes in the transport cycle that might allow the development of advanced therapeutic targets. This is especially attractive for ABC transporters, since the latter are known to mediate drug resistance in cancer cells through a reduction in drug accumulation in tumors [2]. The idea behind this would be the development of chemotherapy treatment as binding of the targeted substrates in the cells can be observed and potentially manipulated by transport inhibition [3]. It has also been hypothesized that ABC transporters mediate drug resistance in cancer through a reduction in drug accumulation in tumors. This hypothesis, however, suggests that chemotherapy effectiveness increases by inhibiting transporters mediated drug efflux validated in model transport systems. Therefore, this thesis might contain useful information and bridge mechanistic information of ABC transporters toward use in drug resistance which is currently undertaken by the cancer therapeutics community [4].Although we took important steps within this thesis, more single-molecule and biochemical studies are need to understand all aspects of the transport mechanism. One limitation of our studies is the fact that the initial transport steps (substrate binding to SBDs) were not yet done with full transporter complexes. While this requires further biochemical work to make our developed FRET assays applicable to entire transporters (in liposomes or nanodiscs) also the usage of energy in the systems via ATP hydrolysis has not yet been considered here. Furthermore, especially for McjD it is attractive to perform more direct probing of the conformational changes in the TMDs and NBDs induced by both ligands. Such observations and the determination of kinetic rates would allow full mechanistic understanding of the transport pathway of McjD and other medically-relevant systems.

References

1. Jones, P.M., George, A.M. (2004) The ABC transporter structure and mechanism: perspectives on recent research. *Cell. Mol. Life. Sci.* 61(6), 682–699
2. Steinbach, D., Legrand, O. (2007) ABC transporters and drug resistance in leukemia: was P-gp nothing but the first head of the Hydra? *Leukemia.* 21(6), 1172–1176
3. Robey, R.W., Massey, P.R., Amiri-Kordestani, L., Bates, S.E. (2010) ABC transporters: Unvalidated therapeutic targets in cancer and the CNS. *Anticancer. Agents. Med. Chem.* 10(8), 625–633
4. Leonard, G.D., Fojo, T., Bates, S.E. (2003) The role of ABC transporters in clinical practice. *Oncologist.* 8(5), 411–424

Samenvatting

Samenvatting

Methoden met één molecuul worden tegenwoordig op grote schaal gebruikt om complexe biologische processen, zoals actief membraantransport, te bestuderen. In tegenstelling tot klassieke bulk-biochemie-experimenten laten de benaderingen in dit proefschrift het gedrag van afzonderlijke moleculen zien en wordt vermeden dat het gemiddelde van een geheel wordt bepaald. Opvallend is dat we in ons werk realtime observatie kunnen aantonen van conformationele veranderingen van membraantransporteurs in bijna-native omstandigheden om hun structuur-functie relaties te begrijpen. In de verschillende hoofdstukken van het proefschrift heb ik me gericht op single-molecule studies van eiwitten en domeinen van ABC-transporters.

Hoofdstuk 1 gaf een uitgebreid overzicht van de biologische betekenis en mechanismen van primaire actieve membraantransporters, de ATP-bindende cassettetransporters. Het is bekend dat deze in alle organismen aanwezig zijn, een van de grootste superfamilies van membraantransporters vertegenwoordigen en centraal staan in veel belangrijke biomedische fenomenen en ziekten [1]. Zoals ik in het hoofdstuk uiteenzet, is een enorme hoeveelheid structurele informatie van ABC transporter verzameld en gebruikt om mechanistische transportmodellen op te stellen, die echter verdere verificatie nodig hebben via aanvullende technieken die dynamische informatie verschaffen (zoals voorzien in dit proefschrift).

In **hoofdstuk 2** beschrijf ik de ontwikkeling van nieuwe technieken voor fluorescentie-labeling van ABC-transporterdomeinen voor Förster Resonance Energy Transfer (FRET) -onderzoek. Ik schets een algemene FRET-labelingstrategie die wordt toegepast op de substraatbindende domeinen (SBD's) van de aminozuurimporteur GlnPQ van L. lactis. Met het verbeterde etiketteringsschema demonstreer ik donor-acceptor met SBD's tot 70%. Onze studies tonen ook aan dat de fluoroforen weinig tot geen invloed hebben op de biochemische eigenschappen van de SBD's op basis van de ontdekking van vergelijkbare bindingsaffiniteit tussen calorimetrie en experimenten met één molecuul. Verder schets ik onze experimentele strategie (gebruikt in hoofdstuk 4) om conformationele toestanden van GlnPQ-SBD's in oplossing en hun interconversiedynamiek te visualiseren.

Hoewel er veel structurele informatie beschikbaar is voor ABC-transporters, is de conformationele dynamiek in ABC-transporters grotendeels ongrijpbaar, maar dergelijke gegevens zijn vereist voor een volledig mechanistisch begrip van transport. Deze beperking is gedeeltelijk opgelost in **hoofdstuk 3**, waar ik structurele en dynamische informatie van het ABC-importeurs modelsysteem GlnPQ van L. Lactis koppel. Onze bevindingen suggereren dat aminozuursubstraten van de transporter worden gevangen via SBD's, die conformationele veranderingen ondergaan van een open-niet-ligand naar een gesloten-ligand-toestand met behulp van een geïnduceerd fit-mechanisme. Onze FRET-resultaten toonden slechts een enkele

lage-FRET piek in afwezigheid van het ligand evenals voor verzadigende concentraties van substraat (hoge FRET). Er werden identieke resultaten gevonden voor verschillende FRET-etiketteringsposities, hetgeen de afwezigheid van artefacten aangeeft. Een directe correlatie van kinetische gegevens, d.w.z. de vrijgavetijd van het substraat van de SBD met in vivo transportsnelheden stelde ons voor het eerst in staat om de eerste stappen van de translocatiecyclus van een ABC-importeur te karakteriseren. In detail kan de levensduur van de gesloten toestand van de SBD een van de bepalende factoren zijn voor de totale transportsnelheid. Uit een kinetisch snelheidsmodel suggereren we verder dat het openen van de substraatbindende domeinen gekoppeld is aan de overgang van de transmembraanpomp die van een naar binnen naar buiten gerichte conformatie overschakelt. Deze bevindingen dragen bij tot een algemeen begrip van het mechanisme van ABC-transport, informatie die alleen toegankelijk werd door het combineren van tools met één molecuul met biochemische gegevens.

In alle voorgaande hoofdstukken werd de smFRET-benadering toegepast op de oplosbare domeinen van ABC-importeurs. In **hoofdstuk 4** werd het met succes overgenomen voor een ABC-exporteur, McjD, in een bijna-native lipidenomgeving. De gegevens van één molecuul bevestigen dat bestaande overtuigingen van conformationele controle van ATP-binding en hydrolyse voor de nucleotide-bindende domeinen, NBD's van McjD: ATP triggers sluiten en hydrolyse induceert dissociatie van de NBD's. Oppervlakte-geïmmobiliseerde McjD in proteoliposomen onthulde dat de NBD's ook een snelle conformationele dynamiek vertonen, zelfs in afwezigheid van ATP. Dus in plaats van alleen ATP-binding die de sluiting van de NBD's drijft, suggereren de gegevens dat de apo NBD's een bijna gesloten toestand kunnen bemonsteren zonder enig nucleotide. Nucleotiden brengen de NBD's echter naar een volledig gesloten dimeertoestand en stabiliseren de gesloten dimeertoestand en verbieden dus terug te keren naar een open dimeer. In tegenstelling tot de dynamische NBD's, onthulden de TMD's van McjD geen conformationele fluctuaties in de afwezigheid of zelfs aanwezigheid van nucleotiden alleen, wat suggereert dat het openen van de periplasmatische poort nauw is gekoppeld aan ATP en binding van het substraat van McjD, de lasso-peptide MccJ25 . Met smFRET konden we ook voor het eerst de opening van de TMD's van McjD laten zien, iets dat nog niet werd bereikt met standaard structurele biologietechnieken. Samenvattend suggereren onze smFRET-gegevens dat ATP- en MccJ25-binding nauw zijn gekoppeld aan de opening van de TMD's, wat anders is dan multidrug ABC-transporters die minder selectief zijn voor hun getransporteerde liganden.

Vooruitzicht

De baanbrekende single-molecule studies die in dit proefschrift worden gepresenteerd over de SBD-, TMD- en NBD-domeinen van verschillende ABC-transporters, effenen de weg voor toekomstige mechanistische studies die toelaten om de transportmechanismen van deze belangrijke moleculaire machines volledig te ontrafelen. Een langetermijndoelstelling van ons onderzoek was om cruciale aspecten van conformationele veranderingen in de transportcyclus te identificeren die de ontwikkeling van geavanceerde therapeutische doelen mogelijk zouden maken. Dit is vooral aantrekkelijk voor ABC-transporters, omdat van deze laatste bekend is dat ze medicijnresistentie in kankercellen bemiddelen door een vermindering van medicijnophoping in tumoren [2]. Het idee hierachter zou de ontwikkeling van chemotherapie zijn, omdat binding van de beoogde substraten in de cellen kan worden waargenomen en mogelijk gemanipuleerd door transportremming [3]. Er is ook een hypothese dat ABC-transporters resistentie tegen geneesmiddelen bemiddelen bij kanker door een vermindering van de accumulatie van geneesmiddelen bij tumoren. Deze hypothese suggereert echter dat de effectiviteit van chemotherapie toeneemt door het remmen van door transporters gemedieerde efflux van geneesmiddelen gevalideerd in modeltransportsystemen. Daarom zou dit proefschrift nuttige informatie kunnen bevatten en mechanistische informatie van ABC-transporters kunnen overbrengen naar gebruik bij geneesmiddelenresistentie die momenteel wordt ondernomen door de gemeenschap van kankertherapeuten [4]. Hoewel we belangrijke stappen in dit proefschrift hebben genomen, zijn meer enkelmoleculaire en biochemische onderzoeken moeten alle aspecten van het transportmechanisme begrijpen. Een beperking van onze studies is het feit dat de initiële transportstappen (substraatbinding aan SBD's) nog niet waren gedaan met volledige transportcomplexen. Hoewel dit verder biochemisch werk vereist om onze ontwikkelde FRET-testen toepasbaar te maken voor volledige transporters (in liposomen of nanodiscs), is hier nog geen rekening gehouden met het gebruik van energie in de systemen via ATP-hydrolyse. Verder is het, in het bijzonder voor McjD, aantrekkelijk om directer onderzoek te doen naar de conformationele veranderingen in de TMD's en NBD's geïnduceerd door beide liganden. Dergelijke waarnemingen en de bepaling van kinetische snelheden zouden een volledig mechanistisch inzicht in het transportpad van McjD en andere medisch relevante systemen mogelijk maken.

Referenties

1. Jones, P.M., George, A.M. (2004) The ABC transporter structure and mechanism: perspectives on recent research. *Cell. Mol. Life. Sci.* 61(6), 682–699
2. Steinbach, D., Legrand, O. (2007) ABC transporters and drug resistance in leukemia: was P-gp nothing but the first head of the Hydra? *Leukemia.* 21(6), 1172–1176
3. Robey, R.W., Massey, P.R., Amiri-Kordestani, L., Bates, S.E. (2010) ABC transporters: Unvalidated therapeutic targets in cancer and the CNS. *Anticancer. Agents. Med. Chem.* 10(8), 625–633
4. Leonard, G.D., Fojo, T., Bates, S.E. (2003) The role of ABC transporters in clinical practice. *Oncologist.* 8(5), 411–424

Ringkasan

Ringkasan

Metodologi molekul tunggal (*single-molecule*) saat ini telah digunakan secara luas untuk mempelajari proses biologi yang kompleks. Salah satu contohnya adalah mekanisme transpor yang menjadi fokus utama dalam laporan ini. Berbeda dengan percobaan biokimia, studi-studi molekul tunggal mengarah pada perilaku individu dari molekul dan dengan demikian karakteristik umum molekul tersebut dapat disimpulkan. Dalam studi molekul tunggal, penggunaan pewarna-pewarna fluorofor dideteksi secara mekanis dan respon reseptifnya direkam secara langsung. Salah satu keunggulan dari pendekatan ini adalah: perubahan konformasi biologis dapat dideteksi dalam lingkungan berpelarut yang dianggap cenderung mendekati kondisi asli di alam.

Dalam tesis ini, saya berfokus pada studi molekul tunggal untuk protein pengikat substrat dan protein pengekspor yang telah disusun ulang di dalam liposom. **Bab 1** menguraikan aktifitas ekspansif salah satu protein transporpada membran yaitu protein kaset pengikat ABC (*ABC-binding cassette*). Seperti yang telah diketahui, protein transpor ABC ditemukan di semua organisme. Protein tersebut mewakili salah satu *super-family* terbesardari protein trans-membran yang memegang peranan sentral dalam banyak fenomena biomedis penting [1]. Dalam beberapa dekade terakhir, informasi struktur dari domain pembangun maupun mekanisme transportasi dari protein transport ABC telah teridentifikasi.

Dalam **Bab 2**, saya menguraikan metode fundamental dari pemutakhiran proses pelabelan fluorofor yang merupakan dasar kunci dari metode *Förster Resonance Energy Transfer* (FRET). Kombinasi antara metodologi molekul tunggal dan pemutakhiran praktis pada proses pelabelan telah terbukti mampu merinci informasi mengenai perubahan konformasi dan dinamika protein pengikat substrat (PPS) pada protein pengimpor ABC tipe I. Penempelan pewarna fluorofor tidak mempengaruhi proses biokimia dari protein. Hal ini dibuktikan oleh konstanta pengikatan yang sebanding antara metodologi molekul jumlah besar (*bulk*) dan metodologi molekul tunggal. Saya juga menemukan bahwa bahwa derajat efisiensi pelabelan juga dipengaruhi oleh pilihan pewarna fluorofor (sebagaimana juga dibahas dalam Bab 4).

Walaupun informasi struktural transporter ABC telah banyak dikemukakan, dinamika konformasi pada protein transporABC masih sulit dipahami atau hanya berdasar pada bukti tidak langsung. Keterbatasan ini diselesaikan dalam **Bab 3** dimana saya menghubungkan temuan struktural dengan informasi dinamika protein yang diperoleh dari studi molekul tunggal. Pengetahuan tentang mekanisme pengikatan dan korelasi kinetiknya di tingkat transportasi *in vivo*, memungkinkan kami untuk pertama kalinya mengkarakterisasi langkah-langkah awal dari siklus translokasi pada importer ABC. Substrat ditangkap melalui protein pengikat substrat (PPS) yang kemudian mengalami perubahan konformasi ke keadaan tertutup mengikuti mekanisme *induced-fit*. Hasil studi ini menunjukkan masing-masing satu puncak histogram pada konsentrasi

jenuh maupun tanpa substrat. Pengikatan substrat dengan afinitas rendah hanya mampu membawa protein ke dalam keadaan semi-tertutup. Hasil yang identik ditemukan untuk beberapa sampel protein dengan posisi pelabelan yang berbeda. Hal ini menunjukkan bahwa mekanisme pengikatan tidak diperngaruhi oleh posisi pelabelan. Protein pengikat substrat (PPS) dari GlnPQ sesekali ditemukan dalam posisi tertutup pada keadaan tanpa substrat. Pembukaan domain dari PPS tampaknya terkait dengan transisi domain trans-membran dari pose terbuka kedalam menuju pose terbuka keluar. Penemuan ini menunjukan pemahaman umum mengenai mekanisme transpor oleh protein ABC, informasi yang hanya dapat diakses dengan menggabungkan metodologi molekul tunggal dengan data biokimia.

Dalam skala yang lebih besar, pendekatan smFRET berhasil diadopsi untuk protein pengekspor ABC, McjD, sebagaimana dibahas dalam **Bab 4**. Data molekul tunggal dari McjD yang diimobilisasi dalam proteoliposom mengungkapkan bahwa domain pengikat nukleotida (DPN) memiliki dinamika konformasi dan tidak statik. Molekul McjD terkadang menunjukkan nilai E* yang rendah (antara 0,3 dan 0,5). Hasil ini menunjukkan bahwa sampel DPN memiliki derajat dimer terbuka dan tertutup yang berbeda. Hasil tersebut juga mengindikasikan bahwa DPN pada McjD dapatditemukan dalam keadaan tertutup meskipun tanpa nukleotida. Selain itu dapat pula disimpulkan bahwa proses pengikatan ATP tidak menginisiasi proses penutupan dari DPN. Nukleotida dapat menggerakkan DPN ke keadaan dimer tertutup sepenuhnya dan dengan demikian menstabilkan keadaan tersebut. Hal ini mencegah kembali terbukanya DPN ke keadaan dimer tertutup. Tidak seperti DPN yang sangat dinamis, pengukuran Domain Trans-membran pada McjD menunjukkan tidak adanya dinamika dengan keberadaan nukleotida saja. Hal ini menunjukkan bahwa pembukaan gerbang periplasmik sangat bergantung pada proses pengikatan ATP dan MccJ25. DPN memiliki konformasi yang berbeda pada keadaan tanpa substrat. Salah satunya adalah pose dimer hampir tertutup yang dapat dipengaruhi oleh ATP untuk membentuk keadaan tertutup penuh. Sebaliknya, domain trans-membran tidak terbuka dengan keberadaan nukleotida saja.TMD dari McjD terbuka untuk melepaskan peptida dengan adanya ATP dan MccJ25 (siklus transportasi). Data smFRET menunjukkan bahwa pengikatan ATP dan MccJ25 sangat berpengaruh pada pembukaan TMD. Hal ini sangat berbeda jika dibandingkan dengan transport ABC *multidrug* lainnya. Saya mengusulkan bahwa: apabila ligan dapat masuk dalam ronggaprotein transpor *multidrug*, protein tersebut akan mengangkut ligan keluar sel. Hal ini dikarenakan pengikatan ligan tidak mempengaruhi dengan pembukaan TMD. Sedangkan transporter ABC yang lebih spesifik hanya akan membuka rongga dengan adanya substrat spesifik.

Pandangan

Studi molekul tunggal yang digunakan dalam tesis ini dianggap sebagai langkah awal untuk studi lebih lanjut. Dalam tujuan jangka panjang, penemuan terkait perubahan konformasi pada protein transpor membran dapat digunakan untuk membawa perubahan dalam tujuan terapetik dimana pengaturan asupan dan penyerapan di seluruh membran dapat dimonitor. Transporter ABC dikenal untuk memediasi resistensi obat pada kanker melalui pengurangan akumulasi obat pada tumor [2]. Hipotesis ini memegang potensi peningkatan kemoterapi efektivitas dengan menghambat transportasi [3]. Hubungan antara relevansi transporter ABC dan resistansi obat saat ini masih diteliti oleh komunitas terapi kanker [4].

Meskipun beberapa penemuan informasi ini telah diselesaikan dalam tesis ini, namun dibutuhkan lebih banyak studi molekul tunggal dan biokimia untuk dapat memahami transporter ini dalam skala yang lebih besar. Sebagai contoh, tesis ini hanya melaporkan langkah awal mekanisme transport, yaitu terikatnya substrat pada domain pengikatan substrat, yang diarahkan pada molekul tunggal. Korelasi dengan eksperimen molekul jumlah banyak (*bulk*) dapat membantu terprediksinya mekanisme transportasi. Akan tetapi menghubungkannya dengan mekanisme hidrolisis ATP dalam domain pengikat nukleotida masih belum dilakukan di sini. Pengamatan terhadap perubahan konformasi dalam domain trans-membran dengan pendekatan molekul tunggal juga penting untuk dilakukan agar dapat memahaminya dengan lebih dalam. Pendekatan molekul tunggal pada domain pengikat ATP dapat menjadi temuan pelengkap ke mekanisme yang diusulkan.

Penelitian pada transporter membran yang dibahas dalam laporan ini bersifat dasar. Studi dengan menggunakan pendekatan molekul tunggal harus menjadi titik awal untuk meningkatkan pemahaman tentang mekanisme transportasi. Peningkatan stabilitas pewarna fluorofor dan penerapannya dalam studi molekul tunggal serta pendekatan untuk subdomain lain dari transporter dapat membawa hasil yang lebih baik.

Referensi

1. Jones, P.M., George, A.M. (2004) The ABC transporter structure and mechanism: perspectives on recent research. *Cell. Mol. Life. Sci.* 61(6), 682–699
2. Steinbach, D., Legrand, O. (2007) ABC transporters and drug resistance in leukemia: was P-gp nothing but the first head of the Hydra? *Leukemia.* 21(6), 1172–1176
3. Robey, R.W., Massey, P.R., Amiri-Kordestani, L., Bates, S.E. (2010) ABC transporters: unvalidated therapeutic targets in cancer and the CNS. *Anticancer. Agents. Med. Chem.* 10(8), 625–633
4. Leonard, G.D., Fojo, T., Bates, S.E. (2003) The role of ABC transporters in clinical practice. *Oncologist.* 8(5), 411–424

Curriculum Vitae

Curriculum Vitae

Personal Details

Name : Florence Agustin Husada
Address : Graviuspad 10, 5641 WK Eindhoven, Netherlands
Telephone : +31 615 31 3266
E-mail : f.a.husada@gmail.com
Date of Birth : 1 August 1990
Nationality : Indonesia

Characteristic :

- **Positive**
  Ambitious, cooperative, hardworking, independent, meticulous, neat, persistent, preventive, punctual, responsible, selective, strict, thoughtful, well organized
- **Negative**
  Intuitive, sensitive, suspicious, quiet, wary

Social :

- Skype florence.010890
- LinkedIn linkedin.com/in/florence-agustin-husada-31343a41/
- Researchgate researchgate.net/profile/Florence_Husada

Educational Backgrounds

2013 – 2018 University of Groningen (Netherlands)
Ph.D of Molecular Microscopy
For dissertation : Single-molecule FRET Reveals Transport Mechanism of ABC Transporter

2012 – 2013 Bandung Institute of Technology (Indonesia)
Master of Biochemistry
For dissertation : Conformational changes in the substrate-binding domains of GlnPQ by single-molecule FRET

2008 – 2012 Bandung Institute of Technology (Indonesia)
Bachelor of Biotechnology
For dissertation : Cloning A-Amylase Bacillus amyloliquefaciends ABBD and its expression in Bacillus megaterium MS941
Degree : Cum Laude

Working Experiences

2018 – present Thermo Fisher Scientific (The Netherlands)

Sales Lead Development Representative

Employee working on :

- Generating qualified leads for the customer relation management
- Increasing the size of the pipeline of the sales field
- Developing conversion lead to business opportunity

2011 – 2011 Indofood Sukses Makmur (Indonesia)

Quality Control Assistant

Internship working on :

- Saturated lipid content control
- Gluten content control

Interests

- **Interests**

  Health aspect :

  Pharmacy in correlation with Ph.D thesis. Observation of living cell systems to induce transport.

  Microscopy in correlation with Ph.D and M.Sc thesis. Using fluorophore to probe conformational state difference of binding protein.

  Food aspect :

  Consumption in correlation with B.Sc thesis. Produce shorter glucose chain by using degrading enzyme.

  Management aspect :

  Organize research project based on personal qualities of being well organized and meticulous and science background.

Bibliography

Florence was born on 1st August 1990 in Bandung, Indonesia. She grew up in the same city and Lippo Cikarang, being part as the youngest daughter with one older sister. In 2009, she was graduated from BPK Penabur Senior High School. With her interest into chemical reaction, she attended Bachelor degree in Chemistry field in Institute Technology Bandung. Graduated with the possibility to apply for an exchange student, Sandwich Program ITB-RUG, she applied and been chosen as the candidate to do her final Master Thesis in University of Groningen, in the group of Prof. Bert Poolman. Gaining the trust from her supervisor, Dr. Giorgos Gkouridis, she was referred to do her Ph.D in the group of Prof. Thorben Cordes. That was when the journey has started.

Doing research in an advancing laboratories wasn't everything needed. It needs persistence, luck, and diligence. She was doing research in a topic of Single-molecule FRET Reveals Transport Mechanism of ABC Transporter. During her Ph.D she joined some scientific conferences and workshop. After 4.5 years, she completed her Ph.D with 5 scientific publications (combined co-authorship), in which three of it are reported as each chapter in this thesis. In 2018, she finished her Ph.D and had one month gap before her company's career in Thermo Fisher Scientific, branch of Eindhoven. She applied the position of Sales because of being triggered to have something new and challenging. Her experience in handling relatively complicated membrane protein during her Ph.D, brought her to understand the hurtle of structural biologist in gaining pure and stable protein. With that as the ground base, she is learning to convince people and direct them to a new straight forward methods, Cryo Electron Microscope. Down the process, she enjoys the new experience she has between traveling around the EMEA countries and developing business for the company.

List of publications

List of Publications

2019 eLife Sciences, (8), 44652

de Boer, M., Gouridis, G., Vietrov, R., Begg, S.L., Schuurman-Wolters, G.K., **Husada, F.**, Eleftheriadis, N., Poolman, B., McDevitt, C.A., Cordes, T.

Conformational and dynamic plasticity in substrate-binding proteins underlies selective transport in ABC importers.

DOI: https://doi.org/10.7554/eLife.44652.004

(publication is not included in this thesis)

2018 The EMBO Journal, 37(21), 100056

Husada, F., Bountra, K., Tassis, K., de Boer, M., Romano, M., Rebuffat, S., Beis, K., Cordes, T.

Conformational dynamics of the ABC trasnporter McjD seen by single-molecule FRET.

DOI: https://doi.org/10.15252/embj.2018100056

2016 Scientific Reports, 18(6), 33257

Ploetz, E., Lerner, E., **Husada, F.,** Hohlbein, J., Weiss, S., Cordes, T.

Förster resonance energy transfer and protein-induced fluorescence enhancement as synergetic multiscale molecular rulers.

DOI: https://doi.org/10.1038/srep33257

(publication is not included in this thesis)

2015 Biochemical Society Transactions, 43(5), 1041–1047

Husada, F., Gouridis, G., Vietrov, R., Schuurman-Wolters, G.K., Ploetz, E., de Boer, M., Poolman, B., Cordes, T.

Watching conformational dynamics of ABC trasnporters with single-molecule tools.

DOI: https://doi.org/10.1042/BST20150140

2015 Nature Structural and Molecular Biology, 22(10), 57–64

Gouridis, G., Schuurman-Wolters, G.K., Ploetz, E., **Husada, F.,** Vietrov, R., de Boer, M., Cordes, T., Poolman, B.

Conformational dynamics in substrate-binding domains influences transport in the ABC importer GlnPQ.

DOI: http://doi.org/10.1038/nsmb.2929

Acknowledgement

Acknowledgement

Dear readers, 4.5 years of Ph.D has come to an end. This period was a wonderful time to bloat science education as well as bearing adversity. This journey would not have been possible without having people around me helping and taking care each other. I ***mainly*** acknowledge here that this thesis is not an invention of myself. It is a result of lots of support from many generous, yet, brilliant colleagues and caring people. This roadway has become an unforgettable moment and I am grateful to have had all these years together with you.

At first, I was not planning to mention all the names who had helped me through this uneasy and unregretful path. But having ever been in that shoes – to trying to find my name in someone's thesis acknowledgement's page – this page is the only one owning the most attention. Regardless my limitation to trace back all long memories during my Ph.D and to mention your name, please do remember, a personal above, GOD, had seen your helping hand which I truly appreciate. Time will come when you will reap what you sow. Thank you so much!

Thinking of "Ph.D", I really cannot stop thanking **Giorgos** for being my supervisor during the first couple months of my Master in Groningen; *thank you for having bigger faith in me than me myself*. February 2012 was kept blowing in my mind when you had promoted my skills, opened up Ph.D door for me, and it had brought me to where I stand right now. You showed and motivated me on having self confidence in research, in which I initially doubted. Thanks Giorgos! **Thorben**, seeing you as a humble professor during my Master, had become one of my reason to start dreaming to become Ph.D. Along the way, you had been proactive to find funding stream, project, collaborator. Coming to its end, you were patience to wait for me to compile this thesis. Just like love and hate relationship, I have no regret of acquiring my Ph.D in yours. **Bert**, our working together was felt short, but in my case, longed to have it back. You have the most gentle way of supervision, like father to his children. It was effortless for me to have my good respect to you. **Kostas Beis** and **Kiran**, thanks for trusting me to collaborate with you in the nice last project during my Ph.D. It was a pleasure to be working together with you. **Ruslan** and **Arnold**, you made my starting days as Ph.D at ease, made my evenings didn't feel that spooky anymore, filled with anticipation to greet you because of your mild nature. Thanks! Without it, I wouldn't have survived in those haunting corridors. **Yusran**, you were coming later in the group, but it was a great reassurance to have a brother at the same time conversant colleague. Our long family-ship is still there, I LEARNED there is no limit to it! **Evelyn**, thanks for your knowledgeable everlasting passion, for showing it's not possible to become bullet proof in science. **Margriet** and **Jan Peter**, thanks for the help to finalize my thesis.

All *Enzymology* members, **Gea**, **Sonja**, **Faizah**, **Ria**, **Lotteke**, **Łukasz**, **Stephanie**, **Joury**, **Mariska**, **Ryan**, **Inda**, **Michiel**, **Aditya**, **Stephan**, **Tjeerd**, **Wojtek**, **Frans**, **Gemma**, **Rianne**, **Boqun**, **Jonas**. If it was not because of the nice atmosphere you provided, my story would have been different.

All *Molecular Microscopy* and Single Molecule Biophysics members, **Sarah** (your name comes first for providing nice coffee chit-chat), Marijn (for all scientific discussion and support), **Kostas** (for your helping hand till the final stage), **Atieh**, **Monique, Nikos**, **Jochem**, **Jasper, Yichen, Joris, Jelle, Lisanne**, **Andrew**, **Enrico**. All *Molecular Biophysics* members, **Wouter, Melissa** (for being a supportive friend and nice sweet-feeder)**, Sourav, Guus, Pedro, Yukun**, and all the new members. Welcome to the world.

All *Indonesian* family in Groningen, people who change misfortune into fortress, make laugh a little louder, make life a little brighter. Being in a foreign country had never been felt more home without you. **Ali**, **Lili** and **Dede** for always being in the same path. These people who shared same roof and were there unconditionally **Caecil**, **Bebel**, **Jeje**, **Ika**, **Audrey**, **Livia**. **Dina**, thanks for all the nice chat and keep sharing same kind of encouragement about every matters. Especially thanks for making this nice cover and be rapidly responsive for all the questions. Thanks for these people who brought laugh and warmth when it was needed **May**, **Salva**, **Fikri**, **Kekei**, **Sasa**, **Ida**, **Rico**, **Jane**, **Ting2**, **Ochin**, **Kukuh**, **Krystle**, **Selva**, **Cory**, **Mei**, **Karin**, **Yaya, Yessi**. It is said there are friends who are as close as family, and I find it in you. Super cooperative family examples, **Bude Arie-Om Herman, Tante Indah-Om Yon, Mas Yayok-Mbak Lia, Mbak Fitri-Mas Kus, Mbak Ica- Mas Kris**, **Mbak Ayu-Mas Zaenal**, **Mas Bin-Ka Copi**, **Mas Ali-Yosay**, **Radit-Nia, Ka Nna-Ka Azis**, **Mas Didik-Mbak Rosel**, **Mbak Laskmi-Mas Kadek**, **Didin-Anis**, **Bu As-Pak As**, **Teh Susan-Kang Bino, Ka Irfan-Teh Liza**, **Adhyat-Nuri**, **Mbak Desti-Mas Iging, Mbak Monik-Mas Fajar** and your all little angels. ITB Sandwich successor, **Ulfah**, **Praw-Ka Insan**, **Felix**, **Aisyah**, **Raissa**, **Nadya**, **Bibit**, **Nisrin, Ila**, **Abed**, **Rizky**, **Nelson**, **Frans**, **Romel**. Fellow friends, **Adel**, **Ka Fean**, **Ka Astri, Mbak Tiur, Bu Ima, Mbak Ira, Mbak Ira Sianturi Mbak Nur, Mbak Erna, Mas Ury, Mas Ronny, Mas Tri, Mas Yoga, Ka Eryth-Ka Iqbal, Sugap**, **Erlang**, **Widi, Shiddiq, Guntur, Mas Udin, Almas,** . To all of you here, *the most beautiful discovery true friends make is that they can grow separately without growing apart*.

All *lifelong family brothers and sisters*, in this system and new system. **Inge**, **Tim-Inge**, **Like-Hans**, **Biljana-Martin Bryan Tyler**, **Tini**, **Martyna**, **Phillia**, **Julia**, **Ruo Mei**, **Seungbok**, **Carol**, **Juliette**, **Carol-Joppe Elliot Charlotte**, **Amber**, **Arjan**, **Steven**, **Michel**, **Muriel**, **Elize**, **Sjantine**, **Rhiannon**, **Desiree-Jonathan**, **Suzy-Gatusso**, **George-Lisa, Abigail-Delon Anya Ziah Leah**, **Sander-Britt**, **Agatha-Aurimas**, **Dorothy-Johan**, **Marlo-Rhia**, **Simon**, **Marloes**, **Ko Ray**, **Ko Irwien**. Proverbs 18:24 *There are companions ready to crush one another, But there is a friend who sticks closer than a brother*.

All *Thermo Fisher Scientific* colleagues, **Ben**, **Max**, **Emine**, **Gaurav**, **Rita, Igor**, **Giullaume**, **Adriana**, **Margarita**, **Aurelien**, **Isabel**, **Florencia**, **Deepak**, **Alevtyna, Mattia**. You came last, but I can't exclude my thanks for your motivation, based on your all own experience, to keep pushing me to the final line of Ph.D.

To those whom love does not go away, **Mama, Papa,** and **Cici**. They walk beside me every day, UNSEEN, UNHEARD, but always near. Still loved, still missed and very dear. Terutama omaon,

yang udah ngijinin ambil sekolah jauh, mau ditinggal sendiri di Indo padahal lagi ga 100% sehat. Tadinya cuma mau untuk 6 bulan, ujung-ujung masih 7 tahun dan still on counting. Thanks for your bless for me, to let me walk in the path I choose and have full trust on me. Sayang omaon =) Buat cicidut, yang udah relain baju2 tebel, alat2 masaknya dicuri buat konsumsi ren di Groningen, sampe kadang ga ngeh baju sendiri ilang kemana, padahal nyasar ke Groningen ato Eindhoven, yang juga ga itungan buat ngebantu mah. Xiexie cici =) Semangat terus buat kita yang milih dengan kemampuan dan pilihan sendiri untuk ngerantau.

For those whom I cannot describe how grateful I am to have walked to you, **Leon, Mama Ria, Papa Bennie, Stefan** and **Anna**. Leon, bedankt voor alles wat je doet en voor alles wat je bent. Ik wil je bedanken dat je me altijd hebt aangemoedigd mijn best te doen, dat je altijd in me gelooft, zelfs als ik niet eens in mezelf kan geloven. Sinds ik je ontmoette, is mijn leven aan het opleven. Er vindt een positieve verschuiving plaats en ik weet dat het iets met jou te maken heeft. Je haalt het beste in mij naar boven, en door jou houd ik niet langer vast aan mijn angsten en laat ik dingen gewoon gebeuren zoals zou moeten. Bedankt voor het openen van een hele nieuwe wereld voor mij. Bedankt dat je het soort vriendje bent dat voor mij en met mij bidt. Ik ben zo gezegend dat ik je in mijn leven heb. Voor het gezin, elk leven is een verhaal, bedankt dat je deel uitmaakt van mijn verhaal.

Last, terima kasih **Yehuwa** untuk segala berkat Engkau. Engkau kasih ren kekuatan dan banyak berkat, yang tidak boleh ren lupa, apa yang ren punya, itu semua adalah dari Engkau.

My acknowledgment to the reading committee and finally the AiO Zernike Institute for funding this Ph.D thesis.

Finally, I would like to thank the reader and all the party that has helped in finishing this thesis. SINCERELY THANK YOU.

Please gather at my last thanks when food is also served.

Notes